Development of a Rubella- Hepatitis C Virus-Like Particle Vaccine Platform

Joshua D. Duncan

BSc, MRes

Thesis submitted to the University of Nottingham for the degree of Doctor of Philosophy

July 2022

Abstract

The Hepatitis C virus (HCV) currently infects 1% of the global population and is attributed to 400,000 deaths annually, thus presenting a major public health threat. Persistent infection results in extensive liver damage and is associated with the development of hepatocellular carcinoma. Current treatments rely on highly effective therapeutic direct acting antiviral compounds. However, these do not prevent reinfection. The current WHO target for HCV elimination by 2030 is unlikely to be met in the absence of a prophylactic vaccine. Approximately 25 % of acute infections spontaneously resolve and several studies have associated this outcome with the rapid production of broadly neutralising antibodies that target the HCV envelope glycoproteins, providing a goal for HCV vaccine candidates.

Virus-like particles (VLPs) offer a highly immunogenic and safe vaccination approach. VLPs can induce greater titres of antibodies compared to subunit vaccines due to the presence of multiple copies of epitopes present in these structures. In addition to this, chimeric VLPs allow the presentation of foreign viral epitopes to the immune system. The Rubella virus (RV) induces long-lasting humoral responses upon exposure following natural infection or vaccination. Recombinant expression of the three RV structural proteins, capsid-E2-E1, leads to the assembly of RV-LPs that are similar to infectious RV in both morphology and immunogenicity.

This project explored the use of RVLPs as a vaccine platform for the presentation of HCV envelope glycoproteins. First an in-house system

for the expression of RVLPs was established and validated. Following this, a panel of Rubella-Hepatitis C virus (RH) chimeras were designed and constructed using homologous recombination cloning methods. Five RH constructs were generated and validated for VLP formation and secretion. Of these constructs, one chimera, RH5, was found to produce chimeric VLPs that incorporated the HCV envelope glycoproteins. Furthermore, the RH5 chimeric VLPs reacted with conformation sensitive anti-HCV antibodies. Finally, immunisation of bovines with RH5 elicited autologous neutralising antibodies. This project described the development and early validation of a novel chimeric vaccine platform for HCV.

Publications

Duncan, Joshua D., Richard A. Urbanowicz, Alexander W. Tarr, and Jonathan K. Ball. 2020. “Hepatitis C Virus Vaccine: Challenges and Prospects.” Vaccines 8(1):1–23. doi: 10.3390/vaccines8010090.

Urbanowicz, Richard A., Theocharis Tsoleridis, Hannah J. Jackson, Lola Cusin, **Joshua D. Duncan**, Joseph G. Chappell, Alexander W. Tarr, Jessica Nightingale, Alan R. Norrish, Adeel Ikram, Ben Marson, Simon J. Craxford, Anthony Kelly, Guruprasad P. Aithal, Amrita Vijay, Patrick J. Tighe, Jonathan K. Ball, Ana M. Valdes, and Benjamin J. Ollivere. 2021. “Two Doses of the SARS-CoV-2 BNT162b2 Vaccine Enhances Antibody Responses to Variants in Individuals with Prior SARS-CoV-2 Infection.” Science Translational Medicine eabj0847. doi: 10.1126/SCITRANSLMED.ABJ0847.

Blok, Andrew J., Pratik Gurnani, Alex Xenopoulos, Laurence Burroughs, **Joshua Duncan**, Richard A. Urbanowicz, Theocharis Tsoleridis, Helena Müller-Kräuter, Thomas Strecker, Jonathan K. Ball, Cameron Alexander, and Morgan R. Alexander. 2020. “Polymer Microarrays Rapidly Identify Competitive Adsorbents of Virus-like Particles.” Biointerphases 15(6):061005. doi: 10.1116/6.0000586.

Napolitano, Federico, Rossella Merone, Adele Abbate, Virginia Ammendola, Emma Horncastle, Francesca Lanzaro, Marialuisa Esposito, Alessandra Maria Contino, Roberta Sbrocchi, Andrea Sommella, **Joshua D. Duncan**, Jospeh Hinds, Richard A. Urbanowicz, Armin Lahm, Stefano Colloca, Antonella Folgori, Jonathan K. Ball, Alfredo Nicosia, Benjamin Wizel, Stefania Capone, and Alessandra Vitelli. 2020. “A next Generation Vaccine against Human Rabies Based on a Single Dose of a Chimpanzee Adenovirus Vector Serotype C.” PLoS Neglected Tropical Diseases 14(7):1–26. doi: 10.1371/JOURNAL.PNTD.0008459.

Declaration

I declare that the work presented in this thesis is my own and has not been previously submitted elsewhere. I also confirm that the experimental data presented here has been the product of my own work unless stated by acknowledgment or reference.

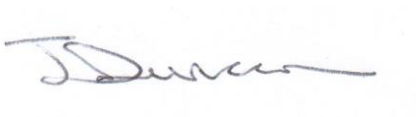

Signature

Date 30/06/2022

The work presented in this thesis is commercially sensitive and should not be publicly disclosed.

Acknowledgements

I would like to thank my supervisors, Prof. Jonathan Ball and Dr Patrick McClure for the opportunity to undertake this PhD project. This has been a challenging project and their continued support and guidance throughout has been essential.

I would like to thank past and present members of the virology research group. In particular, Dr Theocharis Tsoleridis and Dr Joseph Chappell for their support and useful discussions. I would also like to thank Dr Richard Urbanowicz who taught me everything I know about mammalian tissue culture.

I would also like to thank my family and friends who have been a source of great support throughout the course of this project. In particular, I would like to thank my partner Mel whose support has been invaluable.

Contents

List of Figures

List of Tables

Abbreviations

Ab	Antibody
AP	Alkaline Phosphatase
Apo	Apolipoprotein
AR	Antiengic Region
ASC	Antibody-Secreting Cell
BCA	Bicinchoninic acid
BCL	Biological Containment Laboratory
BHK	Baby Hamster Kidney
b-ME	B Mercaptoethanol
bnAb	Broadly Neutralising Antibody
CD81	Cluster of Differentiation 81
cDNA	complementary DNA
ChAd3	Chimp Adenovirus 3
CHO	Chinese Hamster Ovary Cell
co-IP	co-Immunoprecipitation
COPII	Coat Protein Complex II
CRD	Complementarity Determining Region
CRS	Congenital Rubella Syndrome
Cryo-EM	Cry-Electron Microscopy
CTL	Cytotoxic T Lymphocyte
Cyt	Cytoplasmic tail
DAA	Direct Acting Antiviral
DC-SIGN	Dendritic Cell-Specific Intercellular adhesion molecule-3-Grabbing Non-integrin
DENV	Dengue Fever Virus
DHBV	Duck Hepatitis B Virus
DMEM	Dulbecco's Modified Eagle Media
DMSO	Dimethyl sulfoxide
DMV	Double Membrane Vesicles
DNA	Deoxyribonucleic acid
DTT	Dithiothreitol
E	Envelope protein
EC50	Half maximal effective concentration
ECL	Enhanced chemiluminescence
Ecto	Ectodomain
EDTA	Ethylenediaminetetraacetic acid

ELISA	Enzyme-linked Immunosorbent Assay
EndoH	Endoglycosidase H
EqHV	Equine Hepacivirus
ER	Endoplasmic Reticulum
FL	Fusion Loop
GFP	Green Flourescent Protein
Gt	Genotype
HBV	Hepatitis B Virus
HBVsAg	Hepatitis B Virus Surface Antigen
HCC	Hepatocellular Carcinoma
HCV	Hepatitis C Virus
HCVLP	Hepatitis C Virus-Like Particle
HEK	Human Embryonic Kidney Cells
HIV	Human Immunodeficiency Virus
HLA	Human Leukocyte Antigen
HMW	High Molecular Weight
HPV	Human Papillomavirus
HRP	Horseradish Peroxidase
HuAd6	Human Adenovirus 6
HVR	Hypervariable Region
Ig	Immunoglobulin
IgVR	Intergenotypic Variable Region
IL	Interleukin
IFN	Interferon
ISG	Interferon Stimulated Genes
Kda	Kilodaltons
LB	Lysogeny Broth
mAb	Monoclonal Antibody
MBL	Mannose Binding Lectin
MHC	Major Histocompatibility Complex
miR	micro RNA
MLV	Murine Leukaemia Virus
MMR	Measles, Mumps and Rubella
mRNA	Messenger RNA
MVA	Modified Vaccinia virus Ankara
nAb	Neutralising Antibody
NEB	New England BioLabs
NK	Natural Killer
NLR	NOD-Like Receptor
NS	Non-Structural
ORF	Open Reading Frame
PAMPS	Pathogen-Associated Molecular Patterns
PBMC	Peripheral Blood Mononucleocyte
PBS	Phosphate Buffered Saline
PCR	Polymerase Chain Reaction

PEI	Polyethylenimine
pNPP	p-Nitrophenyl Phosphate
PP	Peudovirus Particle
PRRs	Pattern Recognition Receptors
PVDF	Polyvinylidene fluoride
PWID	People Who Inject Drugs
RAS	Resistance-Associated Substitution
RdRp	RNA-dependent RNA polymerase
RH	Rubella-Hepatitis C
RHV	Rodent Hepacivirus
RLR	RIG-I-Like Receptor
RLU	Relative Light Units
RNA	Ribonucleic Acid
RV	Rubella Virus
RV-E2sp	Rubella Virus E2 envelope glycoprotein signal peptide
RVLP	Rubella Virus-Like Particle
SARS-CoV2	Severe Acute Respiratory Syndrome Coronavirus 2
scFv	Single Chain Variable Fragment
SDM	Site Directed Mutagenesis
SDS-PAGE	Sodium Dodecyl Sulfate Polyacrylamide Gel Electrophoresis
sE2	Soluble E2 glycoprotein
SINV	Sindbis virus
SNP	Single Nucleotide Polymorphism
SRBI	Scavenger receptor class B type 1
SSA	Sub-Saharan Africa
ssRNA	Single-stranded Ribonucleic Acid
SV-40	Simian Virus 40
SVC	Spontaneous Viral Clearance
TEM	Transmission Electron Microscopy
TEMED	Tetramethyl ethylenediamine
Tfh	Follicular T cells
Th	Helper T cell
TIM-1	T-cell immunoglobulin and mucin domain 1
TLR	Toll-Like Receptor
TMD	Transmembrane Domain
UL-CDR	Ultra-Long CDR
US	United States
UTR	Untranslated Region
VLDL	Very Low-density Lipoprotein
VLP	Virus-Like Particle
VSV	Vesicular Stomatitis Virus
VSVG	VSV glycoprotein
WHO	World Health Organisation

Chapter 1 Introduction

1.1 Introduction to the Hepatitis C Virus

1.1.1 Impact

HCV is one of the causative agents of chronic viral hepatitis and represents a major threat to global public health. Currently it is estimated that HCV infects approximately 1% of the global population[1]. Annually, 400,000 deaths are attributed to complications arising from chronic HCV infection such as cirrhosis and HCC[2]. In the US, chronic HCV infection is the leading cause of liver transplantation[3] and the number of deaths caused by HCV outnumber those caused by HIV[4]. In response to the public health impact of HCV, the WHO has set 2030 as the target for HCV elimination[5].

1.1.2 Transmission

As a blood borne virus, transmission of HCV occurs through contact with contaminated blood. The highest risk group for acquiring HCV are PWID[6], who become exposed to contaminated blood via the sharing of drug paraphernalia, this is one of the commonest routes of transmission for HCV. Healthcare workers represent another high risk group for HCV infection due to the increased risk of exposure contaminated blood through needle stick injuries[7]. Prior to the screening of blood for medical uses, transfusion of contaminated blood was an additional route of transmission[8,9]. Vertical transmission of HCV can also occur either *in utero* or intrapartum and may represent the main transmission route for HCV in infants[10]. Sexual transmission of HCV can occur and individuals with more than 20 sexual partners are at a higher risk of becoming

infected[11]. Sexual transmission of HCV has been found to be higher amongst homosexual, HIV-positive males[12].

1.1.3 Pathology

Acute HCV infection is defined as the initial 6-month period of infection. Symptoms of acute HCV infection include jaundice, abdominal pain, fatigue, and fever, however approximately 30 % of acute cases present with symptoms with the remaining cases being asymptomatic[6]. Diagnosis of acute infection can be achieved through serological and PCR assays to detect viral RNA[13]. However, given the high proportion of asymptomatic cases, many acute infections may remain undiagnosed. An estimated 25% of acute infections spontaneously resolve within the first 12 months of acquiring infection[14]. Individuals who achieve SVC are more likely to clear subsequent reinfections[14]. In the absence of SVC the infection progresses to chronicity. Chronic HCV can manifest for decades and symptoms include fatigue, weight loss and cryoglobulinemia[15]. Long term infection results in extensive damage of the hepatic tissues leading to cirrhosis[16] which can result in liver failure. In addition to this, chronic infection increases the risk of HCC[17].

1.1.4 Treatment

Currently there are no prophylactic or therapeutic vaccines that target HCV[18], as such treatment relies solely on the use of therapeutic compounds. Initially, HCV was treated with interferon alpha 2a which was replaced with pegylated interferon and ribavirin. This latter treatment achieved successful viral clearance in approximately 50% of

cases[19]. These early approaches have since been improved upon with the availability of DAAs which act as inhibitors of the HCV NS3/4A serine protease, NS5A or NS5B-RdRp[20] and achieve SVR in 95% of cases[21].

Despite the success of DAAs there are multiple draw backs to their use. Firstly, the high cost of these treatments limits their use to higher income countries[22]. Secondly, the use of therapeutics requires the detection of HCV. This can be challenging since acute HCV infections can be asymptomatic and therefore are unlikely to be detected. Thirdly, the efficacy of DAAs vary between HCV genotypes and subtypes[23], some of which encode known RAS[24]. This could limit the efficacy of DAAs in regions with higher frequencies of RAS encoding HCV variants such as regions of SSA which are estimated to harbour the 4r subtype which encodes a NS5A RAS motif[25–28]. Finally, successful DAA treatment does not prevent reinfection[29] therefore arguing for the development of a prophylactic vaccine that could be used prior to infection and also following successful SVR via DAA treatment.

1.1.5 Classification

HCV belongs to the *Flaviviridae* virus family which includes other medically relevant viruses such as yellow fever virus, Zika virus and West Nile virus[30]. Until recently HCV was the sole member of the *Hepacivirus* genus. However, in 2016 Smith *et al.,*[31] published phylogenetic analysis comparing HCV and other *Hepacivirus*-like unclassified viruses with similar genome arrangements. This study proposed the expansion of the *Hepacivirus* genus to include several

new species with demarcation based on analysis of conserved amino acid residues 1123-1566 (NS3) and 2536-3959 (NS5B)(referenced to strain H77(accession number AF011751)[31]. These novel species and HCV have now been named as *Hepacivirus A-N* with HCV being referred to as *Hepacivirus C*[31]. The closest relative of HCV is the *Hepacivirus A* virus, also known as EqHV, which is responsible for acute and chronic viral hepatitis in equids[32,33].

1.1.6 Genetic Diversity

As species HCV exhibits extensive genetic diversity which is driven by the introduction of mutations into the viral genome via the error prone NS5B RdRp[34]. The diversity of HCV is classified into genotypes which are based on a shared nucleotide sequence homology of 70%[35]. There are currently 8 HCV genotypes[35,36]. Intergenotype diversity is further classified into subtypes which are denoted by lower case letters. The nucleotide sequences diverge by 15% between subtypes[35]. At the time of writing there are 90 confirmed subtypes[35].

An additional level of genetic diversity is found in infected individuals with the establishment of a heterogeneous population of closely related HCV isolates, referred to as a quasispecies[37,38]. This population arises due to the propensity of HCV to produce high viral titres coupled with a high mutation rate and a selective pressure driven by the host immune response[39]. Variability within the quasispeices is mostly focused to the immunodominant HVR1 region located at the E2 N-terminus and is linked to nAb evasion and progression to chronicity[39,40].

1.1.7 Epidemiology

HCV is present across the globe and is present on every inhabited continent. The most recent study on the distribution of HCV genotypes was performed by Petruzzeillo *et al.,*[41] in which published data from 2000-2015 were collected to assess regional prevalence of HCV genotypes. This study found that Gt1 was the most prevalent accounting for 49% of cases globally. Gt1 infections were dominant in developed western countries, accounting for 74% of cases in North America[41]. Gt3 was found to be the second most dominant globally whilst Gt4 and Gt2 were third and fourth, respectively. Whilst Gt1 and Gt3 were more prevalent in higher-income countries, Gt4 and Gt5 were found to be more prevalent in developing nations where HCV treatments are limited. Interestingly, Gt4 infections were dominant in Egypt where they accounted for 96% of cases.

1.2 Molecular Biology of the Hepatitis C Virus

1.2.1 Genomic Structure

The HCV genome is a positive ssRNA molecule, approximately 9.6 kb in length. This genome consists of a single ORF that is flanked by UTRs [42]. The 5’ UTR contains an IRES site which is required for the translation of the ORF[43]. The ORF is translated as a 3000-residue polypeptide that is subsequently cleaved via the action of both host signal peptidases and auto-proteases to yield 10 viral proteins (Figure 1.1)[44]. The first three proteins constitute the nucleocapsid core protein, and the two envelope glycoproteins, E1 and E2. The remaining seven proteins are non-structural and are involved in the replication of the viral

genome and assembly of the virus particle. The 3' UTR contains a poly UC tail followed by a conserved X region which act as regulatory elements[45,46] and aid viral genome packaging[47].

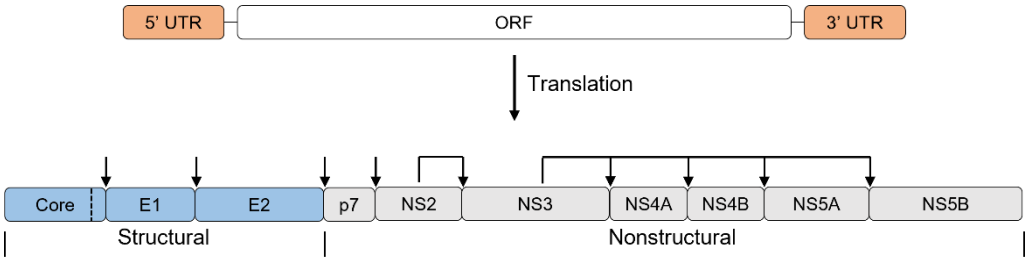

Figure 1. 1 Genome arrangement of the Hepatitis C virus.

The ORF undergoes translation to produce a polyprotein that is subsequently cleaved at sites indicated by the arrows. Structural proteins and p7 are liberated by the action of host cell proteases. Core protein undergoes further cleavage at the C-terminal by signal peptide peptidase (dashed line) to remove the E1 signal peptide. NS2 contains a cysteine protease that mediates cleavage of the NS2/NS3 junction. NS3 encodes an auto protease which cleaves remaining non-structural proteins.

1.2.2 Structural Viral Proteins

1.2.2.1 Core Protein

The HCV-C protein is encoded in the first 191 residues of the polyprotein N-terminus. Initial cleavage occurs in the ER lumen and is mediated by host signal peptidases followed by cleavage by signal peptide peptidase at around residue 177[48]. Mature HCV-C is approximately 21 KDa in size and has two distinct domains (D1 and D2)[49]. The N-terminus domain, D1 consists of residues 1-117 which contain three clusters of basic residues resulting in hydrophilic properties that are involved in RNA binding[50] and dimerization[51]. In contrast, D2 is located at the C-terminus of HCV-C and is hydrophobic in nature allowing for localisation to intracellular membranes[52]. HCV-C

protein has multiple roles in the virus life cycle including nucleocapsid formation and viral genome packaging[49].

1.2.2.2 Envelope Proteins

The HCV genome encodes two envelope proteins, E1 and E2. These proteins are type I transmembrane proteins with N-terminal ectodomains that undergo extensive glycosylation. Following expression, E1 and E2 form intracellular non-covalent heterodimers[53] that are incorporated into the surface of the mature virion and form high order covalent complexes[53] that mediate viral entry into the host cell[54] and are attractive vaccine targets[55].

HCV-E1 consists of residues 192-383 of the HCV polyprotein (H77 isolate)and contains four N-linked glycosylation sites (H77 isolate)[56,57] and 8 cystine residues[58]. The TMD of HCV-E1 contains an ER retention signal[59] and a GxxxG oligomerization motif that is required for the formation of the HCV-E1E2 heterodimer[60]. Structural data for HCV-E1 is limited since this protein is susceptible to rapid proteolytic degradation in mammalian expression systems and requires HCV-E2 for stabilisation[61,62]. Additionally, confirmation-sensitive antibodies towards HCV-E1 are rare[63]. Due to this challenge, bioinformatic analysis was used to predict the structure of HCV-E1 which suggested that it forms a classical truncated class II fusion protein structure similar to those found in Flaviviruses and Alphaviruses[64]. However, a crystal structure of residues 192-271 has been resolved and was found to have structural homology with human phosphatidylcholine transfer protein[65]. A putative fusion peptide at residues 272-285 (Figure 1.2B) suggests

that membrane fusion may be mediated by this protein[65–67]. A similar role has been suggested for *Pestivirus* E1[68]. Finally, HCV-E1 homo-trimers have been reported to be incorporated into the mature virus particle[69]. The formation of homo-trimers is also seen in other viral fusion proteins such as the SARS-CoV2 spike protein (class I), VSV-G protein[70] (class III) and the post fusion arrangement of class II fusion proteins such as RV-E1[71]. Taken together this research suggests that HCV-E1 may represent a novel class of fusion protein.

The E2 protein consists of residues 384-746 of the HCV polyprotein (H77 isolate) and is the larger of the two envelope proteins. The E2 contains up to 11 glycosylation sites depending on the genotype and has three regions of high sequence variability these are the N-terminus region HVR-1[72] (residues 384-410), the HVR-2[73] (residues 450-485) and the C-terminal IgVR[73] (residues 570-581) (Figure 1.2A). The HCV-E2 protein contains multiple linear and discontinuous antigenic domains, which have varying nomenclature and are referred to as domains A-E[74,75], AR1-3[76] and Epitopes I-III[77] (Figure 1.2A). In addition to these domains, AR4 and AR5 regions are present on the HCV-E1E2 heterodimer[76].

Crystallisation of the E2 protein was challenging due to the presence of multiple glycans and the propensity of this protein to form heterogeneous crystals. As a result of this, early structural predictions were based on existing data for the E protein of Flaviviruses[78,79]. However, crystal structures of truncated HCV-E2 core have shown that the protein consists of a central immunoglobulin-like β-sandwich that is

flanked by α-helices[80–82] which form a front and back layer (Figure 1.2B). This arrangement is structurally analogous to domain III of Flavivirus E protein and Alphavirus E1 proteins (Figure 1.2B). The absence of a fusion peptide in HCV-E2 further supports the role of HCV-E1 in mediating viral membrane fusion. Thus, these two proteins likely work in conjunction, with HCV-E2 initiating cell entry via attachment and HCV-E1 completing this process with the membrane fusion event. At the time of writing this mechanism is unique to HCV, thus the HCV-E1E2 heterodimer may represent a novel class of viral fusion protein. A recent preprint study, Torrents de la Peña *et al*., has provided the first resolved structure of the complete HCV-E1E2 in complex with AR4A, AT12009 and IGH505 antibodies[83]. This structure does not fit the current classes of viral fusion protein, further supporting the argument for HCV-E1E2 to be allocated to a novel class.

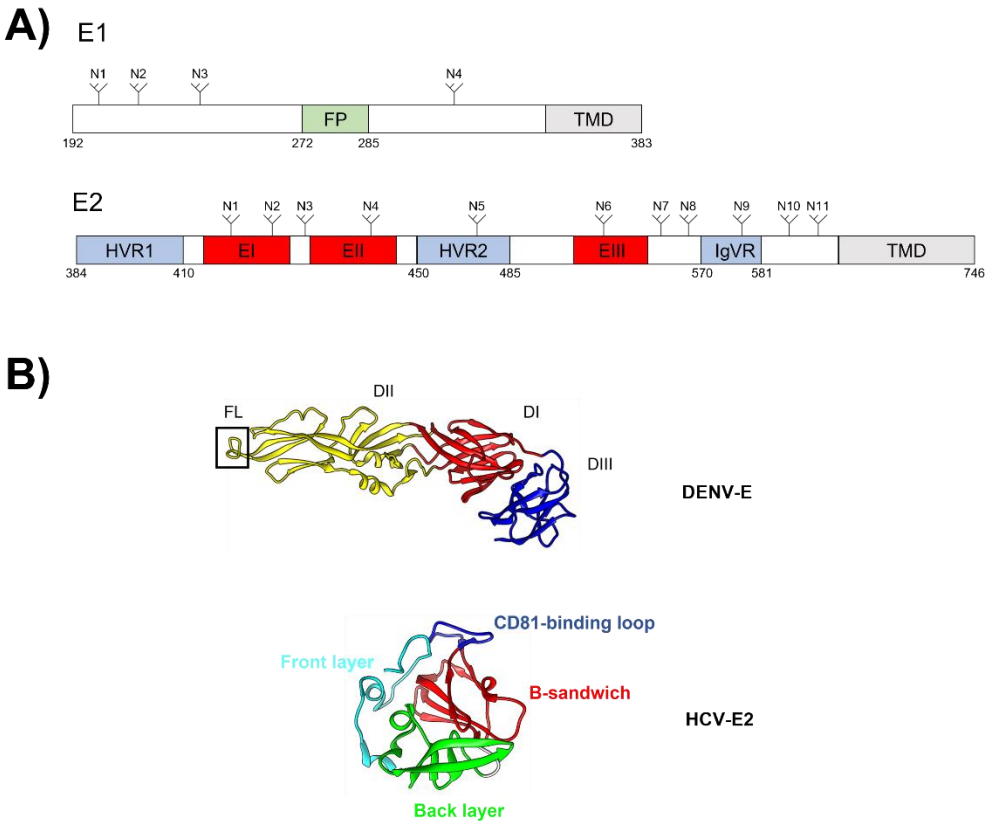

Figure 1. 2 The Hepatitis C Virus envelope glycoproteins.

A) Schematic representation of HCV-E1 and E2 envelope glycoproteins. HCV-E1 contains a putative fusion peptide (FP) and four glycosylation sites (N). HCV-E2 contains three variable regions, hypervariable region (HVR) 1 and 2, and an intergenotypic variable region (IgVR) along with three linear epitopes (EI-III) and 11 glycosylation sites. Both proteins contain transmembrane domains (TMD). The numbering system is relative to the H77 isolate polyprotein. B) The determined crystal structure of truncated HCV-E2 (PDB 6MEH) with labelled regions. For comparison, the crystal structure of DENV-E (1OKE) is displayed, showing the three domains (DI-III). The tip of DII contains a fusion loop (FL).

1.2.3 Non-Structural Viral Proteins

HCV encodes seven non-structural proteins which have roles in virus assembly and genomic replication. The p7 protein belongs to a family of ion channel forming viral proteins called viroporins which also includes

the influenza protein, M2[84] and the HIV protein, Vpu[85]. p7 is 63 amino acids long and is liberated from the HCV polyprotein via host signal proteases[86]. This protein has two TMD regions which span the ER membrane with both N and C termini located in the luminal side[87] and a positively charged cytoplasmic loop with conserved dibasic motif at residues 33 and 35[88], that is critical for activity[89]. p7 monomers oligomerize to form heptamers[90] which act as cation channels[91,92]. Although not required for viral RNA replication, p7 is essential for the production and release of virus particles[93–95] and the establishment of infection *in vivo*[96].

The NS2 protein has a hydrophobic N-terminus with three TMDs[97] and a cytosolic C-terminal that contains a cysteine protease which mediates cleavage of the NS2/NS3 junction[98]. Proteolytic activity requires the formation of NS2 homodimers in which the C-termini form a cysteine protease with two composite active sites each formed by the residues His143 and Glu163 of one monomer and Cys184 of the second monomer[99]. Cleavage of the NS2/NS3 junction is essential for the life cycle of HCV[95], however NS2 is not required for the replication of viral RNA since subgenomic replicons encoding NS3-NS5B are capable of replication[100]. The first TMD region appears to have an important role in the production of infectious virus particles since HCVcc intergenotypic chimeras produce significantly higher titres when NS2- TMD1 is genotype matched with the C-p7 region[101].

NS3 is a multifunctional protein that contains the second autoprotease of the HCV polyprotein, responsible for the cleavage of NS4A, NS4B,

NS5A and NS5B. Structurally, the NS3 protease forms a trypsin-like fold with residues His-57, Asp-81 and Ser-139 forming the active site[102,103]. Activity of the NS3 serine protease also requires NS4A as a cofactor[104–107]. The C-terminal helicase domain functions to unwind viral RNA and functions independently of the NS3 N-terminal protease[106].

NS4A is 54 amino acids in length with a N-terminal TMD followed by a region that interacts with the N-terminus of NS3[108]. The C-terminus of this protein contains and a region rich in acidic amino acids which aides viral assembly and envelopment through interactions with the E1 glycoprotein[109].

The NS4B protein is involved in the formation of the replication complex[110]. This protein is predicted to have four transmembrane domains with both N and C termini regions located on the cytosolic side[111]. The N-terminus contains two amphipathic α-helices which are required for oligomerization[112,113] and results in the formation of the membranous web[114]. The C-terminal domain contains a nucleotide binding motif which suggests that this protein tethers HCV RNA to the replication complex[115,116].

NS5A is a phosphoprotein[117] that consists of an N-terminal membrane associated amphipathic α-helix followed by three structural domains[118]. Domains I and II are required for RNA replication whereas domain III has roles in the assembly of the virus through interactions with the HCV core protein[118].

The NS5B protein is a 66KDa RdRp that consists of 591 amino acid residues located at the C-terminus of the HCV polyprotein. Residues 1-531 form the functional catalytic domain which is anchored to intracellular membranes by a C-terminal TMD[119]. The catalytic region forms subdomains termed fingers, palm and thumb[120]. Residues 1-139 form the fingers domains, the palm domain contains the active site and is discontinuous and made up of residues 188-225 and 287-371, the thumb region stems residues 371-529[120]. *In vitro*, NS5B is capable RNA polymerisation, in the absence of viral and host derived factors[121]. However, *in vivo*, NS5B forms part of the viral replication complex[122].

1.2.4 Structure of the Hepatitis C virus virion

HCV virions are approximately 70-100 nm in diameter and exhibit a high level of structural heterogeneity[123,124]. This is in contrast to members of the *Flavivirus* genus which show highly ordered structures that are approximately 50 nm in diameter and have a symmetrical icosahedral shape[125]. The HCV virion is also associated with host-derived ApoE, B and I proteins[123,124,126–128]. In addition to this, density gradient separation has shown that HCV has a buoyant density of 1.10 g/mL which is lower comparted to other envelope viruses and similar to the density of VLDL [129–131].

1.2.5 Hepatitis C virus Life Cycle

The life cycle of HCV is similar to that of other enveloped RNA viruses which consists of six stages; attachment, entry, genome replication, translation, assembly and release.

The attachment of HCV virion to the membrane of the host cell is achieved through multiple mechanism. One route involves the binding of virus-associated ApoE protein to cell surface heparin sulphate, particularly syndecan-1[132] and syndecan-4[133]. The importance of ApoE in HCV attachment has been shown experimentally, demonstrating that anti-ApoE antibodies can neutralise HCV entry[134] and the addition of ApoE supplements to HCVcc cultures enhances infectivity[127]. HCV-E2 has also been shown to bind cell surface heparan sulphate suggesting that this protein also contributes to viral attachment[135]. Attachment can occur through interactions between virus-associated phosphatidylserine and the cell surface receptor, TIM-1[136].

Once the virion is attached to a permissive cell the entry process is initiated. This process is mediated by the HCV-E1E2 heterodimer and to date four essential host factors have been identified for the HCV entry pathway; CD81[137,138], SR-B1[139], Occludin[140,141] and Claudin[142]. The first stage of entry occurs through the binding of the HVR1 region of HCV-E2 with SR-B1[139]. This interaction induces a conformational change in E2 from a ‘closed’ to an ‘open’ state[143] that exposes the HCV-E2 core and the CD81 binding loop (residues 519-535) allowing for interactions with CD81[80]. This sequence of events is supported by the finding that HCV-E2 mutants harbouring a deletion of the HVR1 region exhibit a higher binding affinity for CD81[144]. Furthermore, despite the high sequence variability, HVR1 sequences maintain similar basic residues suggesting that this feature is required for a role in entry[145]. The formation of the HCV-E2-CD81 complex triggers the recruitment of

claudin and leads to clathrin-dependent endocytosis[146]. The formation of the endosome is followed by a pH decrease which triggers a conformational change to the HCV-E1E2 that leads to membrane fusion[147]. As discussed previously, this mechanism is currently unknown.

Membrane fusion leads to the uncoating of the virus particle and release of the viral genome into the cytoplasm[148]. Translation of the HCV genome occurs in a cap-independent manner via the IRES located at in the 5'-UTR which interacts with the 40s subunit[149–151]. Viral genome replication and translation is enhanced by the host derived miR-122, which is abundant in hepatocytes, representing approximately 70 % of all miRNAs within the liver[152]. The miR-122 binds to the 5' UTR of the viral RNA[153], protecting it from degradation[154]. Expression of viral proteins induces a rearrangement of internal lipid membranes to form a ER derived membranous web which contains both single and double membranous vesicles[114]. This change is mediated primarily by the NS5A and NS4B proteins[155]. DMVs provide the site for the formation of the replication complex in which viral genomic RNA is replicated from a negative RNA template[156].

Virus assembly and budding occurs at the ER. The structural proteins are liberated from the HCV polyprotein via host signal proteases with the ectodomains of the E glycoproteins being translocated into the ER lumen where they undergo folding and form intramolecular disulphide bonds, aided by the chaperone protein calnexin[157]. Formation of the HCV-E1E2 heterodimer also occurs at the ER and the TMD regions of

these proteins are essential for this process[158]. The structural proteins are essential for the assembly and budding of HCV virions this occurs at the ER[131,159] and is tightly linked to VLDL lipid droplet synthesis[160]. Mature infectious HCV particles have been isolated from the ER lumen and COPII vesicles[161], suggesting that following budding, HCV is exported via the Golgi secretory pathway[161].

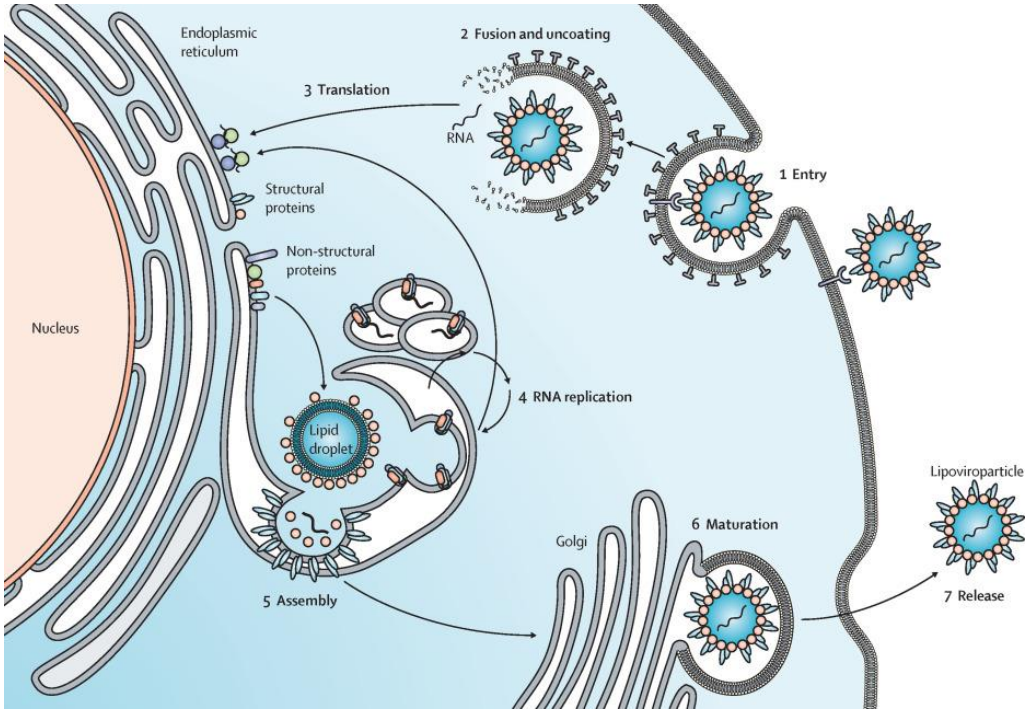

Figure 1. 3 Life cycle of HCV diagram.

Life cycle of HCV diagram, indicating the endosomal entry mechanism, replication in ER invaginations, and budding of new particles through the ER-Golgi membranes. Adapted from Mina *et al*[162].

1.3 Host Immune Responses to the Hepatitis C Virus

1.3.1 Innate Immune Responses

Innate immunity is the first line of defence against a pathogen and the liver provides a unique environment that is enriched with NK cells, Kupffer cells, macrophages and hepatic stellate cells which mediate

innate immune responses[163]. The innate response is initiated by the recognition of PAMPS which are present on viral proteins and RNA. The HCV-E1 and HCV-E2 glycoproteins are virion-associated PAMPS that are recognised by the soluble PRRs such as MBL[164] and L-ficolin[165], and membrane associated PRRs such as DC-SIGN[166]. Intracellular viral PAMPs are located on viral proteins and genomic RNA and are detected via TLRs, NLRs and RLRs[167,168]. Interaction of PRRs and PAMPs trigger signal cascades in innate cells which leads to the production of proinflammatory cytokines IL-1β, IL-18 and type I and type III IFNs[169]. The production of IFNs results in the upregulation of ISGs that establish an antiviral response[170]. However, during HCV infection, viral proteins such as HCV-C, E2, NS5A and the NS3/4A serine protease can inhibit signal cascades leading to reduced expression of ISGs[171–174], providing an opportunity for the virus to evade the innate response and establish a prolonged infection.

Innate immune responses also play a role in SVC. An important example of this is the type III IFN gene *IFNλ4* which exhibits a SNP, referred to as SNP rs12979860. Individuals with a C/C genotype at this SNP achieve significantly higher rates of SVC compared to other genotypes with approximately 50 % of cases clearing HCV[175,176]. In addition to this, the NK cell inhibitory receptor, KIR2DL3 and its HLA-C1 ligand are associated with SVC[177,178]. This results from a reduced inhibition of NK cells, allowing cytotoxic activity towards infected cells[179].

1.3.2 Cell-mediated Immunity

Cell mediated immune responses are one arm of the host adaptive immune response and are mediated by T cells. During viral challenge CD4+ Th cells and CD8+ CTLs perform major roles in controlling infection. These subsets of T cells have distinct functions with CTLs mediating the destruction of virus-infected cells through the recognition of MHC-I restricted viral epitopes that are presented on the surface of infected cells[180]. In contrast to this Th cells recognise MHC-II restricted viral epitopes which trigger the release cytokines such as IFN-γ, which aid the CTL response and the establishment of memory T cells[181–183]. The regulatory roles of Th cells are numerous and a subset of this population, T_{FH} cells, have been shown to aid activation of B cells[182], highlighting their involvement in the establishment of the humoral response.

In the context of HCV infection, cytolytic CTLs and Th cell responses are associated with disease outcome[184]. HCV-specific T cells can be detected during acute infection from week 12 and target epitopes on both non-structural and structural HCV proteins[185]. In patients that progress to chronic infection, the HCV-specific Th cell population collapses[186]. CTLs become exhausted due to prolonged antigenic stimulation[187] and dysfunctional resulting in a reduction in proliferation, loss of cytolytic activity and continued secretion of IFN-γ[187]. This dysfunction is sustained following successful clearance of HCV following DAA treatment[188]. The CTL response can also become ineffective due to the evolution of escape mutants[189]. Circulating T_{FH}

cells persist during chronic infection and migrate to the liver[190]. One study found that limited activation of T_{FH} cells was associated with a delayed expansion of antigen specific memory B cells[191]. Upon viral elimination with DAAs these cells exit the liver and appear to remain functional, suggesting that this population could be a useful target for a vaccine candidate[190,192].

The role of cell mediated immunity in SVC of HCV was initially shown using antibody-mediated depletion of CD4+ Th cells and CD8+ CTLs in Chimpanzees challenged with HCV[193,194]. Blockade of these responses resulted in a failure to control the acute infection[193,194]. Examination of human cellular responses have shown that the generation and persistence of broad HCV-specific CD4+ T cell are associated with SVC[195,196]. Salinas *et al.,*[191] showed that expansion of activated T_{FH} cell during early acute infection was coupled with the early appearance of anti-HCV-E2 memory B cells and the production of bnAbs in acute infections that achieved SVC. Together this shows that cellular immunity plays a key role in SVC and provides an insight into rational vaccine design.

1.3.3 Humoral Responses

The humoral response plays a major role in combatting viral infections. This response is mediated by B cells which become activated following exposure to an antigen and develop into ASCs or alternatively become MBCs which can be recalled following repeat exposure to the pathogen[197,198]. There are multiple mechanisms by which Abs exert antiviral effects such as Ab-dependent cellular cytotoxicity, Ab-

dependent phagocytosis and complement activation[199,200]. Neutralising Abs directly bind to viruses through targeting epitopes present on the surface proteins which may block attachment and/or membrane fusion of the virus[201,202].

HCV-specific Abs can be detected 4-6 weeks after exposure, and these are dominated by IgG1 and IgG3 subclasses which target both structural and nonstructural HCV viral proteins[203–205]. Titres of HCV-specific IgM and IgA are highly variable and are found in both acute and chronic cases[206,207].

HCV exposure also elicits nAbs which exclusively target the E glycoproteins. The first evidence of nAb responses to HCV was reported by Farci *et al*[208] who showed that heat inactivated human serum isolated two years post-infection was able to neutralise HCV and prevent infection in a Chimpanzee model. The timing of the nAb response is crucial to disease outcome. Chronic infection is preceded by a delay in nAb production during the acute phase[14,209], allowing time for the viral quasispeices to become established and adapt to selective pressures exerted by a humoral response leading to the production of a nAb response that is incapable of clearing the infection[40,210]. Although the nAbs elicited during chronic infection are ineffective at resolving HCV infection, isolated mAbs and polyclonal sera from chronically infected individuals can exhibit cross-neutralising properties *in vitro*[191,211,212].

The presence of nAbs circulating during chronic infection has led to controversy regarding the role of humoral responses in SVC. This has been further supported by reports of seronegative individuals undergoing SVC[213,214], suggesting that clearance was achieved solely through cellular immunity. However, both studies defined seronegative using commercially available ELISA that do not detect the HCV E glycoproteins and thus they provide no information regarding the anti-HCV nAb response in these cases. In a recent study, Mina et al[215] demonstrated that serum from highly exposed, yet seronegative individuals exhibited neutralising activity. Multiple studies have correlated SVC with the rapid production of nAbs[209,216–219]. One study by Walker et al[217] showed that SVC was preceded by the production of nAbs with narrow activity towards the founder virus within the first 100 days of exposure. Additionally, circulating nAbs elicited during acute infection display limited SHM, further supporting the hypothesis that early production of nAbs aid SVC[191,220]. Kinchen *et al.,* developed a plasma deconvolution method to assess the types of circulating antibodies and found that SVC was associated with the generation of AR3 and AR4 targeting Abs[218], arguing for the inclusion of these regions in a vaccine.

Further investigation into the B cell responses associated with SVC can highlight the types of Abs that are required for this response and inform rational vaccine design. For example, a recent study using single-cell transcriptomics, identified the V_H3-23 and V_K3-11 families as associated with SVC[191]. Interestingly, these nAbs elicited during SVC show less

SMH compared to circulating nAbs isolated during chronic infection with comparable neutralising breadth[191]. In contrast, other studies have found the V_H1-69 gene to be associated with SVC[220,221]. There are also several bnAbs isolated from chronically infected patients that utilize the V_H1-69 gene[76,191,220,222,223]. Usage of the V_H1-69 gene has been reported for potent antiviral nAbs against influenza and HIV[224].

Taken together these findings show that humoral immunity contributes to SVC and provides a goal for HCV vaccine design. Thus a vaccine should induce bnAbs that target AR3 and AR4 regions and engage B cell lineages that utilize V_H genes associated with SVC.

1.4 Models for Hepatitis C virus Infection

The use of models that simulate viral infection using both *in vitro* and *in vivo* methods are essential for the assessment of vaccine candidate efficacy. *In vitro* models allow for the detection and characterisation of nAb responses in vaccinee sera. *In vivo* models are essential for the validation of vaccine efficacy and safety.

1.4.1 *In vitro* Models

Early attempts to culture HCV *in vitro* from infected human serum were hindered due to low viral titres[225]. This issue was overcome with the isolation of a Gt2a strain, JFH-1, which was unique in its ability to produce high titres of virus when cultured in human hepatocytes[225]. Importantly, JFH-1 derived chimera can be generated in which the 5' core-NS2 region can be replaced with sequences derived from foreign HCV isolates to produce intergenotypic and intragenotypic chimeras[226].

Interestingly the chimera Jcl, derived from $J6_{C\text{-}NS2}$, a gt2a isolate produces up to 1000-fold higher virus titres compared to full length JFH-1 cultures[101]. The generation of chimeras allows for genetically diverse panels of HCV isolates be used to measure nAbs responses elicited by vaccine candidates.

The production of HCVcc requires the isolation of a cDNA clone of the viral genome inserted into a plasmid and placed downstream of an RNA polymerase promoter and upstream of a restriction enzyme site[227]. Bacteriophage RNA polymerase enzymes, SP6 and T7 are typically used in reverse genetic systems, however the T7 enzyme is preferred since it has a higher fidelity rate compared to SP6[228]. The plasmid is linearized by restriction digest and then used as a template for *in vitro* transcription to produce positive RNA transcript run offs. These transcripts are then transfected into permissive cells which are then grown. Confirmation of HCVcc release is typically achieved by serial dilution of the transfected cell supernatant which is then used to infect a permissive cell line which are then stained for the NS5A protein 3 days post infecton[229]. HCVcc methods have been further improved with the selection of permissive cell lines such as the Huh 7.5 cell line[230] which produces greater titres of HCVcc as a result of a mutation which inactivates RIG-I[231]. The advantage of this method is that virus cultures can be established with a known ancestor and any cell culture adaptation mutations can be monitored. However, a disadvantage of the HCVcc model is the need for a BCL-3 laboratory setting, limiting their use to research groups with this resource.

Retroviral pseudotype methods have been established for a wide variety of viruses[232]. This technique utilises the ability of the retroviral Gag protein, from HIV or MLV, to assemble and bud to produce an enveloped particle. Co-expression of foreign viral envelope glycoproteins leads to the incorporation of these proteins into the membrane of the retroviral particle. This results in a retroviral particle with a tropism determined by the foreign viral envelope protein. Furthermore, co-expression of a reporter gene flanked by the retroviral genome packaging signal results in incorporation of reporter-encoding RNA into the PP. Entry of the PP into targets cells is therefore directly proportional to the reporter signal detected in the target cells post-infection. HCVpps have been successfully produced using both MLV[233] and HIV[234] derived packaging systems and show comparable antigenic properties to the HCVcc model[235]. One advantage of this system is that HCVpp are replication-deficient and thus can be produced in a BSL-2 setting, allowing research to be performed in the absence of a BSL-3, HCVcc system. Furthermore, both MLV and HIV derived HCVpp systems can incorporate patient derived HCV-E1E2 glycoproteins which has led to the generation of large panels of HCV-E1E2 isolates that have been characterised using well defined neutralising monoclonal antibodies and patient derived sera[236–238]. The establishment of the patient-derived panels provides a useful tool to assess the efficacy of vaccine candidates. However, at the time of writing there has been no universally agreed standard panel of HCV isolates to assess vaccine efficacy. This contrasts with the field of HIV vaccine research in which

has adopted a HIVpp panel consisting of 109 isolates that was divided into tiers of neutralisation sensitivities[239]. The use of such panels allows for the detailed assessment of neutralisation breadth elicited by a vaccine candidate.

1.4.2 *in vivo* Models

Initially, *In vivo* studies of HCV relied experimental challenge of Chimpanzees which is the only non-human species that are permissive to HCV infection[240]. Use of this model species has recently been halted due to a moratorium on their use in research. Alternative approaches to the Chimpanzee model has been the generation of chimeric mice[241–244]. One such model involves the transplantation of human hepatocytes into young uPA$^{+/+}$-SCID mice resulting in humanized livers that are permissive to HCV infection[241,242]. Another method has been to produce transgenic mice that express human CD81 and OCLN which permits HCV infection and that can become chronic[243,244]. These models have limitations such as using immunocompetent mice, the absence of pathological marks such as cirrhosis and are technically difficult to produce[245]. Additionally, the murine B cell response to HCV-E2 differs to that from humans in that the former produces antibodies skewed towards linear epitopes rather than discontinuous epitopes[246].

An attractive approach to evaluating HCV vaccine candidates is to use closely related *Hepacivirus* species as a model. This approach would allow the testing of a vaccine approach in the context of a natural infection, which cannot currently be achieved for HCV. The closest relative of HCV is the EqHV which can be used to experimentally infect

horses[247]. Alternatively, RHV has been proposed as a model for HCV infection[248]. One clear advantage of utilizing RHV over EqHV is the size and availability of the host organism since rodents are routinely used in biological research. It is important to note the potential limitations that these systems pose. In the case of RHV, the rate of SVC is lower compared to HCV in humans[248] and certain laboratory breeds of rats do not appear to mount a CD8+ CTL response to RHV[249]. Given the importance of SVC and CTL responses in HCV infection the absence of these factors in this model could hinder vaccine research. In the case of EqHV, SVC rates are approximately 60% within two months of infection[250] which is greater than SVC rates of HCV. This discrepancy should be considered when testing vaccine efficacy since the EqHV model could overestimate vaccine efficacy of HCV candidates in humans.

1.5 Approaches to Hepatitis C Virus Vaccine Design

1.5.1 Inactivated Whole Virus

Inactivated virus vaccines have been successfully used for Rabies virus[251], Polio virus[251] and Tick-borne encephalitis[252], a Flavivirus species. Inactivated vaccines are highly immunogenic since they present the virus in a near native confirmation. However in some circumstances the inactivation process can distort epitopes[253,254]. The improvements in HCVcc methods have led to inactivated whole HCV vaccines being investigated[255–257]. These studies have shown that immunisation of mice[255,257] and marmosets[256] with whole inactivated HCVcc derived from a single isolate can elicit bnAb. Pihl *et al*.,[257] found

that the immunogenicity of these particles was increased when administered with the Addavax adjuvant, an analogue of the MF-59 adjuvant has been licenced for human use. Whilst the humoral response to inactivated HCV has been reported, there has been limited data on the cellular immunity following immunisation. Yokokawa *et al*.,[256] showed that IFN-γ expression was greater in spleen cells harvested from marmosets immunised with HCVcc and the K3-SPG adjuvant compared to an Alum adjuvant. Given these results and the continued improvements in HCV purification methods[258,259], it is likely that this candidate will continue to be investigated.

1.5.2 Recombinant Subunit Vaccines

Subunit vaccines are attractive approaches to vaccine design since they have been successfully used for a range of vaccines[260]. To date HCV subunit vaccines have focused on targeting the HCV envelope proteins to elicit a nAb response. Indeed, the first HCV vaccine candidate to reach phase I clinical trials was a subunit vaccine candidate which consisted of full length recombinant expressed E1E2 (rE1E2) derived from the Gt1 reference isolate, HCV-1[261]. In an initial vaccine study, seven chimpanzees were immunised with rE1E2 and subsequently challenged with the homologous HCV-1 strain[262]. Five Chimpanzees exhibited sterilising immunity upon challenge whilst two acquired acute infections that were subsequently cleared[262]. This vaccine candidate was trialled in healthy human volunteers who received 4 µg, 20 µg or 100 µg does of rE1E2, administered with the MF59 adjuvant[261]. Importantly, this vaccine was found to be safely

tolerated in humans which is encouraging since any B-cell targeting HCV vaccines will require these proteins. Immunisation with rE1E2 elicited both HCV-specific humoral and cellular responses with polyfunctional $CD4^+$ T cells being detected and isolated sera exhibiting HCV neutralization activity[261,263]. Further characterisation of the humoral responses using competition ELISA assays showed that circulating nAbs effectively competed for AR3, AR4, AR5, AS412 and the E1 epitope recognised by the IGH526 antibody[264]. An additional study further tested the neutralising breadth of the 13 vaccinee serum samples against a panel of HCVcc isolates from Gt 1-7[265]. When tested as single point 1:50 dilutions, 12 of the 13 sera samples exhibited neutralising activity towards H77 (Gt1a) of which five showed > 50% neutralisation and two showed >80% neutralisation[265]. The three highest neutralising sera samples were further tested against a panel of different genotypes with two samples exhibiting neutralising activity towards all genotypes although the level of neutralisation was variable[265]. Take together these results demonstrate that immunisation with a monovalent rE1E2 vaccine can elicit broadly cross-reactive nAbs in humans, however, the level of neutralising activity was variable between vaccinees.

Despite the encouraging results of the rE1E2 candidate, a major issue for this vaccine was producing enough for commercial scale up. Purification of rE1E2 from CHO cell lysate was performed via lectin based affinity chromatography which was low affinity and co-purified other host cell derived proteins[266]. To circumvent this problem

alternative truncated envelope subunit vaccines have been investigated. One such approach has been to investigate sE2 constructs which have been shown to elicit bnAbs in mice[267]. In addition to this rational design of sE2 lead to the $sE2_{\Delta 123}$ construct in which HVR1 was deleted and HVR2 and IgVR were replaced with G/S linker sequences to focus the immune response to conserved neutralising epitopes[268]. When expressed in mammalian cell culture systems this construct was secreted from transfected HEK-293 cells and SEC analysis showed the presence of mono, dimer and two high molecular weight aggregates, HMW1 and HMW2[268]. Interesting HMW1 fractions elicited the highest anti-HCV-E2 titres compared to mono and dimer[268].

Investigation of sE2 vaccines has shown that truncation of E2 may yield a protein that is sufficiently folded to elicited conformational nAb response[268]. However, a disadvantage of sE2 is that this approach neglects the targeting of AR4 and AR5 which require the formation of the HCV-E1E2 heterodimer[76]. Since mAbs targeting these regions appear to be highly cross neutralising their inclusion in a subunit vaccine would be warranted. Recently there have been multiple efforts to generate sE1E2 constructs. In one approach the expression and immunogenicity of truncated sE1E2, sE2E1 and sE21E was assessed[269]. In this study the TMD of each protein were removed and a linker sequence was inserted. Interestingly the sE21E construct used an inverted HCV-E1 sequence to correct the orientation of HCV-E1 relative to HCV-E2, thus mimicking the arrangement of these proteins in the heterodimer. These constructs were successfully expressed and

secreted by transiently transfected HEK-293t cells and showed reactivity to conformationally sensitive antibodies[269]. However there was no reactivity to AR4A or AR5A antibodies showing that this approach was unable to form these antigenic regions[269]. Other attempts include the insertion of a Fc-tag between the ectodomains of HCV-E1 and HCV-E2 which was compared to rE1E2 in mice and elicited autologous nAbs towards pseudotyped H77 (Gt1a) and heterologous neutralising activity towards SA13 (Gt5a) with similar results[266]. Purification of Fc-tagged proteins has been well documented and is performed regularly at a commercial scale for therapeutic Abs using protein A and/or protein G resins, it's inclusion in an HCV vaccine would therefore aid the upscale process of this candidate. A more recent study reported that insertion of a leucine zipper sequence and a furin cleavage site between the ectodomains of HCV-E1 and HCV-E2 yielded a secreted HCV-E1E2 heterodimer that was recognised by conformation sensitive antibodies, including AR4A and AR5A[270]. This candidate was also shown to elicit similar autologous nAb titres compared to rE1E2 when tested in mice[270]. Given that these reports of sE1E2 are recent it is likely that work is currently being performed to further investigate their use a potential vaccine candidate.

1.5.3 Viral Vector Vaccines

Viral vectors can be used to mediate expression of a target antigen within host cells following immunisation. The intracellular expression of the target antigen results in potent CTL responses[271]. Given the importance of CTL responses HCV SVC, this approach has been

investigated for HCV T-cell targeting vaccines. To date, particular attention has been focused on HuAd6, ChAd3 and MVA derived viral vectors for HCV vaccines[272,273]. In a phase I vaccine trial, a heterologous prime boost of ChA3 and MVA encoding HCV NS3-NS5B of a Gt1b isolate[273]. The encoded NS5b gene was inactivated through mutagenesis and referred to as NSmut[274]. Cellular responses were elicited towards all encoded HCV proteins upon immunisation with ChAd3 -NSmut and these responses were enhanced following a single boost 8 weeks post with MVA-NSmut[273]. This strategy was also tested as a prophylactic vaccine in chronically infected individuals and was found to have limited impact, with a poor CD4+ T-cell response and limited vaccine induced CD8+ T cells[275]. Recently a phase I/II trial was concluded in which the ChAd3-NSmut and MVA-NSmut vaccines were administered to healthy individuals identified as at risk for HCV infection[276]. Whilst this regime failed to prevent chronic infection in vaccinees, there was an observed reduction in viral RNA[276]. This result highlights the need to elicit both cellular and humoral responses in order to control HCV infection.

1.5.4 Virus-Like Particles

VLPs are an attractive approach to vaccine deign as provide a structure that is representative of the native virus whilst lacking a genome and thus both immunogenic and safe[277]. VLPs offer superior immunogenicity compared to subunit vaccines[278] which results from the ability of these structures to drain into lymph nodes ,provide greater

immune cell activation and the presence of multiple PAMPs[277]. To date there are two VLP based vaccines used in humans, HPV and HBV.

HCVLPs were first described by Baumert *et al.,*[279] which were expressed in the SF9 insect cell line that had undergone transduction with a recombinant baculovirus encoding HCV C-E1-E2. HCVLPs were found to accumulate in cytoplasmic vesicles which could be liberated through cell lysis[279]. Further research showed that these VLPs were immunogenic in both mice and baboons[280,281]. More recently, HCVLPs have been revisited and produced using the human hepatoma cell line, Huh 7[282]. These cells were transduced using an adenovirus vector encoding HCV C-E1-E2, and intracellular HCVLPs were harvested following mechanical lysis of the producer cells[283]. These particles have been extensively characterised and show similar morphology to native HCV particles[126,284]. Early vaccine studies showed that immunisation with H77 derived VLPs induced cross reactive Nabs in mice[282]. This work was further developed by generating VLPs derived from Gt1b, 3a and 2a, that were then pooled to make a multi-valent vaccine[285]. This cocktail of VLPs was reported to induce nAb responses in both mice and pigs[285,286]. It should be noted however that whilst these results were described as cross reactive, the neutralisation assays performed were against autologous vaccine strains. To fully assess the neutralisation breadth elicited by this multi-valent vaccine, the sera collected from the vaccinated animals should be tested in an *in vitro* neutralisation assay against a panel of HCV isolates that cover a range of neutralisation sensitivities[238,287]. Finally, it is worth noting that the producer cells for

this vaccine candidate are not suitable for the production of human vaccines since Huh 7 cells are hepatoma cells[288] therefore this candidate would require validation in a cell line that has been approved for human vaccine production.

1.5.5 Chimeric Virus-Like Particles

Chimeric VLPs offer an opportunity to exploit the VLP forming ability of one viral species, to present the epitopes of a foreign virus and thus direct an immune response to these regions[289]. This approach requires the fusion of foreign targets to viral structural proteins to result in incorporation of the target in the VLP. As such this technique is limited to VLP systems that are structurally flexible and can tolerate the presence of the vaccine target.

The HBVsAg is a transmembrane protein that readily forms VLP structures when expressed in a recombinant system[290,291]. This system is the basis of commercial HBV vaccines. HBVsAg contains a hydrophilic loop that is targeted by HBV nAbs and this region may be replaced with foreign epitopes without compromising VLP assembly. Linear epitopes of HCV have been inserted into this region and found to be immunogenic in mice[292,293]. In addition to this, both full length HCV-E1 and HCV-E2 proteins can be incorporated into HBVsAg particles[294]. Immunisation with these particles elicited cross neutralising antibodies in rabbits [294–296]. In a recent study, a related virus, DHBV, was used to generate chimeric VLPs presenting the $sE2_{\Delta 123}$[297]. DHBV was shown to incorporate $sE2_{\Delta 123}$ into VLPs which were reactive to conformation sensitive anti-HCV-E2 antibodies[297]. Immunisation of guinea pigs with a

dose of VLPs equivalent to 10 µg of HCV-E2, elicited nAbs in 4/8 animals with 3 generating nAbs that could neutralise HCV isolates from Gt1-7[297]. These results show that the B cell response in guinea pigs was inconsistent and will require dosage optimisation to improve. In addition, there was no comparison between the immunogenicity of soluble $sE2_{\Delta 123}$ and VLP-associated $sE_{\Delta 123}$. A head-to-head comparison of these vaccines would be useful to further asses the performance of DHBV as a vaccine platform. The use of DHBV may be advantageous, since pre-existing immunity to HBV could impact the efficacy of HBV-derived chimeric vaccine platforms[297].

1.6 Introduction to the Rubella Virus

RV is a positive sense ssRNA virus that exclusively infects humans and is the causative agent of rubella[298], a mild childhood disease that is commonly referred to as German measles. As a respiratory virus, transmission of RV occurs via aerosolized respiratory droplets which are inhaled and establish an infection in the upper respiratory tract[299]. Infection with RV can be asymptomatic or result in mild symptoms which include a maculopapular rash and swollen lymph nodes[299].

RV is a public health concern because of its teratogenic properties which arise when infection occurs during pregnancy leading to infection of the developing foetus and the establishment of CRS[299]. During CRS, RV undergoes replication in a wide range of foetal organs resulting in severe damage that leads to birth defects[299]. Common birth defects caused by CRS are cataracts, congenital heart disease, hearing defects and overall delayed growth of the feotus[299–301]. Outcomes of CRS are

dependent on the time of infection, with the most severe outcomes arising from infection during the first trimester of pregnancy[299].

1.6.1 Classification and Genetic Diversity

RV is a member of the *Rubivirus* genus which belongs to the *Matonaviridae* family. Until recently, the *Rubivirus* genus was classified in the *Togaviridae* virus family along with the *Alphavirus* genus based on similar virion structure of ssRNA genome size[302], prior to the sequencing of the RV genome[303]. Phylogenetic analyse of the RV genome showed that this species shared greater sequence homology with members of the *Benyvirdae* and *Hepeviridae* virus families than members of the *Alphavirus* genus[304], thus arguing for is removal from the *Togavirus* family.

RV was the sole member of the *Rubivirus* genus however advances in metagenomics have led to the identification of a further five species[305–308]. The first of which was the Guangdong Chinese water snake *Rubivirus*, reported in 2018 following a large scale survey of 214 vertebrate species[305]. In addition to this, two *Rubiviruses,* Rustrela virus and Ruhugu virus have been identified in mammalian species in Germany and Uganda, respectively[306]. Interestingly, mammals infected with Rustrela virus were found to suffer acute encephalitis which was absent in infected rodents[306,309].

As a species, RV is divided into two clades, referred to as clades 1 and 2, which share 90 % nucleotide sequence similarity[310]. Clades are further divided into subclades. Clade 1 contains subclades 1a, 1B, 1C,

1D, 1E, 1F, 1G, 1H, 1I and 1J, subclade 1a considered a provisional classification and thus signified by a lower-case letter[311,312]. Clade 2 is divided into subclades 2A, 2B and 2C[311].

1.7 Molecular Biology of the Rubella Virus

1.7.1 Genomic Structure

RV is a positive ssRNA virus with a GC rich 9.6 kb genome that consists of two ORFs, a 5' genomic ORF that encodes a the non-structural proteins p150 and p90[303], and a 3' sub-genomic ORF that encodes the three structure proteins RV-C, E2 and E1(Figure 1.4)[303,313]. The genome is flanked by a 5' UTR and a 3' UTR that encodes a poly A tail[314]. A sub-genomic promoter is located between the two ORFs and is required for the expression of the structural genes[315]. The genome packaging signal resides within the NS-ORF, however packaging requires large regions of this ORF suggesting that genome packaging is dependent upon multiple RNA secondary structures in this region[316].

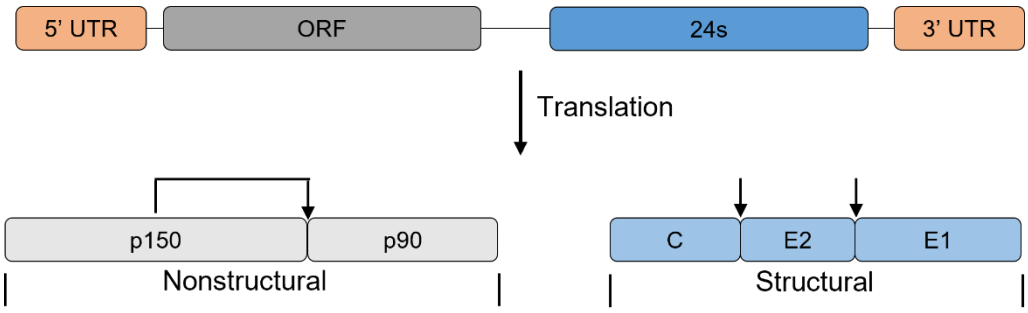

Figure 1. 4 Genome arrangement of the Rubella Virus.

The viral RNA contains a genomic ORF and a subgenomic ORF (24s). Translation of these yields two proteins. The non-structural protein is cleaved by an autoprotease located in the p150 protein. The Structural polyprotein is cleaved by host cell signal proteases.

1.7.2 Structural Proteins

RV-C is 300 residues long with the 22 residues at the C-terminus serving as a RV-E2sp[317]. Following cleavage, the RV-E2sp signal peptide remains attached to RV-C, tethering it to the host ER-membrane. RV-C contains both hydrophobic and hydrophilic regions to allow for both membrane and nucleic acid interactions. RV-C also form disulphide-linked homodimers which are incorporated into the viron[318,319].

RV has two envelope glycoproteins, RV-E2 and RV-E1. The smaller glycoprotein is RV-E2 and consists of 282 residues and is approximately 42-47 KDa[317]. RV-E1 is the larger of the two glycoproteins consisting of 483 amino acid residues and has an approximate molecular weight of 58 KDa[317]. Each of these envelope proteins undergo N-linked glycosylation and it is thought that mature RV-E2 undergoes heterogenous glycosylation since SDS-PAGE separation of this protein shows the presence of a range of different molecular weight isoforms. Both envelope glycoproteins are Type I transmembrane proteins that also have cytoplasmic tails. The transmembrane regions of these proteins are critical for the formation covalently linked RV-E2E1 heterodimers that are required for virus assembly[320].

Currently there is no structural data available for RV-E2. A crystal structure of truncated RV-E1$_{ecto}$ trimers expressed in S2 cells has been reported[71]. These trimers were crystalised at a neutral p*H* and showed that RV-E1$_{ecto}$ has a structure like that of other class II fusion proteins,

with three β-sheet rich domains (Figure 1.5B)[71]. Uniquely, domain II contained two fusion loops at residues 88-93 and 131-137 which were in close proximity to form a fusion surface that was stabilised by a Ca^{2+} ion that interacted with residues N88 and D136[71]. The presence of Ca^{2+} has been shown to be critical for virus infectivity since mutagenesis of one the contact residues is lethal to cell cultured RV[321].

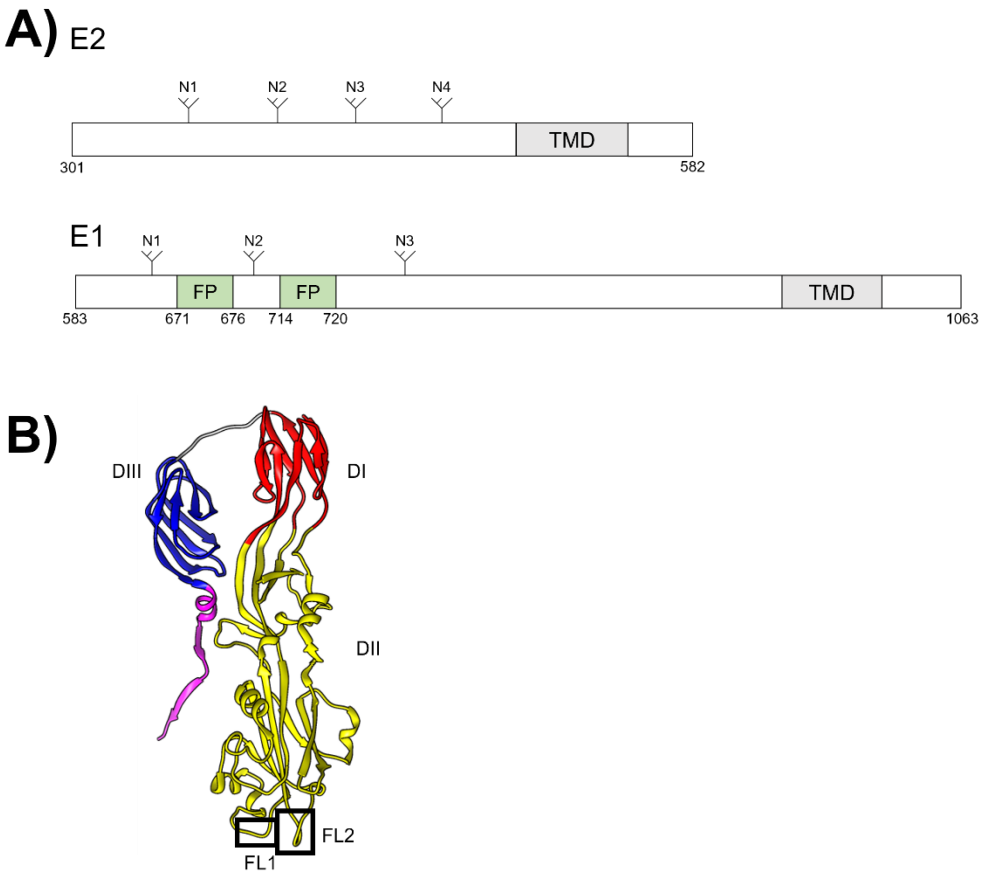

Figure 1. 5 The Rubella Virus envelope glycoproteins.

A) Schematic diagrams of the RV-E2 and RV-E1 glycoproteins. RV-E1 contains three glycosylation sites (N) and contains two fusion loops (FL1 and FL2). RV-E2 contains four glycosylation sites. Both glycoproteins contain a single transmembrane domain (TMD). **B**) Crystal structure of RV-E1 (PDB 4B3V) showing three domains (I-III) and C-terminal stem region (purple). The two fusions loops form a 'fusion surface' at the tip of DII.

1.7.3 Rubella Virus Assembly

Virus assembly occurs in the *cis* Golgi compartment and is mediated by the three RV structural proteins which must converge at the budding site[322]. Since these proteins are initially localised to the ER upon expression a series of trafficking event must occur to reach the budding site. RV-C is tethered to ER membrane via the C-terminal RV-E2sp, this association with an intracellular lipid membrane determines the subcellular localisation of the protein. The cytoplasmic tail of RV-E2 is seven residues long, of which five are arginines. This positively charged domain is required for the localisation of RV-C to the Golgi. Garbutt *et al.,*[320] demonstrated that mutagenesis of three arginine residues to alanine prevent virus assembly and resulted in RV-C being absent from the Golgi. However assembly was not hindered when the arginine residues were replaced with lysine residues, showing that the function of the RV-$E2_{cyt}$ in RV-C localisation is mediated by the positive charge of this domain[320]. This process could be similar to the budding process of *Alphaviruses*, in which a critical interaction between the cytoplasmic domain of E2 and preassembled nucleocapsid is required for budding although the exact driving force for this process remains unknown[323].

Formation of the RV-E2E1 heterodimer is necessary for RV assembly[320]. Heterodimerisation is mediated by the correct folding of the ectodomain and TMD regions since replacement of these regions with analogous regions of other viral envelope proteins prevents dimer heterodimer formation[320,324]. The C-terminus of RV-E1 contains an ER retention signal, since when this protein is expressed in the absence of

RV-E2, it remains in the ER[325]. In contrast, when expressed alone, RV-E2 accumulated at the Golgi due to a Golgi retention signal located in the TMD region of this protein[326]. Formation of the RV-E2E1 heterodimer results in the masking of the RV-E1 retention signal and export of this complex to the Golgi in a COPII-dependent manner[327]. Thus, RV viral assembly is tightly linked to the correct heterodimer formation.

Knowledge of the budding process for RV remains incomplete. It is likely that this process is driven by interactions between the RV-C and the C-termini of the RV-E2E1 heterodimer since RV-C does not undergo budding in the absence of envelope heterodimer. This contrasts with other viruses, for example the Gag polyprotein of retroviruses can drive the budding to form enveloped particles in the absence of a viral glycoprotein[328].

Following budding, RV virions undergo a maturation process in the Golgi lumen. The mechanism for this is currently unknown, however TEM has shown that immature virions have a uniform electron density which is then develop into a distinguishable core structure upon maturation[329,330]. Cyro-EM of mature RV virions has shown that these structures are approximately 90 nm in diameter and are pleomorphic[330]. However, a common feature is the arrangement of anti-parallel rows of the RV-E2E1 heterodimers[330,331].

1.8 Adaptive Immune Responses to Rubella Virus

1.8.1 Cellular Immunity

RV specific cellular responses are observed following natural infection or vaccination[332,333]. This response can be detected approximately seven days prior to the appearance of anti-RV IgG[332]. Mapping studies have shown that all three structural proteins contain MHCII restricted epitopes that stimulate CD4+ T cell proliferation[334–338]. Additionally, the N-terminus of RV-C contains a MHCI restricted epitope[337].

1.8.2 Humoral Immunity

Humoral responses towards RV begin within the first week of exposure with the production of IgM[339,340]. Interestingly, this response differs between natural infection and vaccination, with higher IgM titres observed following infection and vaccination inducing longer lived IgM[339]. RV-specific IgG can be detected within three weeks of exposure[339]. The affinity of circulating anti-RV IgG increases over a period of 3 months following exposure[339] and these antibodies remain detectable for decades. RV-E1 has multiple neutralising epitopes that span residues 202-283 of the protein[341].

1.8.3 Vaccination

Immunity to RV infection is achieved through natural infection or vaccination with the attenuated isolate RA27/3. This strain was developed in 1965 when RV was isolated from the lung tissue of an aborted foetus and subsequently attenuated by serial passage in the human cell line,WI-35, at 30°C[342]. Attenuation resulted in the loss of transmissibility and pathogenicity when administered to vaccinees[342].

Despite the safety of this vaccine, it is currently not recommended for use during pregnancy[341]. In addition there are rare cases of vaccine associated complications such as chronic arthritis[343] and Guillain–Barré syndrome[344].

Today the RA27/3 strain is administered as part of the tri-valent MMR vaccine. MMR vaccination is performed during childhood with the first dose at 1 years old and a second dose at 3 years old[345]. Following the first MMR dose, approximately 95 % of vaccinees are seropositive for RV[345]. The immunity elicited towards RV is long lasting with anti-RV antibodies being detectable in vaccinee sera decades after immunisation[346].

1.9 Applications of the Rubella Virus in Novel Vaccines

1.9.1 Live Attenuated Rubella Viral Vector

The ability of RV to induce long lasting immunity and to be safely tolerated as a vaccine has led to interest in its use as a vaccine platform. Development of a live, attenuated Rubella vaccine vector has been ongoing for the past decade[347–350]. Initial work made use of the previously reported Not deletion[351], a deletion of residues 512-720 of p150 which can be tolerated by RV. With this in mind, Spadaccini *et al.,*[350] demonstrated that this region could be replaced with GFP which was tolerated by RV and led to GFP expression in RV-infected cells. Insertion of foreign viral epitopes within this region can elicit immune responses in mice and non-human primates[347]. RV has also been shown to tolerate insertions of foreign viral epitopes within the RV-24s structural ORF. Insertion of HIV epitopes, fused with the RV-$E2_{TMD}$ are

incorporated into the mature RV virion[348]. This highlights the ability of RV to function as a chimeric vaccine platform and shows that the assembly process of the virus can withstand the presence of foreign viral epitopes.

1.9.2 Rubella Virus-Like Particles

The ability of the RV structural proteins to form VLPs in a genome-independent manner was first reported by Hobman *et al.,*[327]. In this system a cDNA clone of the 24s ORF was transduced into a COS cell line. Following this RVLPs were detected in cell media and electron microscopy showed the presence of VLPs with similar morphology to native RV. In addition these VLPs produce similar anti RV antibody titres in mice compared to native infectious RV virions, showing that RVLPs are immunogenic[322].

1.10 Project Overview and Aims

As previously described, nAb responses directed towards the HCV-E1E2 proteins play a major role in HCV SVC. Therefore, a B cell targeting HCV vaccine should aim to elicit this response. The ability of RV to induce long-lived humoral responses, form VLPs and exhibit structural flexibility made this virus an interesting candidate for a novel chimeric VLP based HCV-targeting vaccine. This project set out to develop a novel Rubella-Hepatitis C (RH) VLP vaccine platform in which the HCV-E1E2 proteins could be presented on the surface of RVLPs. To investigate this approach, the project set out to achieve the following aims:

1. Establish and validate an in-house system for the production and detection of RVLPs. This system would allow for the testing of chimeric VLP constructs.
2. Design and express a panel of RH chimeric constructs. The assembly of RVLPs requires the correct trafficking of the RV-E proteins to the Golgi[320]. This is mediated by the TMD and cytoplasmic tails of these proteins[320]. A panel of RH chimeras were designed in which the ectodomains of the RV-E proteins were replaced with those of HCV-E proteins (Figure 1.6). These chimeras were validated to produce chimeric RH-VLPs.
3. The final aim was to investigate the immunogenicity of the chimeric VLPs. To test this, the VLPs were incorporated into an ongoing study to isolate anti-HCV monoclonal antibodies form immunised bovines. Whilst this approach was not a vaccine trial it provided insight into the ability of the VLPs to generate an anti-HCV response.

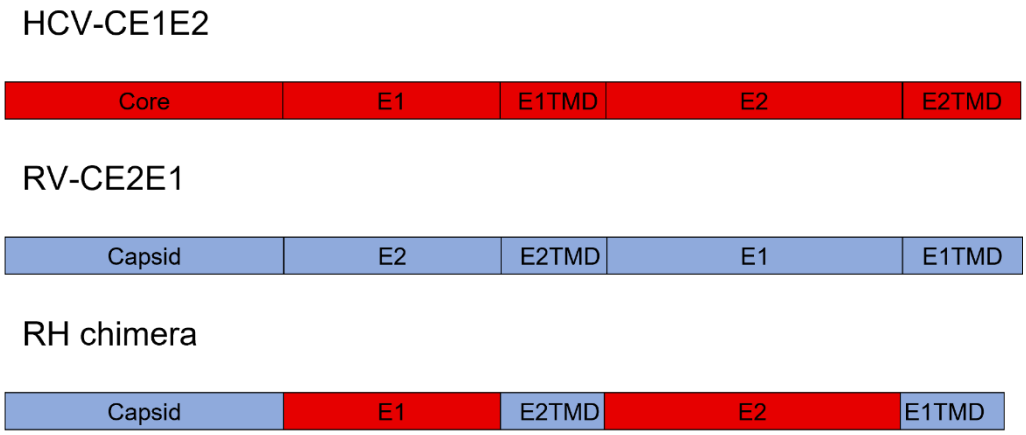

Figure 1. 6 Schematic diagram outlining the design of Rubella-Hepatitis C Chimeras.

The ectodomains of the Rubella virus envelope glycoproteins were replaced with the ectodomains of the Hepatitis C virus envelope glycoproteins and tested for the assembly of chimeric virus-like particles.

Chapter 2 Materials and Methods

2.1 Plasmids and Constructs

All viral genes used in this project were subcloned into the mammalian expression vector, pcDNA3.1 (Invitrogen), with exception of VSV-G (GenBank accession ACK77583.1) which was expressed in a pMD2.G vector (Addgene plasmid# 12259). The E1E2 sequence of HCV reference isolate H77[352] (GenBank accession AF011751) and RV-24s region of the RA27/3[353] vaccine strain of RV (GenBank accession JF727654) were used to generate RH chimeras. The H77-E1E2 genes were readily available in the laboratory at the start of this project. For RV-24s, synthetic gene fragments of RV-C and RV-E2E1 (corresponding to RV genome nucleotides 6512-7411 and 7316-9703, respectively) were purchased from GeneStrings (GeneArt, Thermo Scientific) as lyophilized preparations which were resuspended in DEnuclease-free water (Thermo Fisher Scientific) to a final concentration of 50 ng/µL and stored at -20 ºC. Fragments were designed with the following 5' tag,5'-*CAGTGTGGAATTC*ACC-3' (Sense), and 3' tag, 5'-TAAGAATTCTGCAGATATC-3' (antisense), which included vector specific regions homologous to EcoRI-digested pcDNA3.1, a Kozak sequence on the 5' tag and a stop codon on the 3' tag.

2.2 Antibodies

Detection of RV-E1 and RV-E2 was achieved using mouse anti-RV-E1 (G36S clone, Thermo Fisher Scientific) and mouse anti-RV-E2 (D92G clone, Thermo Fisher Scientific) antibodies, respectively. Both

antibodies were supplied at a concentration of 100 µg/mL and were used in western blot experiments at a 1:20 dilution. RV-C was detected using the mouse anti-RV-C antibody, 9B11 (Abcam). This was supplied at a concentration of 1 mg/mL and diluted 1:1000 for western blot experiments. Polyclonal rabbit sera, 7w7[354], raised against RV-C was previously provided by Tom Hobman (University of Alberta). The loading control antibodies used in this project were goat anti-GAPDH (Genscript) and mouse anti-β-actin (Thermo Fisher Scientific) which were each used at a 1:1000 dilution. Western blot detection of HCV-E2 was achieved using a humanised AP33 kindly provided by Prof Arvind Patel (University of Glasgow). The anti-HCV-E2 antibody, 1:7 was kindly provided by Mats Person (Karolinkska Institutet). The anti-HCV-E2 antibodies HC33.4, HC84.26, AR3A and AR4A were kindly provided by Justin Bailey (Johns Hopkins School of Medicine). Mouse monoclonal anti-HCV-E1 antibody was purchased from Native Antigen.

Secondary antibodies used for western blots were conjugated to HRP enzymes. Detection of mouse primary antibodies was achieved using an anti-mouse-HRP antibody (Dako) at a concentration of 1:1000. Human antibodies were detected using the anti-Human, Fc specific antibody (Sigma-Aldrich) at a 1:1000 dilution. Goat antibodies were detected using a mouse anti-goat-HRP (Sigma-Aldrich) at 1:5000 working dilution.

2.3 Primers and PCR

Oligonucleotides were purchased from Eurofins Genomics or Merck. Upon receipt, lyophilized primers were resuspended in nuclease-free

water to a final concentration of 100 µM and working solution were made at 10 pmol/µL. Primers were stored at -20 ºC and discarded after 5 freeze/thaw cycles.

For amplification of targets required for cloning, high-fidelity Q5 polymerase 2x master mix (New England Biolabs) was used. In brief, 25 µL reactions were set up according to the manufacturer's instructions. PCR protocols were performed as follows; initial denaturation at 98 ºC for 30 sec, 35 cycles of melting at 98 ºC for 10 sec, annealing for 20 sec and extension at 72 ºC for 30 sec/Kb, with a final extension at 72 ºC for 2 min. Primer annealing temperature was predicted using the NEB TM calculator (available at tmcalculator.neb.com; New England BioLabs). PCR products were purified using a Monarch® PCR clean kit (New England BioLabs).

Colony PCR screening of transformed *E.coli* colonies was performed using HotStarTaq DNA polymerase (Qiagen). For detection of recombinant pcDNA3.1 plasmids, screening was performed with T7F 5'-TAATACGACTCACTATAGGG-3' (sense) and bGHR, 5'-TAGAAGGCACAGTCGAGG-3' (antisense) primers. The colony PCR protocol was performed as follows; initial denaturation at 95 ºC for 15 min, 25 cycles of melting at 94 ºC for 30 sec, annealing for 20 sec, extension at 72 ºC for 1 min/Kb, final extension at 72 ºC for 10 min.

2.4 DNA Electrophoresis

Agarose gels were freshly made for DNA electrophoresis. In brief, 2 g agarose (Sigma-Aldrich) was dissolved in 100 mL TAE buffer by

heating with gentle agitation. Once dissolved, the solution was cooled and 5 µL ethidium bromide (10 mg/mL) was added and mixed before being poured into gel casts and left to set for 20 min. Set gels were placed in chambers filled with TAE (0.5 µg/ mL ethidium bromide) and used within two days. DNA samples were prepared for electrophoresis by mixing 5 µL of sample with 0.5 µL 10x TriTrack loading buffer (Thermo Fisher Scientific). Samples were loaded alongside 3.5 µL GeneRuler molecular ladder (Thermo Fisher Scientific). Gels were run at 90 V for 36 min and DNA bands were visualised using a UV transilluminator.

2.5 Sanger Sequencing

All sequencing was performed externally by SourceBioscience (Nottingham). Plasmids and PCR products were prepared for sequencing according to company specifications with plasmids submitted at a final concentration of 100 ng/µL and PCR products submitted as 1:10 dilutions in nuclease-free water. For sequencing inserts in the pcDNA3.1 vector, a T7F primer, 5'-TAATACGACTCACTATAGGG-3' (sense), and bGHR primer, 5'-TAGAAGGCACAGTCGAGG-3' (antisense), were used. For complete coverage of chimeras, an additional HCV-E1F 5'-CGCAGCTTCGACGTCATATC-3' (sense) primer was used.

2.6 Design and Chimera cloning

Chimeric constructs were designed based on TMD predictions made using the DASTM online software[355]. Constructs were made using two cloning approaches (Figure 2.1A)which made use of two homologous

recombination techniques, Gibson Assembly, and In-Fusion cloning. All primer sequences can be found in appendix 1.

Cloning method 1 (Figure 2.1A), used SDM and Gibson assembly cloning methods. First, SDM was used to create Rubcas vectors. Rubcas F and RubcasR primers were used to delete RV-E2 and RV-E1 regions from pcDNA3.1-RV-24s by PCR with Q5 polymerase. The RV-E1 C-terminus was maintained and varied between RH constructs. Rubcas primers also introduced a BsiWI restriction site. PCR products were used in a SDM kit reaction (New England BioLabs). In brief, 1 µL of PCR product was added to 5 µL 2x KLD reaction buffer, 1 µL10 x KLD enzyme mix and 3 µL nuclease-free water. The KLD reactions were incubated at room temperature for 5 min and then transformed into *E.coli* cells and isolated plasmids were confirmed by Sanger sequencing. Rubcas vectors were linearized by incubating 50 µg of Rubcas plasmid was with BsiWI enzyme at 55 ºC overnight. BsiWI was inactivated by heating to 65 ºC for 20 min. Linearization of Rubcas vectors was confirmed by DNA electrophoresis. Next, the ectodomain regions of HCV-E1 and HCV-E2 were amplified. HCV-E1 was amplified with a RH-E1F primer that encoded a 5'-15 bp homologous tag to the 3' end of RV-C gene in the Rubcas vector, and a RH-E1R primer which was specific to the 3' end of HCV-E1 and this position varied between chimeras. The RH-E1R primer also contained a large 5'-tag that encoded half of the RV-E2 C-terminus region. RH-E2 was amplified with a RH-E2F primer that was specific to the 5' end of HCV-E2 and contained a 5'-tag that encoded the remaining half of the RV-E2 C-

terminus region and an additional 20 bp region that was homologous the first 20 bp of the of the 5' tag of the RH-E1R primer. RH-E2R was specific to the 3'-end of the HCV-E2 which varied between chimeras and contained a 5'-tag specific to the RV-E1 C-terminus region in the Rubcas vector. Amplicons were purified by PCR clean up kit (New England BioLabs) and quantified using Nanodrop. Chimeras were assembled using Gibson assembly. Briefly, Rubcas, RH-E1 and RH-E2 were used at a 1:2:2 ratio, respectively, with reactions performed at a final volume of 10 µL and incubated at 50 ºC for 15 min. Finally, 2 µL of each reaction was transformed into *E. coli*.

Cloning method 2 used the In-Fusion cloning method (Figure 2.1B). First, pcDNA-RV-24s was linearized by PCR using RH-Vec primers. Like the Rubcas primers, RH-Vec-R primers were specific to the 3' end of RV-C and RH-Vec-F was specific to the 3'-end of RV-E1 which varied between chimeras to include different regions of the RV-E1 C-terminus. Amplification of RH-Vec was achieved using Q5-polymerase. RH-E1 and RH-E2 were amplified in the same way as described for cloning approach 1. PCR products were purified and quantified. In-fusion cloning were set up in 2.5 µL reactions with RH-Vec, RH-E1 and RH-E2 used at a 1:2:2 ratio, respectively, in a final volume of 2 µL which was mixed with 0.5 µL 5x In-Fusion enzyme mix (Takara BioTech). Reactions were incubated at 50 ºC for 15 min and transformed in *E. coli* cells immediately.

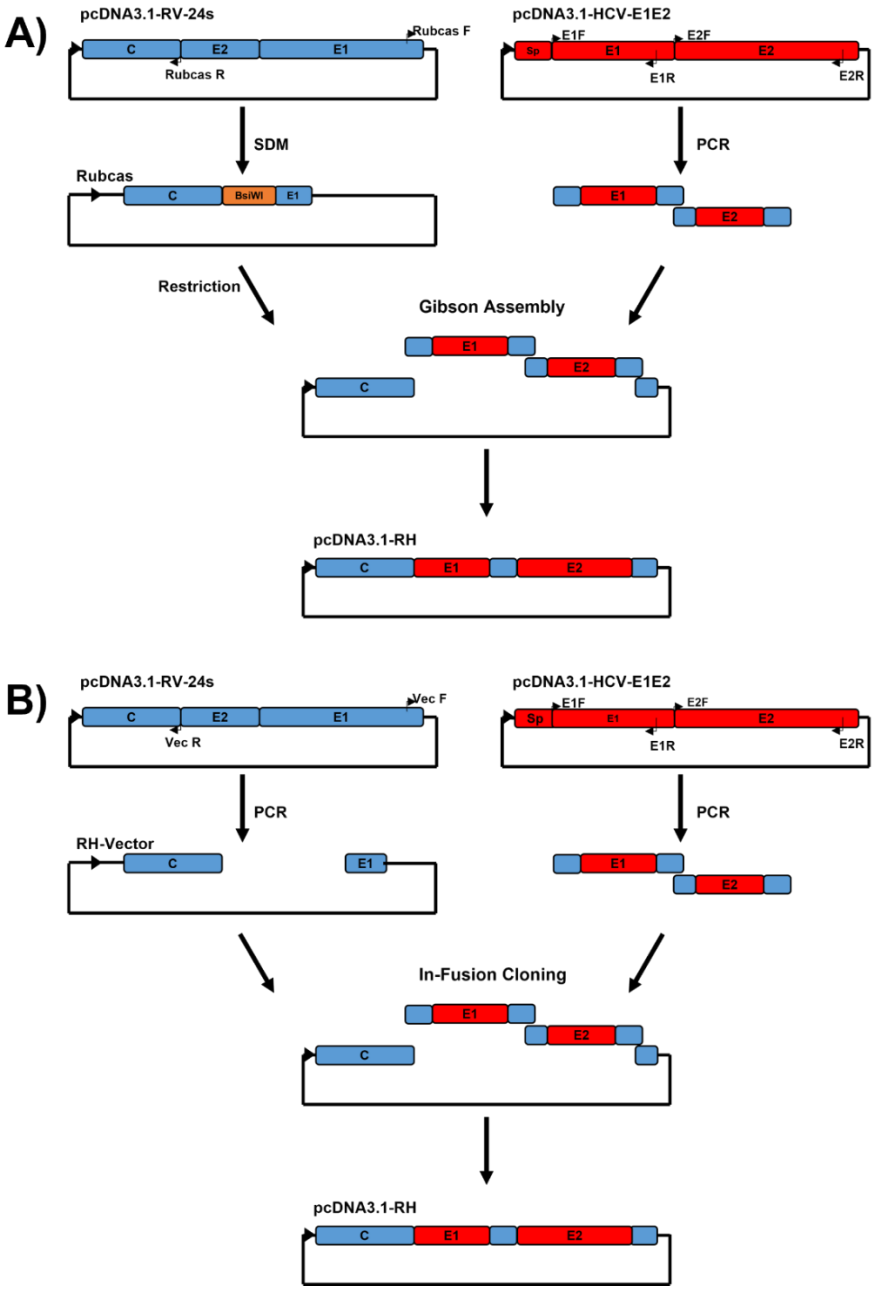

Figure 2. 1 Cloning approaches used to generate RH chimeras.

A) Cloning approach 1, Rubcas vector was made by site directed mutagenesis to delete RV-E2 and most RV-E1 ectodomain and insert a BsiWI site. Rubcas vector was digested and HCV-E1 and HCV-E2 ectodomains were amplified with primers encoding tags homologous to the 3' end of RV-C and 5' end of RV-E1-C-terminus. Inserts and digested Rubcas were used in a Gibson assembly reaction for homologous recombination. **B)** Cloning approach 2, linearized RH-vector was produced by PCR amplification of pcDNA3.1-RV-24s. HCV-E1 and HCV-E2 ectodomains were amplified using the same method as cloning approach 1. Vector and inserts underwent homologous recombination by In-Fusion cloning.

2.7 Bacterial transformation

Plasmids were transformed into Stellar (Takara Bio) or DH5α (New England BioLabs) *E. coli* competent cells via the heat shock method. Briefly, competent cells were thawed on ice and incubated with a plasmid preparation for 30 min. The heat shock method was then performed on both Stellar and DH5α cells by placing the aliquots in a water bath set at 42 °C for 45 seconds and 30 seconds, respectively. The cells were placed on ice and diluted in 250 µL prewarmed SOC media (Takara Bio), then incubated at 37 °C in a shaking incubator set at 300 rpm for 1 hr. Following this, 50 µL of the transformed cell suspension was spread on to a prewarmed LB agar plate supplemented with ampicillin at a final concentration of 100 µg/mL and incubated overnight at 37 °C. Single colonies were picked for colony PCR screening. Positive colonies were used to seed suspension cultures for plasmid purification.

2.8 Plasmid purification

2.8.1 Miniprep

Single colonies of transformed *E.coli* were picked from a LB agar plate and used to inoculate 5 mL suspensions of LB-ampicillin Broth (100 µg/mL). Suspension cultures were incubated at 37 °C overnight on an orbital shaker set at 225 rpm. Grown cultures were harvested by alkaline lysis using a GenElute miniprep kit (Sigma-Aldrich). Briefly, cells were pelleted by centrifugation at 12,000 x *g* for 5 min. The supernatant was discarded, and pellets were resuspended in 200 µL of RNAse containing resuspension buffer. Cells were then lysed with the

addition of 200 µL of lysis buffer and incubated at room temperature for 3 min. Lysis reaction was stopped by the addition of 350 µL of neutralisation buffer which was mixed thoroughly by gentle inversion. The solution was then centrifuged at 12,000 x *g* for 10 min to pellet cell debris and precipitate. The supernatant was collected and loaded onto a centrifuge column and centrifuged at 12,000 x *g* for 1 min. The flowthrough was discarded and 750 µL of wash buffer was loaded on to the column and centrifuged at 12,000 x *g* for 1 min. The flowthrough was discarded, and the column was placed into a clean collection tube. Plasmids were eluted in 50 µL of sterile molecular grade H_2O and centrifuged at 12,000 x *g* for 1 min. Purified plasmids were quantified using a Nanodrop spectrophotometer (Thermo Fisher).

2.8.2 Midiprep

Single transformed *E.coli* colonies were picked and used to inoculate 5 mL suspension cultures. Following overnight incubation, 50 µL of the culture was used to inoculate 50 mL of LB broth in a 250 mL baffled Erlenmeyer flask (Corning) which was then incubated overnight at 37 ºC with agitation at 225 rpm. The culture was harvested, and plasmid was purified using the GenElute Midiprep HP kit (Sigma-Aldrich). In brief, the suspension culture was centrifuged at 4500 *x* g for 10 min to pellet cells. The supernatant was discarded, and cells were resuspended with 4 mL of chilled resuspension buffer containing RNAse. Cells were then lysed with 4 mL of lysis buffer and incubated at room temperature for 5 min. Lysis was halted by the addition of 4 mL of chilled neutralisation buffer. Following this 3 mL of binding buffer was added and the sample

was loaded into a syringe filter and incubated at room temperature for 5 min. Spin columns were prepared with 4 mL of column preparation solution and centrifuged at 3000 *x* g for 2 min. The following centrifugation steps were performed at 3000 *x* g for 2 min. Flowthrough was discarded and sample was loaded onto the column and centrifuged. The column was washed with 4 mL of wash 1 solution and centrifuged followed by a second wash with 4 mL of wash 2 solution. Residual wash solution was removed by an additional centrifugation step. The column was transferred to a fresh collection tube and 1 mL of elution buffer was added and incubated for 1 min at room temperature followed by centrifugation at 3000 *x* g for 5 min. Eluted plasmid was quantified using a NanoDrop one (Thermo Fisher Scientific). Plasmids were stored at 4 ºC for further use.

2.9 Mammalian cell culture

2.9.1 Maintenance of adherent cell lines

Adherent cell lines HEK-293T, Huh 7 and Vero-E6 were grown in DMEM (Gibco) supplemented with 10 % heat inactivated foetal bovine serum (Gibco) and 1 % non-essential amino acids (Gibco). Cells were incubated at 37 °C and 5 % CO_2. Cultures were passaged using trypsin digest every 3-4 days and cells were discarded at passage 50. In brief, DMEM was removed, and the cell monolayer was washed with 8 mL of PBS. The PBS was removed and 7 mL of trypsin-EDTA (0.05 %) (Gibco) was added to the cells and incubated at room temperature for 5 min. Once the monolayer was detached from the flask, trypsin digestion was inactivated by the addition of 10 mL of DMEM. The cell suspension

was then transferred to a 50 mL centrifuge tube (Falcon) and made up to a 50 mL volume with DMEM. Cells were then counted with a haemocytometer and centrifuged at 300 x g for 7 min. Supernatant was removed and pelleted cells were resuspended in 10 mL of fresh DMEM. New cultures were seeded at a cell density of 1-3 $x10^4$ cells/ cm^2. The final media volumes for a T175 and T75 flasks (Corning) were 30 mL and 12 mL, respectively.

2.9.2 Maintenance of Suspension Cell Line

FreeStyle™ 293-F cells (Thermo Fisher Scientific) were cultivated in FreeStyle™ F17 expression medium (Thermo Fisher Scientific) supplemented with 1.5 % GlutaMAX™ (Gibco). Non-baffled Erlenmeyer 125 ml and 250 mL flasks (Corning) were used for 40 mL and 80 mL cultures, respectively, and were agitated at 135 rpm and incubated at 37°C with 8% CO_2. Smaller 15 mL cultures were propagated in 50 mL mini bioreactors (Corning) and agitated at 250 rpm. Cells were passaged every 3-4 days and subcultures were seeded at a density of 3 $x10^5$ cells/mL. Cultures were discarded after the 30^{th} passage.

2.9.3 Generation of retroviral pseudotype particles

PPs where generated using the MLV packaging system, as previously described[356]. In brief, $1.2x10^6$ HEK-293T cells were seeded in a 10 cm^2 Primaria coated dish (Corning) in 5 mL DMEM and incubated overnight. Prior to transfection, 2 µg of MLV-Gag-Pol (phCMV-5349)[233], MLV-Luciferase (pTG126) and a plasmid encoding either HCV-E1E2 or VSV-G, were diluted in Opti-MEM to a final volume of 300 µL and mixed with a solution of 276 µL reduced serum Opti-MEM (Gibco) and 24 µL of the

cationic polymer, PEI (Life Sciences) (1 mg/mL PEI, 150 mM NaCl, p*H* 7.0). The plasmids and PEI were incubated for 1 hr at room temperature. DMEM was removed from the 10 cm^2 dish of HEK-293t cells and 7 mL of Opti-MEM was added slowly to minimise cell detachment. Plasmid-PEI solution was added into a dropwise manner to ensure even distribution. Cells were incubated for 6 hrs at 37 ºC, after which the Opti-MEM was replaced with 10 mL DMEM. Transfected cells were grown for 72 hrs and harvested. HCVpp containing supernatant was passed through a 0.45 µM syringe filter (Sartorius) and stored at 4 ºC. Producer cells were washed with 1 mL of room temperature PBS and detached from the dishes using a cell scrapper (Sarstedt). Disassociated cells were transferred to a 1.7 mL microcentrifuge tube and lysed in 1 mL of lysis buffer (50 mM Tris, p*H* 7.4, 1% Triton, 1 mM EDTA, 150 mM NaCl, protease inhibitor tablet (Sigma-Aldrich)).

2.9.4 *In Vitro* Pseudotype Particle Infection Assay

Huh 7 cells were plated 24 hrs prior to neutralisation assay at a density of 15 $x10^3$ cells/ well in a 96 well, white, flat bottom plate (Corning). DMEM was removed and 100 µL of PP supernatant was added per well and cells were incubated for 4 hrs at 37 ºC, 5 % CO_2. Following infection, supernatant was removed from the Huh 7 cells and replaced with 200 µL DMEM and were grown for 72 hrs at 37 ºC, CO_2. Luciferase activity was measured using the Promega Luciferase assay kit. In brief, DMEM was removed from Huh 7 cells and 50 µL lysis buffer (Promega) was added per well and incubated for 30 min at room temperature with

agitation. Luciferase activity was measured using a FLUROstar Omega plate reader that was primed with luciferase substrate (Promega) and injected 50 µL immediately before measuring luciferase activity. For reading HCVpp infected cells, the gain was set to 3600 and for VSVpp infected plates, the gain was set to 2000 to prevent signal saturation.

2.9.5 Virus-Like Particle Expression and Purification

VLPs were expressed in both HEK-293T and HEK-293F cell lines. Transfection of HEK-293T cells was performed as described for the generation of HCVpps. These cells were transfected with 2 µg of RV-24s or chimera construct. Transfection of HEK-293F cells was performed as follows in 15 mL, 30 mL, and 60 mL cultures. Briefly, 24 hrs prior to transfection cultures were seeded at a density of $7x10^5$ cells/mL. Enough plasmid to reach a final concentration of 1 µg/mL in transfected cultures was diluted in Opti-MEM to a final volume of 500 µL. PEI was at a 3:1 ratio with plasmid and diluted in Opti-MEM to a final volume of 500 µL. PEI and plasmid solutions were mixed and incubated at room temperature for 1 hr. The HEK-293F cultures were counted and the density was adjusted to 1. $x10^6$ cells/mL. The plasmid, PEI and Opti-MEM solution was added to cells and the transfected culture was grown for 72 hrs at 37, 8% CO_2 with rotation. To harvest the supernatant, cultures were subjected to centrifugation at 300 *x* g for 5 min to remove cells. The supernatant was further clarified by additional centrifugation at 3000 *x* g for 20 min. Finally, supernatant was passed through a 0.22 µM filter (Sartorius) and stored at 4 ºC.

Purification of VLPs was achieved by pelleting the supernatant onto a 20 % sucrose cushion. Briefly, sucrose was dissolved in PBS (Sigma-Aldrich) to a final concentration of 20 % (w/v) and 1 mL or 3 mL was loaded into a 10.4 mL or 26.3 mL polycarbonate ultracentrifuge tube (Beckman- Coulter), respectively. Harvested supernatant was gently pipetted onto the sucrose cushion and samples were centrifuged at 110,000 x g for 2.5 hrs at 4 ºC. The 10.6 mL and 26.3 mL tubes were centrifuged in a Type 70 Ti rotor (Beckman-Coulter) and Type 70.1 Ti rotor (Beckman-Coulter), respectively. Following centrifugation, supernatant was discarded, and pellets were resuspended overnight in 50 µL PBS and stored at –20 ºC.

2.10 Protein Quantification

All protein samples were quantified using the BCA protein estimation kit (Thermo Fisher Scientific) according to the manufacturer's instructions. Assays were performed in low-binding 96 well plates (Thermo Fisher Scientific). Cell lysate and pelleted supernatant samples were diluted 1:5 in lysis buffer and 1:2 in PBS, respectively. A standard curve was made by serially diluting a BSA standard (Thermo Fisher Scientific) to 2 mg/mL, 1.5 mg/mL, 1 mg/mL, 0.75 mg/mL, 0.5 mg/mL, 0.25 mg/mL, 0.125 mg/mL, and 0.025 mg/mL. The diluent used to prepare the BSA standards was lysis buffer and PBS for cell lysates and supernatant pellets, respectively. A total of 10 µL of protein sample or standard was added per well and 200 µL of freshly prepared BCA working reagent (50:1 ratio of reagent A and B, respectively) was added. The microtitre plate was then incubated at 37 °C for 30 min and absorbance was

measured at 595 nm using a FLUROstar Omega plate reader. The absorbance values for the BSA samples were used to generate a standard curve from which the concentrations of unknown samples were interpolated.

2.11 SDS-PAGE

Electrophoretic separation of protein samples was achieved using hand cast polyacrylamide gels. Gels were made in duplicate and cast using the Mini-PROTEAN® Tetra System (Bio-Rad). In brief, 15 mL of resolving gel solution (12 % acrylamide, 380 mM Tris-HCl, p*H* 8.8, 0.1 % SDS, 0.002 % ammonium persulfate, 0.0015 % TEMED) was poured into two 1.0 mm thick gel casts and overlayered with 400 µL of 100 % propan-2-ol. The resolving gel was incubated for 30 min at room temperature to allow polymerization to occur. The propan-2-ol was removed and the top of the resolving gel was extensively washed with dH_2O and dried. Stacking gel solution (5 % acrylamide, 122 mM Tris-HCl, p*H* 6.8, 0.1 % SDS, 0.001 % ammonium persulfate, 0.002 % TEMED) was poured onto the resolving gel and a well comb was inserted into the gel cast. The stacking gel solution was incubated at room temperature for 30 min to allow for polymerisation. Immediately following preparation, polyacrylamide gels were placed in a tetra cell (Bio-Rad) tank filled with SDS-PAGE running buffer (25 mM Tris base, 192 mM glycine, 0.1% SDS).

Protein samples were mixed with 4 x Laemmli buffer[357] (277.8 mM Tris-HCl, p*H* 6.8, 44.4 % (v/v) glycerol, 4.4 % SDS, 10 % β-ME) and heated to 95 °C for 10 min. For nonreducing SDS-PAGE, β-ME was omitted

from the Laemmli buffer. Samples were loaded onto the polyacrylamide gel alongside 4 µL of Spectra Broad Range Molecular weight marker (Thermo Fisher Scientific). Reduced proteins were separated by running the polyacrylamide gel at 70 V for 20 min followed by 150 V for 50 min.

2.12 Western Blot

Following SDS-PAGE, polyacrylamide gels were equilibrated in chilled transfer buffer (25 mM Tris, 192 mM glycine, p*H* 8.3) for 10 min at room temperature. PVDF membrane (Amersham) was activated in 100 % methanol for 3 min and equilibrated in chilled transfer buffer along with blotting paper. After equilibration, the gel, PVDF and blotting paper were assembled onto a Trans-Blot Semi dry cell (Bio-Rad) and run at 100 mA for 1 hr. Following transfer, the PVDF membrane was incubated in blocking solution (PBS, 0.1 % Tween 20, 10 % skimmed milk) overnight at 4 ºC. Blocking buffer was removed and 10 mL of primary antibody, diluted to a working concentration in buffer (PBS, 0.1% Tween 20, 5% skimmed milk), was added to the membrane and incubated at room temperature for 1 hr with gentle agitation. Primary antibody solution was removed and the PVDF membrane was washed three times for 10 min in TPBS (0.1% Tween-20). All primary antibodies were detected using secondary HRP-conjugated antibodies. A freshly made secondary antibody working solution was added to the membrane and incubated at room temperature for 1 hr with gentle agitation. The secondary antibody solution was removed, and the membrane was washed a further three times for 10 min in TPBS. Detection of

membrane bound HRP was achieved using ECL substrate (Thermo Fisher Scientific). In brief, 500 µL of each ECL substrate solution was mixed during the final membrane wash. PVDF membrane was removed from PBST and placed on a clear plastic sheet. ECL substrate was added in a dropwise manner to the membrane to ensure complete coverage and incubated at room temperature for 1 min. Excess ECL substrate was removed by wicking. A second clear plastic sheet was placed over the membrane and HRP activity was visualised using a gel box. Captured images were exported as TIF files.

2.13 ELISA Assays

2.13.1 Lectin capture ELISA

Lectin capture of HCV glycoproteins was performed as previously described[358]. Lectin from *Galanthus nivalis* (GNA) (Sigma- Aldrich) was diluted in 0.05 M carbonate-bicarbonate, p*H* 9.6, to a final concentration of 10 µg/mL and 50 µL per well of a Nunc MaxiSorp flat bottom plate (Thermo Fisher Scientific). Plates were incubated overnight at 4 °C and the coating solution was removed, and wells were blocked for 2 hrs at room temperature with 200 µL of 5 % skimmed milk TPBS. Blocking solution was then removed and the plate was washed once with 200 µL of TPBS followed by a 90 min incubation at room temperature with diluted antigen. Following removal of the sample each well was washed in 200 µL TPBS three times and 50 µL of primary antibody diluted in TPBS was added for 1 hr at room temperature. Plates were washed a further three times in 200 µL TPBS and incubated with 50 µL of AP-conjugated secondary antibody diluted in TPBS for 1 hr. Plates were

washed a final three times in TTBS and tapped dry. Detection of bound AP was achieved by adding 50 µL of pNPP substrate (Sigma-Aldrich) to each well and measuring absorbance at 405 nm using a FLUROstar® Omega plate reader.

2.13.2 Rubella Capsid Protein Capture ELISA

SwELISA was used to detect enveloped RV-C. MaxiSorp plates were coated overnight at 4 ºC with 50 µL/ well of anti-RV-C (9B11) diluted in 0.05 M carbonate-bicarbonate buffer to a concentration of 1 µg/mL. Coating buffer was removed, and wells incubated with 200 µL of block solution (3% BSA, TPBS) for 2 hrs. VLP samples were incubated in 1% triton or PBS (native form) and incubated at for 30 min at room temperature with occasional agitation. Blocking solution was removed and wells were washed once with 200 µLTPBS. Wells were then incubated with 50 µL of sample for 90 min at room temperature. Each sample was used in triplicate and paired with an untreated with VLP sample. Sample was removed and wells were washed three times with 200 µL TPBS. Captured RV-C was detected by addition of 50 µL polyclonal rabbit sera (7w7) raised against RV-C used at a 1:1000 dilution. Wells were incubated with sera for 1 hr at room temperature. Sera was removed and wells were washed a further three times with 200 µL TPBS. Secondary anti-rabbit IgG- AP conjugate (Sigma) was diluted 1:1000 and 50 µL was added per well and incubated for 1 hr at room temperature. Secondary antibody was removed, and wells were washed three times with TPBS. Detection of bound AP was achieved by

adding 50 µL of pNPP to each well. Absorbance was measured at 405 nm using a FLUROstar® Omega plate reader.

2.14 Immunoprecipitation of VLPs

VLPs were isolated from cell culture supernatant using immunoprecipitation with Protein A Dynbeads (Thermo Fisher Scientific). Samples were pre-cleared with 15 µL of Protein A beads overnight at 4 ºC with rotation. 15 µL magnetic protein A beads were incubated with 5 µg of anti-envelope protein antibody in a total volume of 250 µL and incubated at room temperature for 1 hr with agitation. Antibody-conjugated beads were pelleted gently by placing the microcentrifuge tubes in a magnetic rack (Thermo Fisher Scientific), supernatant was removed, and the antibody-bound beads were washed once in 200 µL of TPBS. Antibody-bound beads were added to the precleared samples and incubated overnight at 4 ºC with agitation. Beads were pelleted and the supernatant was removed. The beads were then washed twice in 200 µL of TPBS. Pelleted beads were resuspended in 20 µL PBS (1% Triton) and incubated at room temperature for 30 min with occasional agitation. Beads were pelleted and supernatant was collected and used for western blot analysis. Removal of antibody-antigen complexes from the beads was achieved by the addition of 20 µL Leammeli buffer with added β-ME. The beads were then incubated at 95 ºC for 10 min before pelleting and collection of the supernatant.

2.15 Endo H and PNGase treatment

Deglycosylation of protein samples was performed using either Endo H or PNGase F (New England BioLabs). In brief, 20 µg of total protein was used for each 20 µL reaction. Samples were incubated at 37 °C for 2 hrs to ensure complete cleavage of glycan groups. Samples were then reduced with 6.7 µL of 4x Laemmeli buffer and heated to 95 °C for 10 min. Reduced samples were subsequently separated by SDS-PAGE and target proteins were detected by western blot.

2.16 Electron Microscopy

Pelleted supernatant was resuspended in 50 µL fixing buffer (3% glutaraldehyde, 0.1 M sodium cacodylate). Electron microscopy was performed by Nicola Weston (Nanoscale and Microscale Research Centre, University of Nottingham). Images were captured using a JEM-2100F field emission electron microscope (JEOL).

2.17 Bovine Immunisation Methods

2.17.1 pMam-IgKL and sE2 Subcloning

The soluble protein expression cassette pMam-IgKL was designed by Jonathan Ball and consisted of an Ig kappa leader sequence, enterokinase site, twin strep tag, and a 6 x His-tag. A BtmI site was located between the kappa leader sequence and enterokinase site to allow for insertion of genes of interest (Figure 2.2). The pMam-IgKL was purchased from Genstrings and subcloned into EcoRI digest pcDNA3.1. Vector was linearised by restriction with BmtI (New England BioLabs).

Soluble HCV-E2 constructs were designed based on previously published construct which encoded residues 384-645 (H77 polyprotein numbering)[82]. The E2 ectodomains of HCV isolates UKNP2.4.1, UKNP1.18.2, UKNP4.1.1 and UKNP3.1.1 were amplified from pcDNA3.1 plasmids containing the full E1E2 sequences of these isolates using the primers described in (Table 2.1). Amplicons were subcloned into BmtI digested pMam-IgKL vectors (Figure 2. 2) and sent to Arvind Patel's laboratory for expression and purification of sE2 for bovine immunisations. In addition to these sE2 constructs, purified sE2 from isolates 1a80, 1b34 and J6 were provided by Justin Bailey.

Table 2. 1 sE2 PCR Primers.

Name refers to the UKNP isolate designation. Bold, underlined regions represent homologous tags to subclone the amplicon into BmtI digested pMam-IgKL vector. Annealing temperatures (Ta) were determined using the NEB Tm calculator**.**

Name	Sequence (5'-3')	Ta
2.4.1F	**CCAGGTTCCACTGG**tGAGACTCATACCACCGGC	66
2.4.1R	**TTGTCGTCGTCGTCG**ccaatGTTGCATGCTGCTGACAATC	
1.18.2F	**CCAGGTTCCACTGG**tCGGACCCGCACGACGGGG	69
1.18.2R	**TTGTCGTCGTCGTCG**ccaatATTGCACGCGGCGTTGAGCC	
4.1.1F	**CCAGGTTCCACTGG**tCAGACACGTTTGACTGGG	64
4.1.1R	**TTGTCGTCGTCGTCG**ccaatGTTGCATGCCACTTCCATCC	
3.1.1F	**CCAGGTTCCACTGG**tTCTACATACACCACCGGT	63
3.1.1R	**TTGTCGTCGTCGTCG**ccaatGTTGCAAGCGGCGGTAAACC	
6.1.2F	**CCAGGTTCCACTGG**tGCAACCACCACCACCGCC	64
6.1.2R	**TTGTCGTCGTCGTCG**ccaatATTACATGCAGCGTCAAACC	

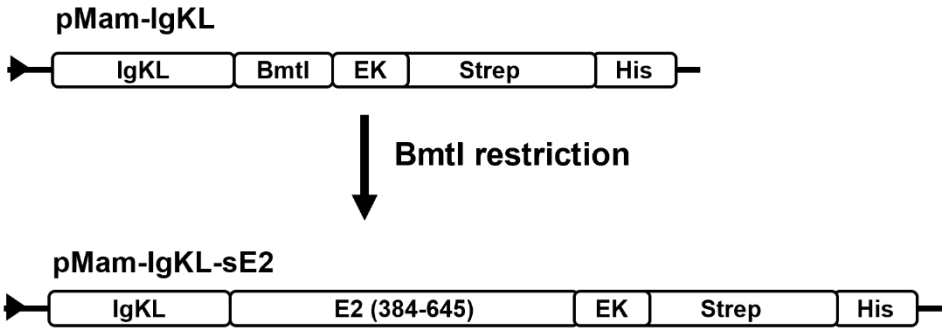

Figure 2. 2 pMam-IgKL expression cassette schematic diagram.

Cassette consisted of a Ig Kappa leader sequence (IgKL), BmtI restriction site, enterokinase cleavage site (EK), twin strp tag (Strep) and 6x His tag (His). Cassette was subcloned into pcDNA3.1 and linearized by restriction digest using bmtI. Linearized pMam-IgKL was then used as a vector for the insertion of HCV-E2 ectodomains (E2 384-645) by homologous recombination.

2.17.2 Bovine Immunisations

Two Holstein bullocks were immunised with 250 µg sE2 protein or 250 µg of RH5-VLPs. For the sE2 immunisation, the immunogen was diluted in sterile PBS to a final volume of 500 µL and mixed with 500 µL of the MF59®-like adjuvant, AddaVax™ (Invivogen). Purified VLPs were diluted to 500 µL in sterile PBS and mixed with 500 µL TiterMax® gold adjuvant (Sigma-Aldrich). Immunisations were administered in the right shoulder of each animal.

2.17.3 Isolation of Bovine Sera and PBMCs

Bovine blood was collected following immunisation via jugular bleeds resulting in approximately 50 mL per animal per bleed. Blood samples were diluted at a 2:1 ratio with prewarmed RPMI-1640 medium (Gibco). 20 mL of diluted blood was gently loaded onto 10 mL of prewarmed

Histopaque-1077 and centrifuged at 800 x *g* for 30 min in a swing out rotor. The top plasma layer was collected and stored at -20 ºC for further use. The PBMC layer was collected with a 1 mL pasture pipette, placed in a fresh 50 mL tube, and diluted with 50 mL of RPMI-1640. The diluted PBMCs were counted using a haemocytometer and centrifuged at 400 x *g* for 10 min. Cells were resuspended in mammalian cell freezing media (FBS, 10% DMSO (Sigma-Aldrich)) at a density of $20x10^6$ cells/mL and stored in liquid nitrogen vapour in 1 mL aliquots.

2.17.4 Bovine Sera Reactivity ELISA

Detection of anti-HCV antibodies in bovine sera was achieved using GNA-capture ELISA as previously described in this chapter. Lysates of transfected cells expressing HCV-E1E2 were incubated on GNA coated plates at a total protein concentration of 0.5 mg/mL. ELISA plates were blocked with 3% BSA TPBS for 2 hrs. The BSA was essentially bovine IgG-free. Aliquots of isolated bovine plasma were heat inactivated prior to use by incubation at 56 ºC for 30 min. Plasma was diluted 1:100 in PBST and added to the plate for 1 hr. Bound bovine IgG was detected with an anti-Bovine AP (Sigma-Aldrich) at a 1:2000 dilution.

2.17.5 *In vitro* Pseudoparticle Neutralisation Assay

Neutralisation of PPs was tested by incubating the PP supernatants with heat inactivated bovine sera for 1 hr. In brief 270 µL of PP supernatant was added to a V-well plate and incubated with 30 µL bovine sera at a 1:10 dilution in PBS (Sigma-Aldrich), making the final concentration of sera 1:100. PPs were incubated with Bovine sera from

different timepoints at a single concentration. An uninhibited control of 270 µL PPs mixed with 30 µL PBS was used to define 100 % infectivity with 0 % infectivity defined by 270 µL ΔE mixed with 30 µL PBS. PP supernatant and sera were incubated in V-well plates for 1 hr at room temperature and then used to infect Huh 7 cells as previously described in this chapter. Following infection, PPs were removed from the cells and replaced with 200 µL DMEM supplemented with Penicillin-Streptomycin (Thermo Fisher Scientific) at a final concentration of 1 % (100 units/mL penicillin, 100 µg/mL streptomycin). Luciferase activity was measured in the same manner as described for the *in vitro* infection assay.

2.18 Statistical Analysis

All statistical analysis was performed using GraphPad Prism 9 software. To determine significance between multiple sample means, a one-way ANOVA was performed. To identify which sample means were significant, Tukey's multiple comparison test was performed.

Antibody EC_{50} values were determined using sample mean values from each dilution point and curve fitting using a non-linear regression, variable slope model in GraphPad Prism 9.

Chapter 3 Generation of Rubella Virus Like Particles

3.1 Introduction

The generation of RVLPs was initially described by Hobman *et al.,*[327]*.* In this study a cDNA clone of the RV-24s ORF was subcloned into a pCMV5 plasmid and transiently expressed in COS and BHK-21 cell lines. Further studies have also made use of transiently transfected CHO[320] and developed BHK-21 cells that stably expressed RV-24s[322]. To date there are no reports of RVLP production in HEK cell lines.

The first stage of this project set out to establish an in-house system to produce RVLPs which could then be applied to the expression of chimeric VLPs. The expression of RVLPs using the HEK-293T was investigated since these are a human derived cell line and are regularly used in our laboratory for mammalian protein expression.

3.2 Results

3.2.1 Subcloning the Rubella virus 24s ORF

The RV genome has a GC content of 69%[303]. This characteristic makes wild-type RV sequences less amenable to manipulation using molecular biology techniques such as PCR and homologous recombination cloning techniques, and lead to difficulties in plasmid propagation in transformed *E. coli* cells. Thus, the first step of establishing a RVLP system was to generate a sequence that decreased the GC content. To achieve this, the RV-24s sub genomic ORF was codon optimised for human cell expression using the GeneArt Strings service (Thermo Fisher Scientific). Codon optimisation reduced the GC content from

69% to 59% (Figure 3.1A). Given the size limitation of 3 Kb for nucleotide fragment synthesis, optimised RV-24s sequence was deconstructed into two nucleotide fragments encoding RV-C and RV-E2E1. The synthesized fragments were designed with 15 bp vector specific homologous tags which allowed for direct infusion cloning in to *EcoRI* digested pcDNA3.1. Colony PCR screening of transformed *E. coli* colonies with vector specific primers showed the insertion of approximately 1 Kb in 2/8 colonies for RV-C, and 2.4 Kb in 7/8 colonies for RV-E2E1 (Figure 3. 1B). One positive colony from each construct was selected and confirmed with Sanger sequencing. Full-length RV-24s was reconstituted by amplification of RV-C and RV-E2E1 to produce fragments with homologous tags at the 3' end and 5' end, respectively. Amplification was confirmed by gel electrophoresis (Figure 3. 1C) and the products were subcloned into pcDNA3.1 by In-Fusion cloning. Colony screening PCR confirmed the presence of an insert that was approximately 3.2 Kb in 14/16 colonies (Figure 3. 1C). Sanger sequencing confirmed the insertion of codon optimised RV-24s in pcDNA3.1.

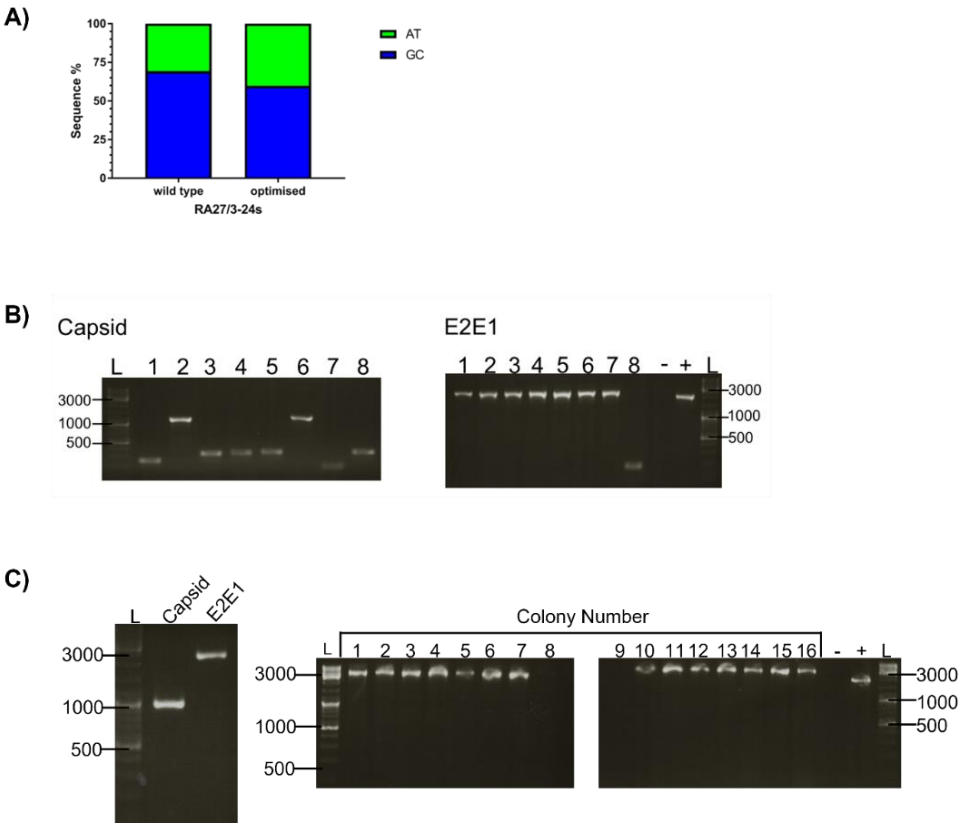

Figure 3. 1 Subcloning of codon optimised RV-24s in to a pcDNA3.1 vector.

A) Nucleotide composition comparison between the wild-type RV-24s ORF (GenBank accession JF727654.2) and a sequence codon optimised for human cell expressing using GeneArt Strings (Thermo Fisher Scientific). **B)** DNA electrophoresis of colony PCR screening following in-fusion cloning of codon optimised RV-C and RV-E2E1 in *EcoRI* digested pcDNA3.1. Transformed colonies were screened with T7F and bGHR primers. **C)** Reconstruction of the complete codon optimised RV-24s ORF. RV-C and RV-E2E1 amplicons were amplified by PCR and subcloned in pcDNA3.1 vector via homologous recombination. Transformed *E.coli* colonies were screened using T7 and bGHR primers. Colony PCR positive (+) control was pcDNA3.1-H77E1E2, negative (-) control PCRs contained no template. Ladder (L) band numbers refer to size in bp.

3.2.2 Expression of Rubella 24s in two mammalian cell lines

The RV-24s encoding plasmid was transiently expressed in both Vero and HEK-293T cell lines. Vero cells are commonly used to propagate RV in cell culture[317] and therefore were used as a control group for the expression of RVLPs. Following transfection with pcDNA3.1-RV-24s, culture supernatants were pelleted on a 20% sucrose cushion and producer cells were lysed. Western blot analysis confirmed the presences of RV-C and RV-E2 in transfected HEK-293T cells (Figure 3. 2). Surprisingly, no detection of RV structural proteins was found in Vero cell lysates whilst the GAPDH loading control confirmed that cell lysate protein was successfully transferred (Figure 3. 2), showing that RV-24s was not sufficiently expressed in the Vero cell line. Pelleted supernatant from transfected HEK-293T contained detectable levels of RV-C and RV-E2, indicative of RVLP secretion. RV-C was detected as a single band with an approximate molecular weight of 36 KDa, in line with previously published data[327]. RV-E2 migrated as a smear pattern, approximately 42- 47 KDa (Figure 3. 2), suggesting that this protein underwent heterogenous glycosylation as has been reported previously[359].

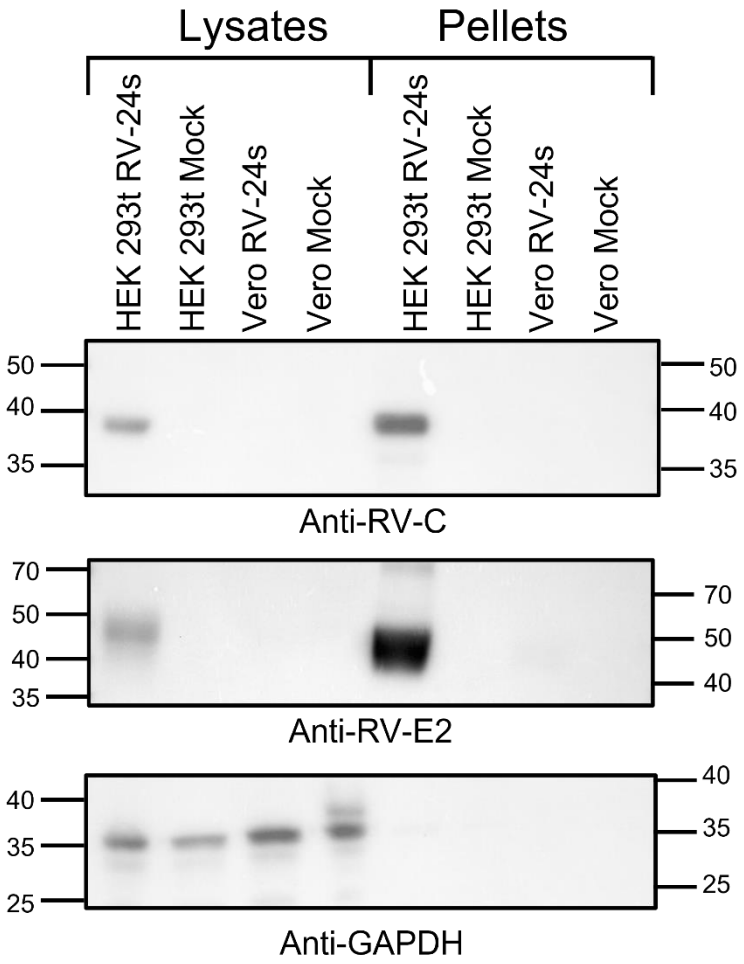

Figure 3. 2 Western blot detection of intracellular and extracellular RV-C, RV-E2 and GAPDH from mammalian cells transiently transfected with pcDNA3.1-RV-24s.

Transfected cells were lysed 72 hrs post transfection and supernatant was pelleted through a 20 % sucrose cushion. All samples were quantified by microBCA assay. A total of 10 µg protein was loaded per lane of each cell lysate. A total of 5 µg of protein was loaded per lane of each pellet sample. Protein was separated by SDS-PAGE using a 12 % acrylamide gel. RV-C was detected using the mouse anti-RV-C monoclonal antibody, 9B11 (Abcam), used at 1 µg/mL. RV-E2 was detected with a mouse anti-RV-E2 monoclonal antibody use at 5 µg/mL. A GAPDH loading control was included. Numbers denote KDa values shown by a molecular weight marker. Mock cells were included to confirm specificity of the anti-RV antibodies.

3.2.3 Expression of Rubella Virus-like Particles in HEK-293T Cells

To further investigate the expression of RV-24s in HEK293T, cultures were transfected with RV-24s or RV-C plus RV-E2E1 encoding plasmids and secretion of structural proteins was compared to a background signal produced by cultures transfected with either RV-C or RV-E2E1 alone. Transient expression was confirmed by western blot analysis of transfected cell lysates. Western blot of the pelleted supernatant showed the presence of RV structural proteins (Figure 3. 3). RV-C was detected in RV-24s, RV-C+E2E1 and RV-C pelleted supernatant however more intense bands were observed in RV-24s and RV-C+E2E1 samples. RV-E2 and RV-E1 proteins were detected in RV-24s, RV-C+E2E1 and RV-E2E1 pellet samples, with RV-24s and RV-C+E2E1 pellets showing more intense signals for both glycoproteins compared to the RV-E2E1 pellet. No RV protein bands were observed in mock samples. Taken together these results show that the secretion of RV structural proteins was increased in cells transfected with all three RV-24s structural proteins which was indicative of RVLP production.

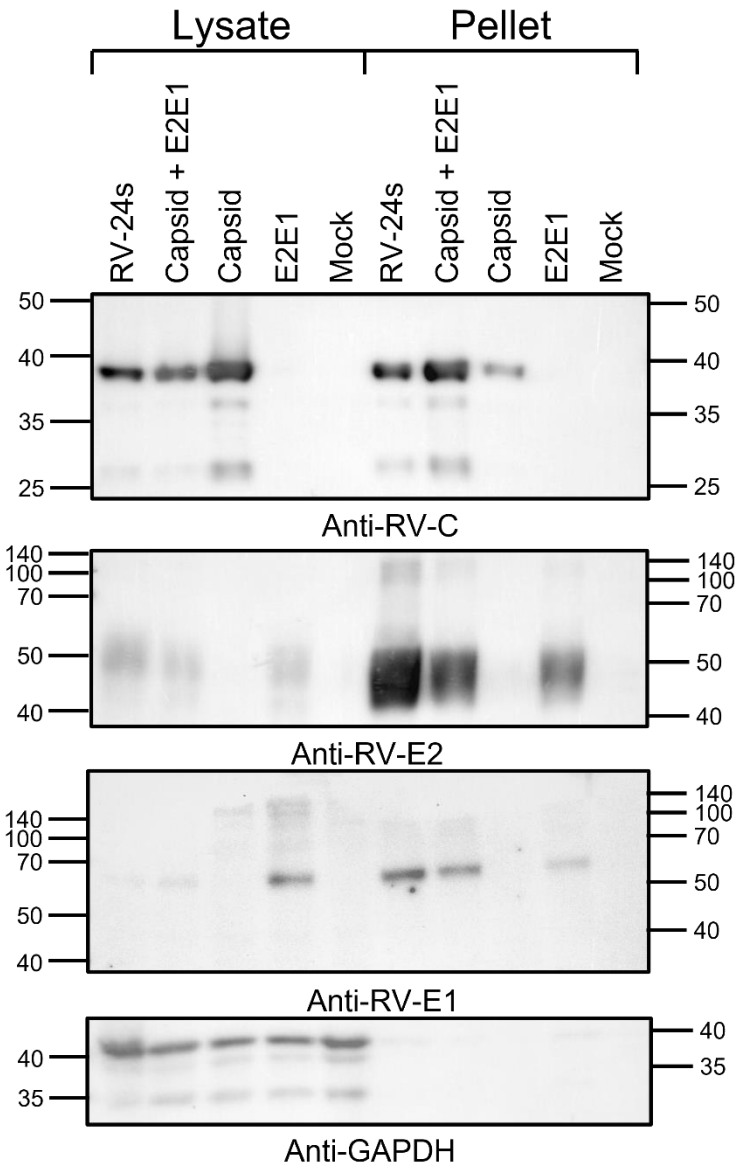

Figure 3. 3 Western blot detection of RV structural proteins from transfected HEK-293T cells expressing complete RV-24s in cis and in trans.

Transiently transfected HEK-293T expressing RV24s, RV-C+RV-E2E1, RV-C, RV-E2E1 with mock transfected cells as a negative control. 10 µg of total protein of cell lysate was loaded per lane. 5 µg of total protein of pelleted supernatant was loaded per lane. SDS-PAGE was performed on 12 % acrylamide gels and protein was transferred to PVDF. Numbers denote KDa of molecular weight marker.

To further validate the secretion of RV-E1 and enveloped RV-C, antigen capture ELISAs were performed (Figure 3. 4). A GNA lectin capture assay, with RV-E1 detection, was used to assess secretion of viral glycoproteins in RV-E2E1 expressing cell lysates, HCV-E1E2 lysate as a GNA capture positive control. This approach failed to detect RV-E1, with the highest concentration of lysate showing no signal above the background signal produced by mock cell lysates. This showed that RV-E1 was unable to be captured by the GNA lectin (Figure 3. 4A). To overcome this, pelleted supernatant was serially diluted and coated directly to microtitre plates (Figure 3. 4A). Lysate samples were not directly coated due to the high total protein content of these samples. Direct coating of RVLPs lead to a detection of RV-E1 in both RV-E2E1 and RV-24s pellets with signal being decreasing with sample concentration (Figure 3. 4B). In line with the previous anti-RV-E1 western blot data, expression of RV-E2E1 alone resulted the release of extracellular RV-E1, however the RV-24s pellet produced a greater signal. Next, pelleted supernatant from RV-24s transfected cells were tested for the presence of enveloped RV-C. This was achieved by developing an RV-C capture ELISA assay, in which wells were coated with an anti-RV-C monoclonal antibody and incubated with samples that were untreated or lysed in 1% Triton for 30 min. Differences observed between Triton treated and native samples would confirm the presence of enveloped RV-C. This assay was performed with both supernatant and pellets from RV-24s, RV-C, RV-E2E1 and mock cell cultures. Supernatant from RV-24s and RV-C expressing cultures showed mean

absorbance values that were greater than both mock and RV-E2E1 supernatants (Figure 3. 5), demonstrating the specificity of this assay and confirming the previous western blot analysis showing the presence of extracellular RV-C in the absence of RV-E2E1 (Figure 3. 3). There was no significant difference observed between native and triton treated RV-24s and RV-C supernatants. However, when pelleted supernatants were used in this assay, a significant increase in absorbance was detected in Triton-treated RV-24s compared to the untreated sample ($p<0.0001$) (Figure 3. 5B). This increase was not observed in the pelleted RV-C supernatant. This showed that expression of RV-24s, but not RV-C, in HEK-293T cells led to the secretion of enveloped RV-C.

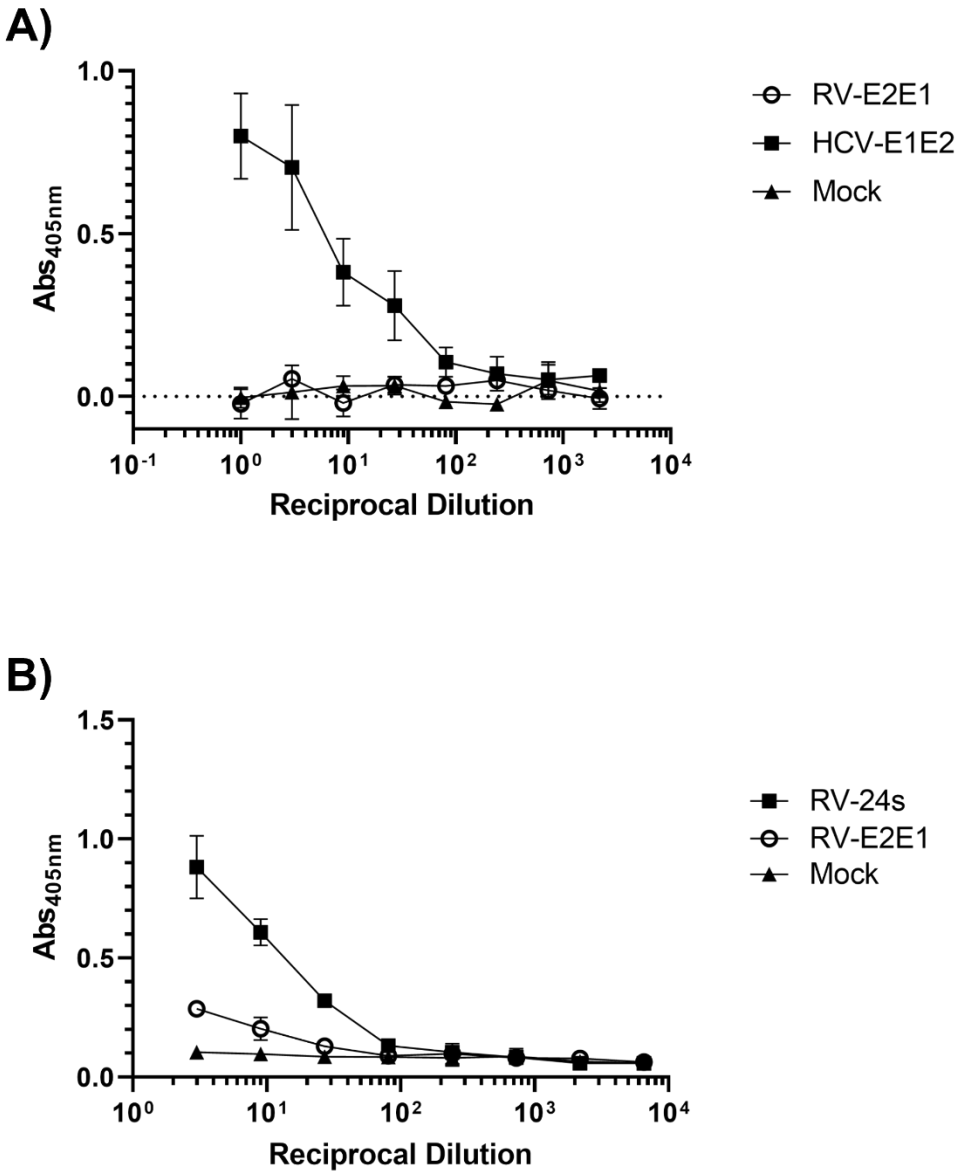

Figure 3. 4 ELISA detection of RV-E1.

A) GNA capture ELISA was performed to detect expression of RV-E1 in cell lysates. HCV-E1E2 (H77 isolate) was used as a positive control for the assay and mock cell lysates was used as a negative control. Lysates were serial diluted 3-fold, starting at a 1:3 dilution**. B)** Pelleted supernatant from RV-24s, RV-E2E1 and untransfected mock cells were serially diluted 3-fold and directly coated onto microtitre plates. Bound RV-E1 was detected using a mouse anti-RV-E1 monoclonal antibody at a 1 µg/mL. concentration. HCV-E1E2 was detected with AP33 used at a 1 µg/mL concentration. Error bars represent standard deviation.

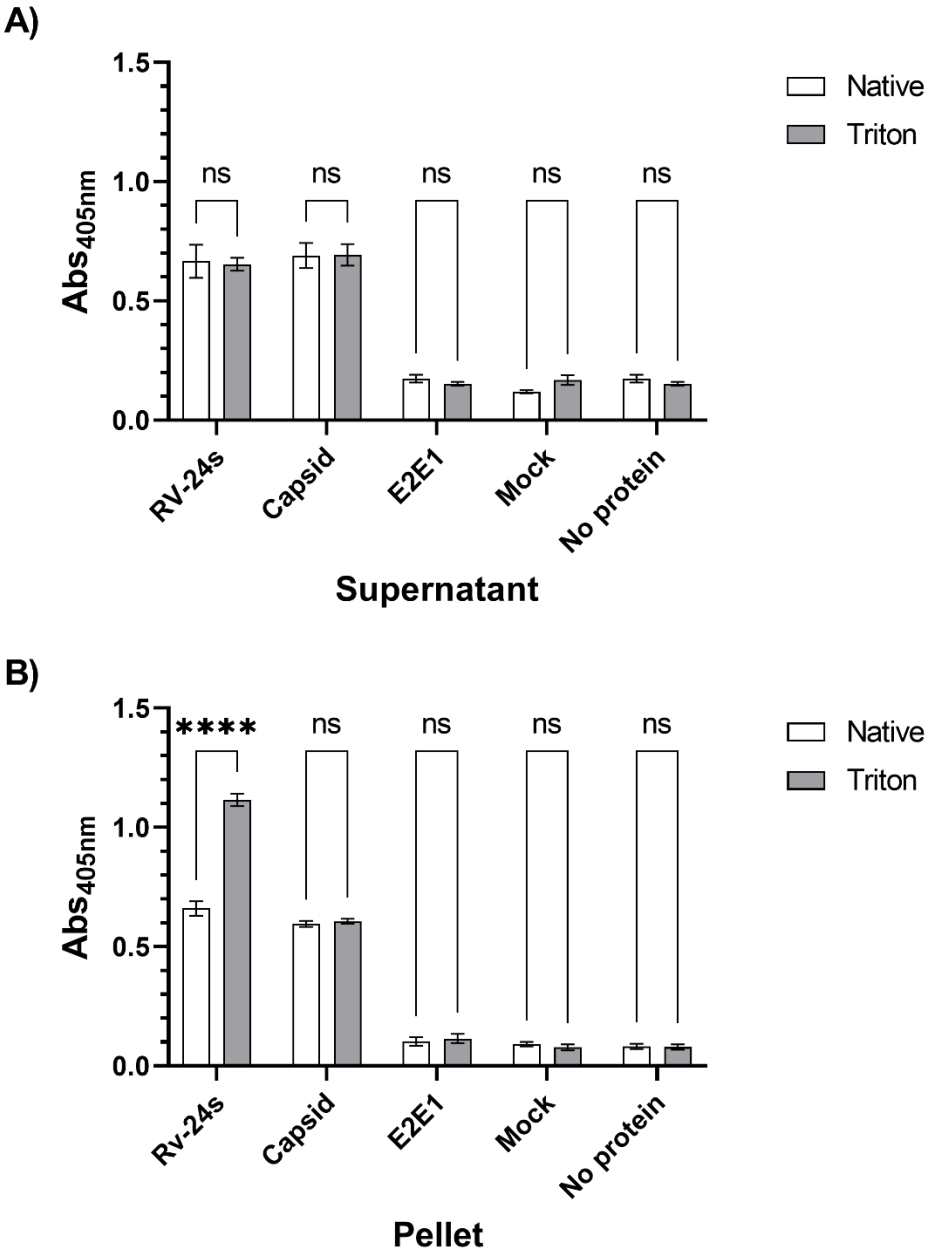

Figure 3. 5 Detection of RV-C in native and Triton treated pelleted supernatant by RV-C capture ELISA.

Supernatant from transiently transfected HEK-293T cells expressing RV-24s, RV-C, RV-E2E1 and untransfected mock cells was pelleted and added to microtitre plates coated with anti-RV-C at 1 µg/mL. Native pellets were untreated, triton treated pellets were incubated in 1% triton for 30 min at room temperature. Captured RV-C was detected with polyclonal anti-RV-C rabbit serum, 7w7, used at a 1:1000 dilution. Two-way ANOVA was performed to test for statistical significance. Error bars represent standard deviation. **** represents $p<0.0001$, ns represents $p>0.05$.

To further validate this system, a co-IP assay was performed to show that enveloped RV-C was associated with RV-E1. For this experiment, an anti-RV-E1 monoclonal antibody was captured on magnetic protein G beads and incubated with transfected cell supernatant. Following an overnight incubation and washing, captured complexes were eluted using 1% Triton and tested by western blot for the presence of RV-C. The rationale for this elution method was to test for RV-E1-associated enveloped RV-C which would provide clear evidence of RVLPs. Western blot analysis detected RV-C in the elution from anti-RV-E1 coated beads (Figure 3. 6A). Importantly, no RV-C was eluted from protein G beads coated with an anti-HCV-E2 antibody or from beads lacking an antibody. This showed that the capture of RV-C was antibody-dependent and not a result of non-specific binding to the protein G beads. The co-IP purified RV-C isolated was further characterised by a non-reducing SDS-PAGE followed by western blot (Figure 3. 6B). In the absence of the reducing agent, DTT, RV-C migrated as a single band with a molecular weight of approximately 70 kDa, the expected weight of a RV-C homodimer. Under reducing conditions, RV-C showed a molecular weight of approximately 36 kDa. In contrast, intracellular RV-C from RV-24s expressing cells, showed the presence of both monomeric and homodimer RV-C under non-reducing conditions. Taken together this data showed that expression of RV-24s in HEK293T cells leads to the secretion of enveloped, covalently linked RV-C homodimers that were associated with the RV-

E1 glycoprotein thus providing strong evidence for the presence of RVLPs.

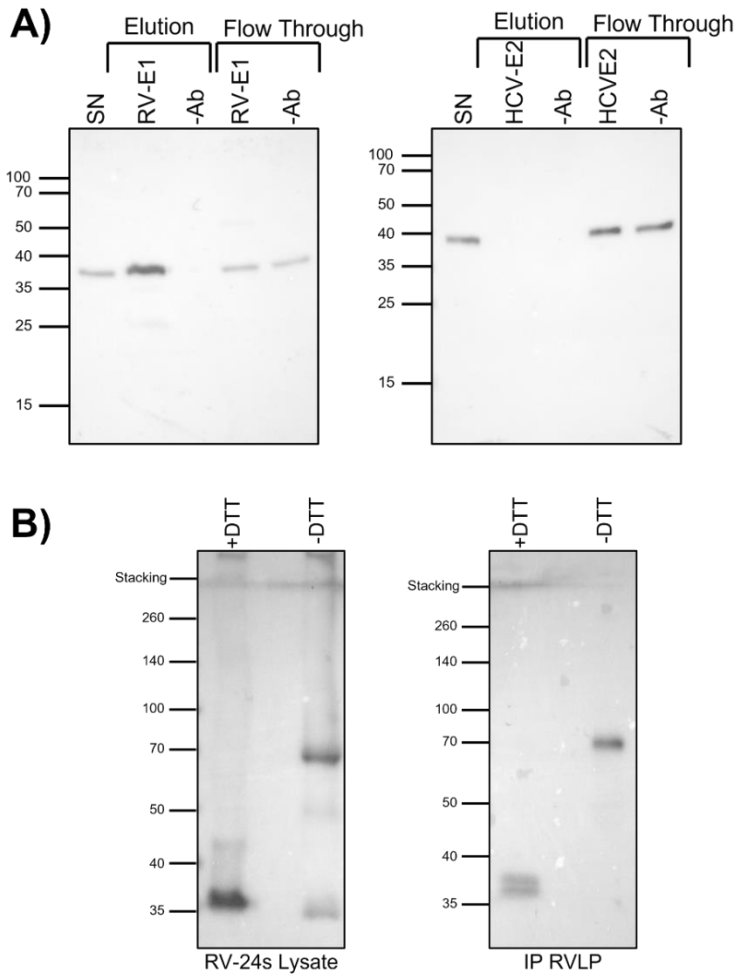

Figure 3. 6 Immunoprecipitation of RVLPs and non-reducing SDS-PAGE of intracellular and extracellular RV-C.

A) Immunoprecipitation of RVLPs from HEK-293T supernatant. Protein G beads were precoated with anti-RV-E1 monoclonal antibody and captured RVLPs were lysed in 1% triton. Release of RV-C from lysed RVLPs was detected by anti-RV-C western blot. Protein G beads without Ab and coated with anti-HCV-E2 antibody, 1:7, were used as negative controls. **B)** Non-reducing and reduced RVLP-transfected HEK-293T cell lysates and immunoprecipitated RVLPs were used in SDS-PAGE and RV-C was detected by western blot. Non-reduced samples were boiled in Laemmli buffer without DTT, reduced samples were boiled with DTT.

Finally, TEM was used to visualise RVLPs. Pelleted supernatants of RV-24s expressing HEK-293T cells were fixed in 3% glutaraldehyde, loaded onto copper grids and negatively stained. The electron micrographs showed that these pellets contained multiple pleomorphic structures in both mock and RVLP samples (Figure 3. 7). It was not possible to distinguish RVLPs using this method.

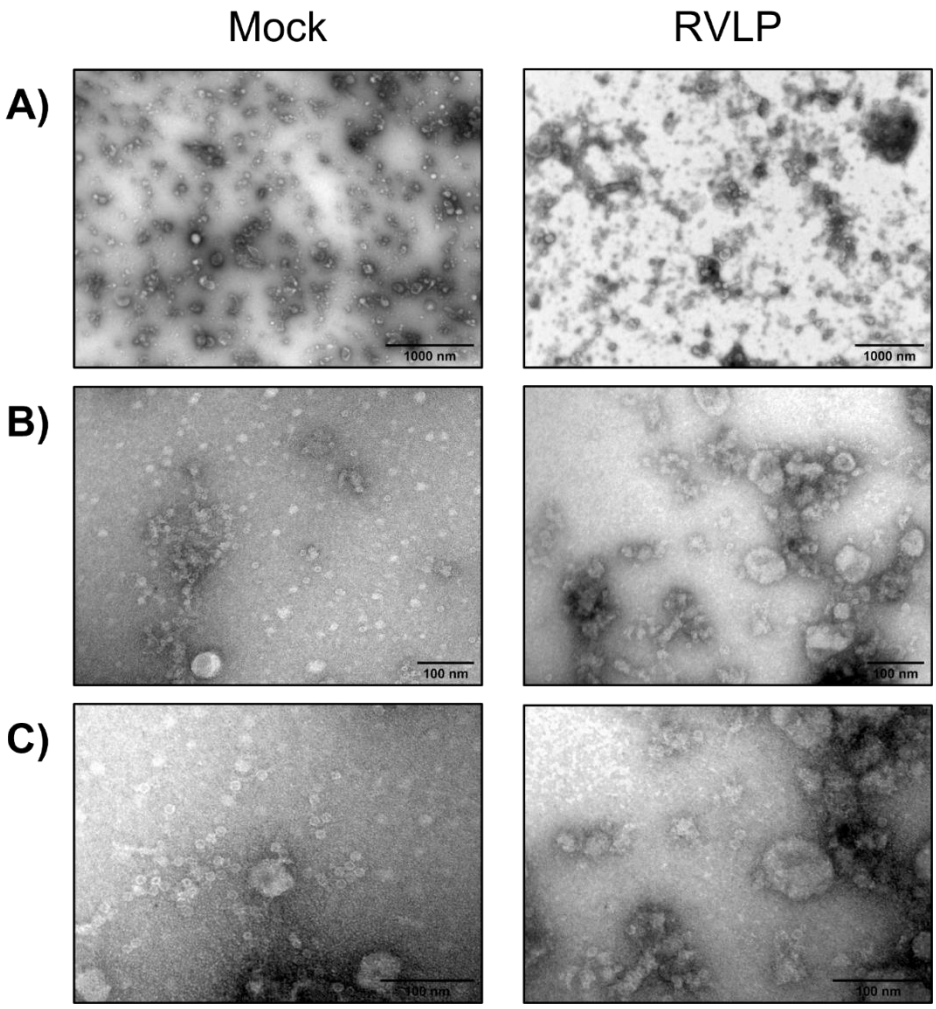

Figure 3. 7 Electron microscopy of pelleted RVLP and Mock HEK-293T Supernatant.

Supernatants were purified on a 20 % sucrose cushion and resuspended in 0.1 M sodium cacodylate, 3 % glutaraldehyde. Samples were loaded onto copper grids and negative stained. Images were taken at 16,500 x (**A**), 135,000 x (**B**) and 220,000 x (**C**).

3.3 Discussion

Previously described methods to produce RVLPs have made use of multiple different mammalian cell lines although the use of human cells and in particular the HEK-293T cell line, have not been reported in the literature. This cell line has been used to express a range of VLPs[360–364] and is routinely used in our laboratory for recombinant protein expression. When considering mammalian expression systems to produce human vaccines, and in particular constructs that encode viral glycoproteins, the use of a human based expression system allows for translational modifications that are more representative of the wild-type virus, which has implications for the antigenicity of a vaccine. For these reasons the HEK-293T cell line was assessed to produce RVLPs. Side-by-side comparison with the Vero cell line showed that RV structural proteins are expressed and secreted in HEK-293Ts. Interestingly expression of RV-24s was not detectible in Vero cells. This may be due to multiple factors; first, Vero cells originate from the species *Chlorocebus sabaeus* whilst the RV-24s sequence was codon optimised for human cell expression. Secondly the transient transfection method could be less efficient in Vero cells compared to HEK-293T cells. This factor could be overcome with an investigation into optimal conditions for transient transfection. However, given the successful expression of RVLPs using the HEK-293T cell line, optimisation of a Vero expression system was outside the scope of this project.

The expression data shown in this chapter confirmed that transient expression of RV-24s in HEK-293T cell cultures resulted in the

secretion of the three RV structural proteins and that RV-C was enveloped by a detergent-sensitive lipid membrane. Surprisingly, pelleted supernatant from RV-C or RV-E2E1 expressing cultures contained a detectable level of their respective structural proteins. This was in contrast to Hobman *et al.,*[327], who reported that the secretion of RV structural proteins was dependent on the expression of RV-C, RV-E2 and RV-E1. This difference could be explained by different detection sensitivities since different primary antibodies were used in this study compared to the previous described. Additionally, the pelleted samples produced for this work were concentrated using a sucrose cushion method which may result in the sedimentation of host cell debris. Given that all three RV structural proteins are tethered to a lipid membrane, it is likely that this background signal is the result of host cell debris. Previous studies used purified RVLPs that were separated by density on a sucrose gradient. This method would remove host-derived cell debris and thus remove the background signal. Another reason for the difference may be due high levels of expression in transiently transfected HEK-293Ts due to the constitutive expression of the SV-40 T antigen which increases plasmid replication in the nucleus resulting in greater expression efficiency[365–367]. Since the expression vector used in these experiments was the pcDNA3.1 which encodes an SV-40 ORI and would therefore be replicated within HEK-293T cells.

The isolation of detergent sensitive homodimeric RV-C is strong evidence for the presence of RVLPs. Non-reducing SDS-PAGE of the purified RV-C showed that this protein forms covalent homodimers

which is in line with previous studies[318]. RV-C contains two cysteine residues, Cys[153] and Cys[197], and crystal structures of residues 127-277 of RV-C have shown that the dimer has twofold symmetry with intermolecular disulphide bridges formed between Cys[153] and Cys[197], although Cys[153] has been identified as non-essential for RVLP assembly[368]. The mature RV virion has been estimated to contain approximately 230 RV-C homodimers[331] and these are arranged in parallel strands under the lipid envelope that run in a perpendicular orientation to the RV-E2E1 heterodimers on the virus surface[319,330].

The use of TEM to visualise virus particles has been well documented and it's use for visualising both intracellular and extracellular RV virions has been reported[369]. In this study applying TEM to pelleted cell supernatant showed the presence of multiple structures in both mock and RVLP samples, showing that host cell derived particles co-sediment with RVLPs when purified using the sucrose cushion method. The lack of distinguishable RVLPs also suggests that these particles are expressed at low levels. It is also important to highlight that all the TEM data published by the Hobman and Gillam research groups on RVLPs was on intracellular particles which can be clearly identified by the homogenous electron dense spherical structures within the lumen of the *cis* Golgi apparatus[327]. Other studies investigating infectious RV, purified using sucrose gradients have detected extracellular particles with electron dense cores and a double-shell architecture[329–331,369,370]. These structures were absent from the TEM data collected for this chapter. Furthermore, a protruding glycoprotein spike structure is often

not visible for RV[317], in contrast to other viruses such as coronaviruses which have clearly identifiable surface spike structures[371]. There are multiple approaches to improve this experiment which could be employed separately or simultaneously. Firstly, sample purity could be improved by further purifying RVLPs on a sucrose gradient. This method would allow for the separation of sub cellular particles based on density thus removing impurities and enriching for RVLPs. This method would require validation by collecting fractions of the sucrose gradient and performing a western blot for the three RV structural proteins. Fractions that contain RV-C, RV-E2 and RV-E1 could then be pooled and imaged. Secondly, immunogold labelling could be used to stain the sample once on the copper grid. A primary anti-RV-E1 antibody could be used followed by a gold conjugated secondary antibody. This would allow for specific identification of RVLPs, in addition the association of a gold particle of known size would allow for accurate measurements of RVLPs to be performed. This approach has previously been used to image HCVLPs[372]. Additionally, the transient transfection protocol could be optimised to increase RVLP production. Optimisation of this system would require varying the amount of plasmid used in each transfection and could also test a variety of different transfection reagents such as the commercial reagents, Lipofectamine (Thermo Fisher Scientific) or Trans-IT (Mirus Bio). Additionally, a stable transfected HEK-293T could be generated and compared to different transient systems to select the optimal culture conditions. Following optimisation, cell cultures could be scaled up to increase the amount of input material. Larger volumes of

supernatant could initially be purified on a 20 % sucrose cushion and resuspended pellet could then be pooled to increase the VLP density. Finally, different methods of sample preparation for TEM analysis could be explored. Common sample preparation requires directly coating a sample onto charged copper grids however one approach could be to pre-coat a copper grid with an anti-RV-E1 antibody prior to the addition of a VLP sample, thereby increasing the capture of RVLPs to the grid. A similar approach has been used to visualise HCV virions[123]. Ideally all of these improvements would be used simultaneously to generate robust informative TEM data.

This work has validated the expression of RVLPs using the HEK-293T cell line. Another approach to confirm the expression of RVLP and demonstrate functionality, would be to use a reporter system. One such system that has been reported is the reverse genetics system in which a cDNA clone of the RV genome was modified to replace the RV-24s ORF with a GFP reporter gene[373]. This plasmid was linearized and used as a template for *in vitro* transcription to produce mRNA transcripts that were then transfected into a RV-24s stable expressing BHK-21 cell line. This led to the encapsidation of reporter viral genomes into the RVLPs and thus produced reporter viruses were capable of single round of infection that could then be measured by GFP expression in the permissive cell line. Further work by Claus *et al.,*[316] used this system to identify a potential genome packaging signal located between nucleotides 3986-5284. This was confirmed when insertion of this region into a SINV replicon and resulted in

encapsidation of progeny RNA into RVLPs. With this information it could be possible to develop a simpler RV based reporter system in which producer cells are co-transfected with RV-24s and a reporter plasmid in which the reporter gene is flanked by the RV packaging signal. A similar approach has been used for a SARS-CoV2 VLP reporter system[364] in which the genome packaging signal was placed upstream of a luciferase reporter gene which was subsequently packaged into VLPs and expressed in cell lines permissive to SARS-CoV2 entry.

Towards the end of this project, an attempt to recapitulate a RVLP reporter system was made. cDNA synthesis was performed on RNA extracted from a single dose of the MMR vaccine. Unfortunately given time constrains of this project, a full cDNA genome of the RA27/3 genome was not recovered. Future work should establish a reporter system to further aid the validation of RVLP-based chimeras.

Chapter 4 Design and Expression of Chimeric Virus-Like Particles

4.1 Introduction

The primary aim of this project was to investigate the use of RVLPs to incorporate HCV envelope proteins as a potential vaccine candidate for HCV. A successful HCV B cell targeting vaccine will likely require the presentation of correctly folded HCV-E1E2 ectodomains to ensure that nAbs targeting key antigenic regions, such as those defined by mAbs AR3, 4 and 5, are elicited upon vaccination[18]. Thus, ensuring the correct folding of the HCV-E1E2 was critical criteria for the screening of chimeras.

The previous chapter detailed the establishment and validation of the RVLP system in our laboratory. Compared to other VLP producing systems which can require multiple plasmids at highly specific ratio such as SARS-CoV2 VLPs[364], the expression of RVLPs required the transfection of a single plasmid encoding the RV-24s region. Previous studies have demonstrated that RVLP assembly requires the correct trafficking of RV-E2E1 to the budding site at the *cis* Golgi compartment[320]. Trafficking of the RV-E2E1 is mediated by TMD and cytoplasmic regions of these proteins. RV-E1$_{TMD+Cyt}$ harbour a ER retention signal[325] and export to the Golgi is mediated by RV-E2$_{TMD}$ as evidenced by the observation of chimeric VSV-G-E2$_{TMD+Cyt}$ accumulation in the Golgi network when expressed in CHO cells[326]. RV-E2$_{TMD+cyt}$ regions are critical for heterodimerisation[320] which results in the RV-E1 ER retention signal becoming masked leading to export to

the Golgi in a COPII mediated manner[327]. RV-E1$_{cyt}$ region is not critical for RVLP assembly, however virions appear to accumulate within the Golgi lumen and are not secreted when this region is replaced with analogous regions of VSV-G[320]. Whilst these experiments were informative, they provided limited insight into the structural flexibility of RVLPs. For example, fusion of RV-E1$_{TMD+cyt}$ to the VSV-G$_{ecto}$ abolished RVLP formation confirming the importance of the formation of the RV-E2E1 heterodimer in RVLP assembly. However, in this study there was no chimera included in which dimer forming ectodomains were fused to each of the RV E C-termini. Thus, it was unclear if RVLP assembly could tolerate the inclusion of two foreign envelope protein ectodomains. A level of structural flexibility has been demonstrated in the attenuated full-length RV platform[347,348].Insertion of HIV-GP140 epitopes fused to the RV-E2$_{TMD}$ have been shown to incorporate in the secreted virions[348]. This demonstrated that RV assembly can tolerate the insertion of small foreign epitopes when fused to the RV-E2 C-termini. However, this construct also included full length RV-E1 and RV-E2 proteins, which would facilitate assembly, and it is unclear if the chimeric HIV-RV-E2 protein was incorporated passively since this protein would likely be present at the site of assembly.

The objectives of this chapter were to first design chimeric RV-HCV glycoproteins using predictions of the TMD regions for each of the envelope glycoproteins to produce chimeras with different HCV-E$_{ecto}$ and RV-E$_{TMD+cyt}$ fusion points. Secondly, chimeric glycoproteins were generated using homology recombination cloning techniques to

produce constructs in which chimeric glycoproteins were placed downstream and in frame of RV-C. These constructs were expressed and characterized using anti-HCV-E antibodies to assess folding and VLP formation.

4.2 Results

4.2.1 Design of Chimeric Rubella- Hepatitis C Virus Glycoproteins

The first stage of designing the RH constructs was to define the TMD regions of the HCV and RV E proteins. Prediction of the TMD regions of each protein was made using the DASTM tool[355]. This algorithm predicts the TMD based on a hydrophobicity profile determined by a sliding window consisting of 11 residues and based on the Engelman-Steitz hydrophobicity scale[355,374]. A comparison is then made between the query sequence and a reference library of known transmembrane proteins[355]. This approach provides an important advantage over other tools which make predictions based upon a hydrophobicity profile alone which results in wrongly labelling hydrophobic regions of globular proteins are TMD regions[355].

Predictions of RV and HCV envelope protein TMDs were made using the deduced amino acid sequences of the RA27/3 and H77 isolates, respectively (Figure 4. 1). TMD regions were defined as residues that scored 2.5 and above by the DASTM tool. The TMD regions of HCV-E1 and HCV-E2 were predicted encompass residues 353-378 and 716-734, respectively, whereas the RV-E2 and RV-E1 TMD regions were predicted to include residues 526-570 and 1033-1050, respectively. These predictions are similar to the TMD regions defined in the

literature for these proteins[326,375,376]. The results of these predictions were used to define the TMD and the ectodomain regions of each viral E protein.

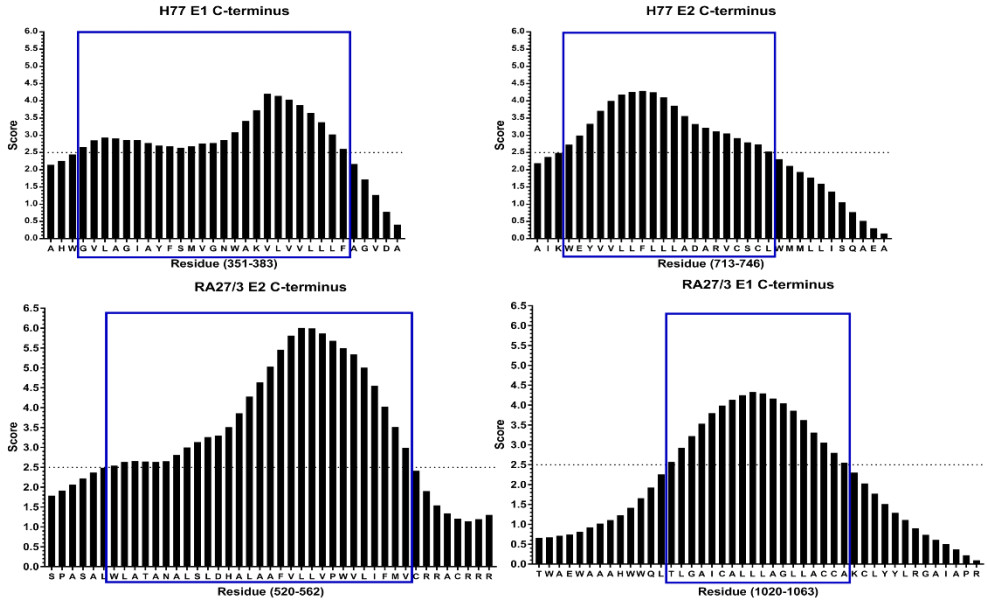

Figure 4. 1 Prediction of TMD regions for RV and HCV envelope glycoproteins using DASTM.

Graphical representation of TMD predictions made using the DASTM online tool. HCV-E1 and HCV-E2 predictions were made using the H77 isolate (GenBank accession AF011751), with amino acid residue numbering corresponding to their position in the full-length polyprotein sequence. RV-E2 and RV-E1 TMD predictions were made using the vaccine strain RA27/3 (GenBank accession JF727654) with residue numbering corresponding to the position in the subgenomic 24s ORF. Blue boxes highlight the predicted TMD regions.

The prediction of the TMD regions allowed a panel of five RH constructs to be deigned (Figure 4. 2). Three of these constructs, RH1, RH2 and RH5 were designed to fuse HCV-E_{ecto} to the RV-E_{TMD} regions, since the TMD regions of the RV-E proteins are required for trafficking and VLP assembly. The junctions for RH1 had been previously designed by Jonathan Ball and Felix Ray. A further two constructs, RH3 and RH4

were designed to include the HCV-E_{TMD} regions with the RV-E_{cyt} residues. These constructs because the HCV-E TMD domains have important roles in HCV-E1E2 heterodimerization and it was unclear if the cytoplasmic domains of RV-E proteins would facilitate VLP assembly.

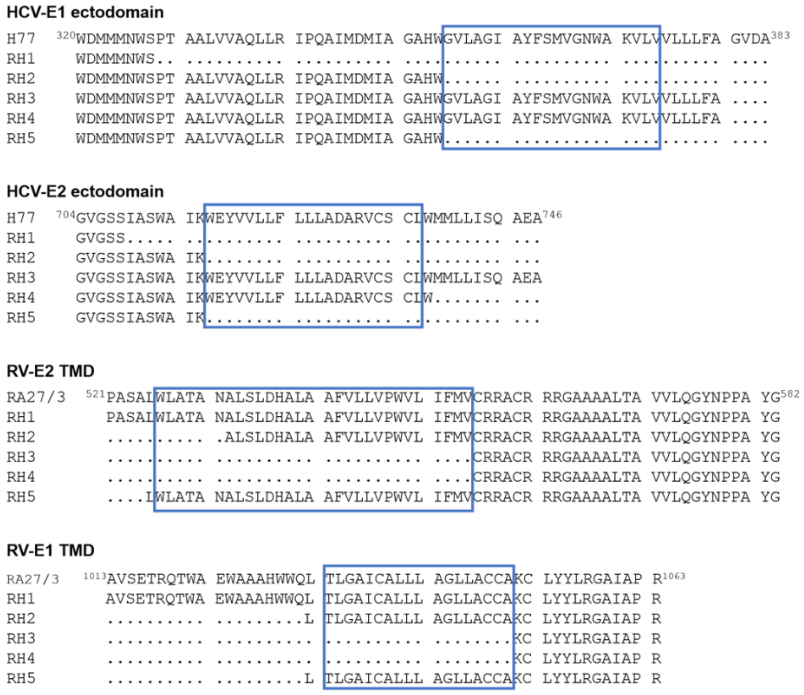

Figure 4. 2 Alignment of RH chimeric glycoprotein amino acid sequences.

HCV regions were numbered according to the H77 reference isolate polyprotein. RA27/3 regions are numbered according to the residue number in the structural 24s ORF. Blue boxes demark the predicted TMD regions of each glycoprotein.

4.2.2 Validation of Rubella virus Capsid Cleavage from Hepatitis C virus E1E2 glycoproteins

Having designed the RH chimeric glycoproteins, the next step was to assess if these constructs could be expressed *in cis* or *trans* with RV-C. The RV-E2sp is located at the C-terminus of RV-C and is required for

translocation of the RV-$E2_{ecto}$ into the ER lumen[359] and retention of RV-C to the intracellular membranes[377,378]. *Cis* expression of RH glycoproteins would require efficient cleavage of the RV-E2sp from the N-terminus of the HCV-$E1_{ectodo}$. To test this, a chimeric construct was designed in which the RV-C gene replaced the HCV-E1sp, termed RcapHE1E2. This was made by amplifying RV-C and HCV-ΔspE1E2 by PCR with primers that introduced homologous tags for recombination (Figure 4. 3A). Homologous recombination was performed using In-fusion cloning and was confirmed with colony PCR screening (Figure 4. 3B) and Sanger sequencing. To assess the cleavage of RV-E2sp from HCV-E1, RcapHE1E2 was used to generate pps using the MLV system, since infectious pps would require cleavage of the RV-E2sp junction. Following expression RcapHE1E2pps were tested in an infectivity assay in the Huh 7 cell line (Figure 4. 3C). Interestingly, pps generated using the RcapHE1E2 plasmid showed no significant difference ($p>0.05$) in RLU compared to HCV-E1E2pps, demonstrating that sufficient cleavage and translocation of HCV-E1 occurs when placed downstream of a RV-E2sp sequence. Additionally, the co-expression of RV-C with HCV-E1E2 also lead to no significant difference in RLU ($p>0.05$) compared to HCV-E1E2pps however the mean RLU was decreased. This was likely due to competition between RV-C and HCV-E1E2 plasmid promoters for cellular expression machinery. This data showed suggested that *cis* expression of chimeric glycoproteins with RV-C would be a valid approach to chimera design.

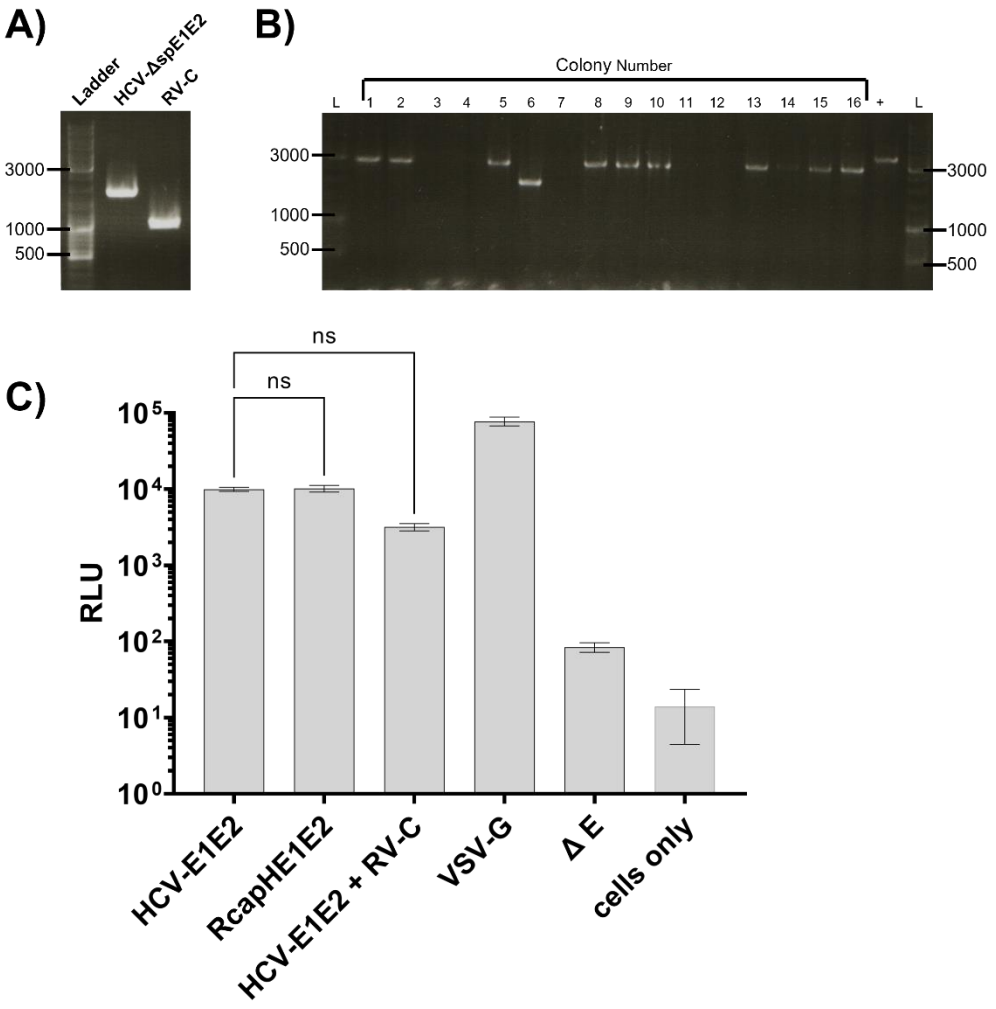

Figure 4. 3 Validation of RV-E2sp cleavage form HCV-E1.

A) PCR amplification of RV-C and HCV-ΔspE1E2 was confirmed by DNA electrophoresis. **B**) Amplicons ligated and subcloned in to pcDNA3.1 and a colony screen PCR was performed on transformed *E. coli* cells. **C**) Infectivity assay using Huh 7 cells. PPs were generated using a MLV backbone system and co-expression with the following glycoprotein encoding plasmids; full-length HCV-E1E2 (H77 isolate), RcapHE1E2, full-length HCV-E1E2+ RV-C, VSV-G. ΔE control served as a negative control that lacked a viral glycoprotein. Cells only served as an addition negative control to identify background luminescence of non-infected Huh 7 cells. Statistical significance was determined using one-way ANOVA, non-significance (ns) was determined when $p>0.05$.

4.2.3 Assembly of Chimeric constructs

To generate recombinant plasmids of the RH panel, primers were designed to amplify the HCV-E_{ecto} regions and introduce large tags via the HCV-$E1_{ecto}$ reverse primer and HCV-$E2_{ecto}$ forward primer that would encode the RV-$E2_{TMD/cyt}$ region upon homologous recombination. The first attempt to generate the RH2 and RH3 constructs used Gibson assembly[379] (Figure 4. 4). Initially, a pcDNA3.1 plasmid encoding wt RV-24s sequence was used as a template for an SDM reaction to delete residues 301-1032 for Rucas2 and 301-1050 for Rubcas3 and introduce a restriction site for the BsiWI restriction enzyme (Figure 4. 4A). Amplification of the wt RV-24s plasmid was successful with both sets of Rubcas primers. High molecular wight DNA bands were observed when separated by electrophoresis, however the agarose concentration was not low enough to provide sufficient resolution to determine an accurate molecular weight for each amplicon, which would be expected to be approximately 6.5 Kb (Figure 4. 4A). The PCR products were used in an SDM reaction and transformed into competent *E. coli* cells and confirmed by sangar sequencing. The HCV-E_{ecto} regions were amplified and subcloned into BsiWI digested Rubcas vectors using Gibson assembly (Figure 4. 4B). Following transformation of *E. coli* cells, colony screen PCRs were performed to confirm the insertion of chimeric glycoprotein sequences (Figure 4. 4C). All screened colonies showed the presence of Rubcas vectors and not inserts of an expected 3 kb size that would correspond to a complete chimeric construct. The Gibson assembly reactions were repeated twice

for both RH2 and RH3 constructs, and these failed to produce amplicons of the correct size. This data shows that this cloning approach was not suitable to generate RH chimeras.

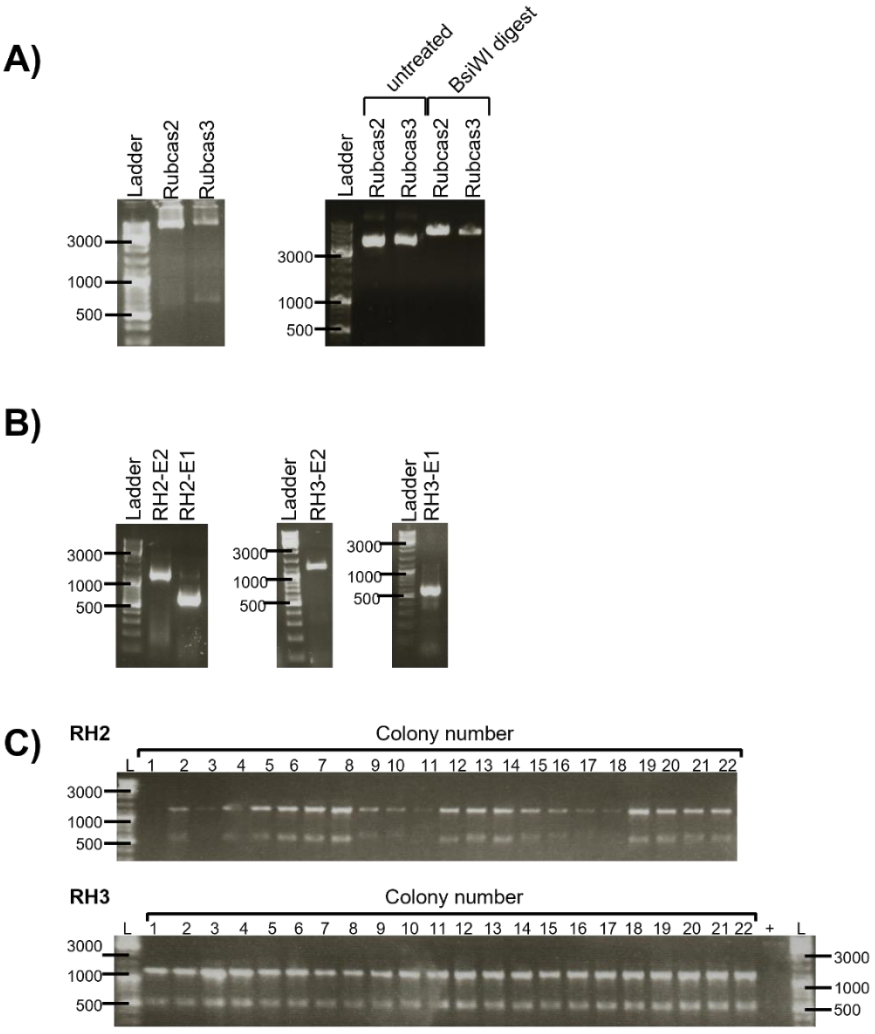

Figure 4. 4 Gibson assembly cloning approach to generate RH chimeras.

A) Rubcas constructs were generated by PCR amplification from pcDNA3.1-RV-24s template with RubcasF and RubcasR primers which was confirmed by DNA electrophoresis. Rubcas products were ligated using a site directed mutagenesis approach. Rubcas plasmids were linearised by BsiWI digestion prior to Gibson assembly. **B**) HCV envelope glycoprotein ectodomains were amplified by PCR with primers to introduce homologous recombination tags in addition to the RV-E2-TMD region. Amplification was confirmed by DNA electrophoresis and these products were used in a Gibson assembly reaction with respective linearized Rubcas vectors. **C**) Colony screening PCRs of RH2 and RH3 transformed *E. coli* colonies using T7F and bGHR primers. Positive control (+) was pcDNA3.1-RV-24s. Numbers denote in each ladder (L) lane correspond to band size (bp).

The second cloning approach used the In-Fusion cloning method and the RV-24s template was the codon optimised sequence described in the previous chapter. The codon optimisation process reduced the GC content from 69 % to 59 % (Figure 3. 1A) making it more suitable for molecular techniques. In contrast to the previous cloning approach the Rubcas vectors were not produced. Instead of this, the vector was amplified by PCR using a reverse primer specific to the 3' end of the RV-C sequence and a forward primer specific to the RV-$E1_{TMD}$. The amplification of the HCV-E_{ecto} regions was the same as previous the previous method with the exception that the RV specific tags matched codon optimised sequences.

PCR amplification of the RH vectors was successful and produced large molecular weight bands (Figure 4.5A). The amplification of all HCV-E_{ecto} was also successful and produced amplicons of approximately 700 bp and 1.2 Kb for RH-E1 and RH-E2, respectively (Figure 4. 5A). The vector, RH-E1 and RH-E2 components of each construct were recombined in a 2.5 µL In-Fusion reaction. Colony PCR screening confirmed the presence of 3 Kb amplicons between the T7 and bGH regions of the pcDNA3.1 plasmid (Figure 4. 5B). Some bands were observed that were above 3 Kb, which would correspond to full length RV-24s region and shows that the pcDNA3.1-RV-24s template was present from the vector PCR amplification. Colonies that showed an insert of the expected size for a complete chimera were selected for sequencing and confirmed to be correct (Figure 4. 5B).

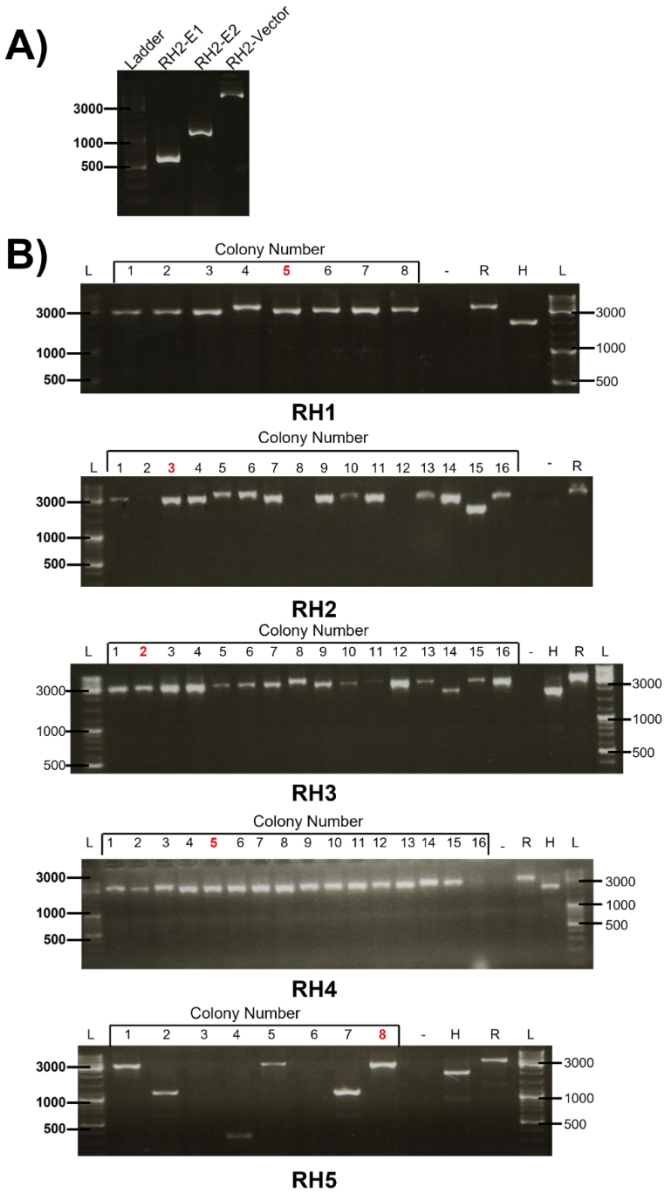

Figure 4. 5 In-Fusion cloning approach to produce generate chimeric constructs.

A) An example of PCR amplification of RH-E1, RH-E2 and RH-Vector products separated by DNA electrophoresis on a 2% agarose gel. **B**) Colony screen PCR products generated using T7F and bGHR primers to amplify plasmid isolated from transformed *E. coli* colonies. Negative (-) control was a PCR that lacked a plasmid template, pcDNA3.1-RV-24s (R) and pcDNA3.1-HCV-E1E2 (H) controls were included as positive PCR controls and to identify template flowthrough. The numbers noted in each ladder lane referred to the size of each band (bp). Colonies that were confirmed by Sanger sequencing and used in future expression experiments are coloured in red.

4.2.4 Expression of RH Chimeras in the HEK-293T cell line

To test the RH panel, the plasmids were expressed in HEK-293T cells using the process described for RVLPs in in chapter 3. HCVpps and RVLPs were also expressed as positive controls for HCV-E1E2 and RV-C, respectively. The RcapHE1E2 plasmid (described in section 4.2.2) was also included.

Intracellular HCV-E2 was detected by western blot with a humanized AP33 antibody (Figure 4. 6). The strongest signals were present in the HCVpp and RcapHE1E2 lysates followed by RH5, RH1 and a faint signal for RH2, RH3 and RH4. This variation in E2 signal was not due to variable sample loading since the samples were normalized for total protein and the actin loading control showed similar levels of protein per lane (Figure 4. 6). The migration of the RH-E2 proteins was comparable to HCV-E2, with migration corresponding to approximately 65 KDa. This molecular weight was in line with previously published values[380]. RV-C was detected all RH, RV-24s and RV-C expressing cell lysates. This protein produced a band of approximately 36 KDa which was in line with the observations in chapter 3 and published values. HCV-E1 was detected in the lysates of HCVpp and RcapHE1E2 with an approximate molecular wight of 35 KDa, whilst faint signals were observed for this protein in all the chimera lysates (Figure 4. 6).

Extracellular viral proteins were detected by western blot on sucrose pelleted supernatants (Figure 4. 6). Samples were normalized by total protein loaded per lane of the acrylamide gel. Of the RH chimeras, RH5 showed a strong signal for HCV-E2 whilst RH1 and RH2 produced faint

signals. RH3 and RH4 lanes did not show a detectable signal for HCV-E2. RH5-E2 has a higher molecular weight than the HCV-E2 incorporated into HCVpps, with the most species corresponding to 65-70 KDa or 70-100 KDa, respectively. Differences in predicted molecular weight do not account for this change and could be the result of differential glycosylation between the two glycoproteins which would in turn alter the migration pattern. Release of RV-C was also observed in RH5, although RH2 produced a similar signal. The strongest RV-C signal was detected in the RV-24s pellet. Interestingly, pelleted RH5 was the only chimera sample to be recognised by the anti-HCV-E1 antibody. Furthermore, RH5 showed a higher level of HCV-E1 than HCVpps. The RH5-E1 protein had an approximate molecular weight of 39 KDa which was heavier than HCV-E1 which had a molecular weight of 35 KDa.

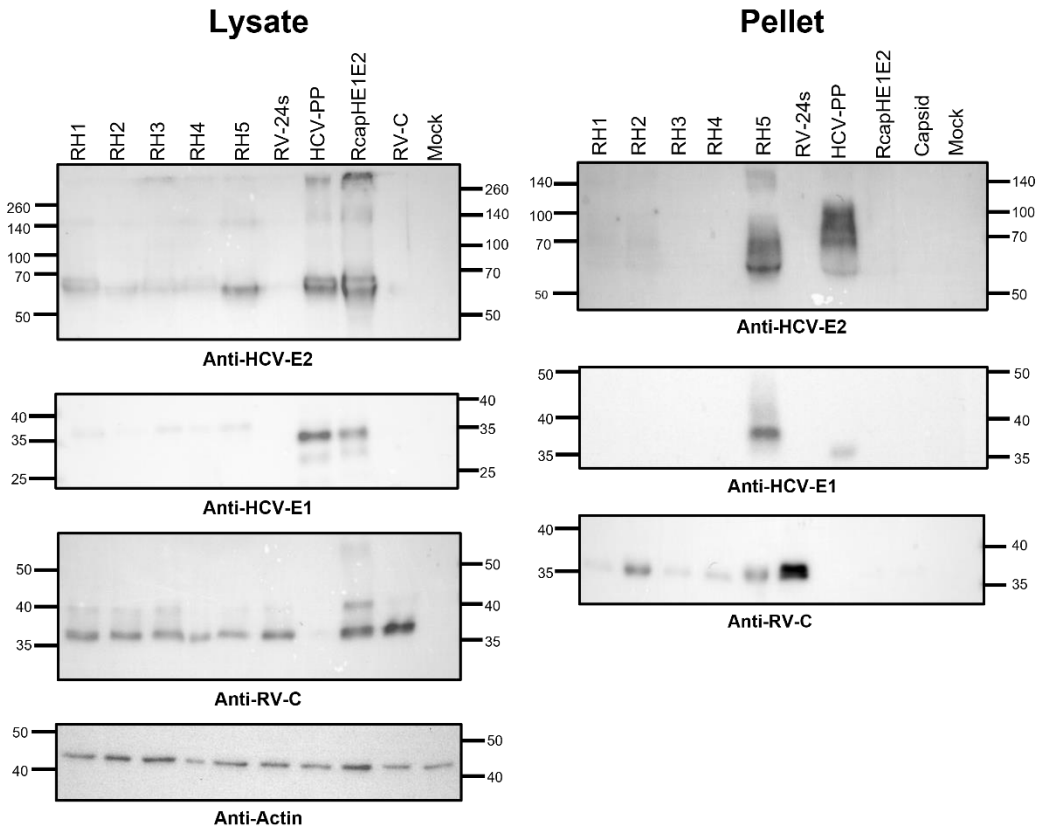

Figure 4. 6 Western bot detection for the expression of RH chimeras in the HEK-293T cell line.

HEK-293T cells were seeded in 10 cm^2 dishes 24 hrs prior to transfection with 2 µg of each plasmid and grown for 72 hrs. Cells were lysed in lysis buffer and supernatant was pelleted on a 20 % sucrose cushion and resuspended in 50 µL PBS. All samples were quantified by BCA total protein estimation assay. A total of 10 µg and 5 µg of total protein was loaded per lane of a 12 % polyacrylamide gel for lysate and pellet samples, respectively. Proteins were separated by SDS-PAGE and transferred to PVDF membranes using a Semi-dry transfer method. Humanised AP33 was used at a concentration of 1.5 µg/mL to detect HCV-E2, a commercial mouse anti-HCV-E1 antibody was used to detect HCV-E1 at a concentration of µg/mL. RV-C was detected using the mouse antibody, 9B11 antibody at a concentration of 1 µg/mL. As a loading control for the western blot assay, actin was detected using a mouse anti-actin antibody at a final concentration of 0.5 µg/mL. Mouse and Human antibodies were detected with anti-mouse-HRP and anti-Human-HRP secondary antibodies, respectively, each used at a 1:1000 dilution.

Next, a GNA capture ELISA was used to investigate the expression of HCV-E2 and gain insight into the conformation of the HCV-$E2_{ecto}$ for each of the chimeras. Two well characterised anti-HCV-E2 antibodies were used to detect HCV-E2, the mouse derived AP33 which binds to the linear domain E epitope in a semi-conformational fashion[381], and the conformation-sensitive, human derived antibody,1:7[211]. Both intracellular and extracellular HCV-E2 was measured using cell lysates and pelleted supernatant, respectively (Figure 4. 7). Intracellular HCV-E2 was detected for all chimeras with both antibodies producing signals above the background values observed in the negative controls (Figure 4. 7A). Of the chimeras, RH5 gave the highest signal for both antibodies, although these values were lower than the positive controls with exception to the 1:7 signal for RcapHE1E2, which had a low signal. In agreement with the western blot data, the highest extracellular RH-E2 signal was detected in pelleted RH5 supernatant which was significantly higher than the background signal produced by expression of HCV-E1E2 for both AP33 ($p<0.0001$) and 1:7 ($p<0.01$) antibodies (Figure 4. 7B).

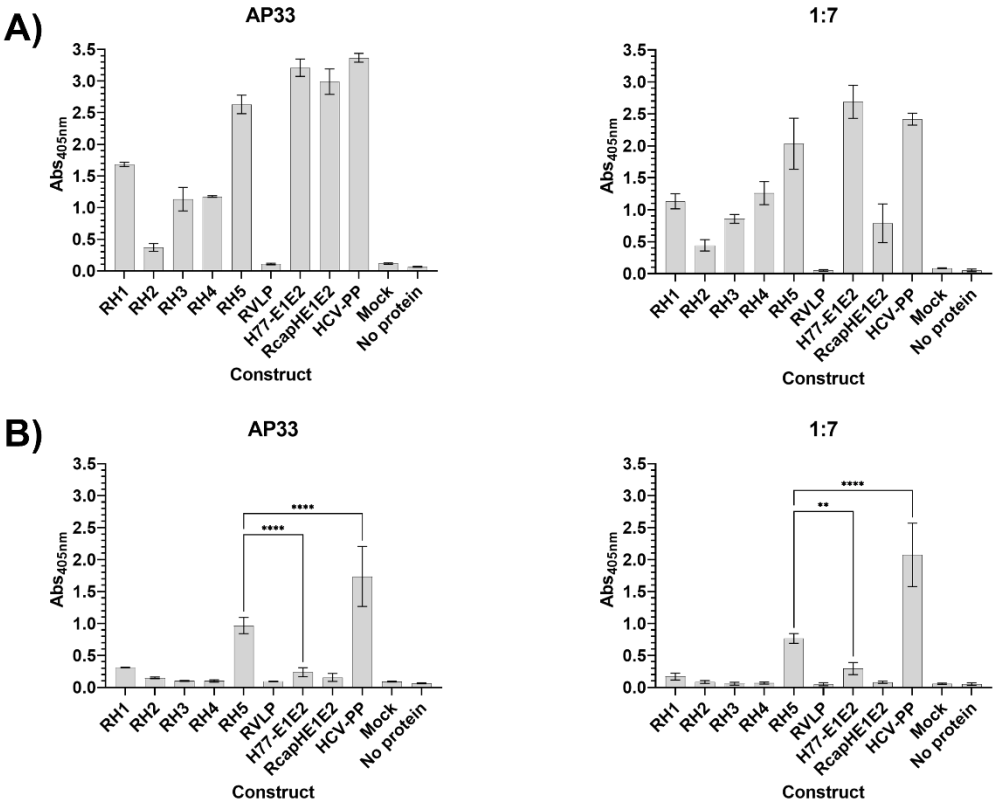

Figure 4. 7 GNA-capture ELISA of RH chimera expressing HEK-293T cell lysates and pellets.

ELISA plates were precoated with GNA lectin at a final concentration of 10 µg/mL in coating buffer. **A**) Lysates of transfected HEK-293T cells were captured on to GNA coated plates. Lysates samples were normalised to a total protein concentration of 1 mg/mL prior to capture. **B**) Pelleted supernatant harvested from transfected HEK-293T cells was loaded onto GNA coated ELISA plates. Samples were normalised to a total protein concentration of 0.5 mg/mL. Detection of bound HCV-E2 was achieved using humanised AP33 and 1:7 each at a final concentration of 10 µg/mL. Bound primary antibodies were detected using an anti-Human-AP conjugated secondary antibody at a 1:2000 dilution. Bound AP activity was measured by addition of a pNPP substrate. Absorbance was measured 30 min after the addition of pNPP. Statistical significance was determined using an one-way ANOVA, $p<0.0001$ (****), $p<0.01$ (**).

4.2.5 Expression of RH Chimeras in the HEK-293F Cell line

Expression of the chimera panel was also tested in the suspension cell line, HEK-293F. These cells are derived from the same ancestor as HEK-293T but lack the SV-40 T antigen. These cells offer advantages over HEK-293T, such as greater recombinant protein expression and maintenance in serum-free media. In addition, these cells have been approved for commercial vaccine production.

The expression of each chimera was performed in a scaled down, 15 mL culture. The experimental design mimicked that of the HEK-293T expression experiments except for the HCVpp control group. Initial GNA capture ELISA data of HEK-293F pellets no significant level of HCV-E2 was seen in HCVpp producer cells. An infection assay was performed using the supernatant of HCVpp and VSVpp producing HEK-293F cells. There was no detectable RLU produced in infected Huh 7 cells infected with $HCVpp_{HEK\text{-}293F}$ and VSV-G infection exhibited a significant reduction in RLU. This data confirmed that HEK-293F were unable to produce detectable levels of HCVpp. As such the HCVpp control group was expressed in HEK-293T.

Detection of viral proteins was confirmed by western blot analysis (Figure 4. 8). A similar pattern of expression was observed in HEK-293F to HEK-293T. In this system, RH5 produced the highest signal for HCV-E2 in the pelleted supernatant, and it had an apparent molecular weight of approximately 70 KDa. However, a higher molecular weight band was also observed of 140 KDa, possibly representing a homodimer, was observed in this lane. Faint signals for HCV-E2 were

detected in the pellets of RH1 and HCV-E1E2. Interestingly, all pellet samples from cultures expressing RV-C showed signals for this protein. In contrast to the HEK-293T expression data, RV-24s showed a weaker signal compared to the chimeras with RH4 and RH5 showing the highest levels of secreted RV-C.

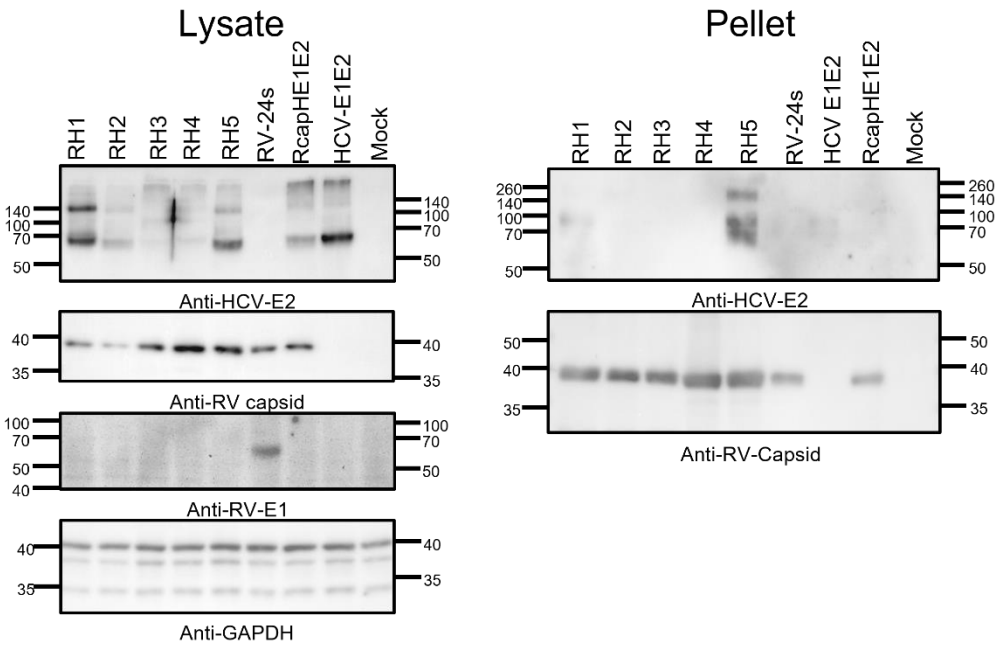

Figure 4. 8 Western bot detection for the expression of RH chimeras in the HEK-293F cell line.

HEK-293F cells were seeded at 0.7x10^6 cells/mL in 15 mL cultures 24 hrs prior to transfection with 15 µg of each plasmid and grown for 72 hrs. Cells were lysed in lysis buffer and supernatant was pelleted on a 20 % sucrose cushion and resuspended in 50 µL PBS. All samples were quantified by BCA total protein estimation assay. A total of 10 µg and 5 µg of total protein was loaded per lane of a 12 % polyacrylamide gel for lysate and pellet samples, respectively. Proteins were separated by SDS-PAGE and transferred to PVDF membranes using a Semi-dry transfer method. Humanised AP33 was used at a concentration of 1.5 µg/mL to detect HCV-E2. RV-C was detected using the mouse antibody, 9B11 antibody at a concentration of 1 µg/mL. RV-E1 was detected using a mouse anti-RV-E1 antibody at a final concentration of 1 µg/mL. As a loading control for the western blot assay, GAPDH was detected using a goat anti-GAPDH antibody at a final concentration of 0.5 µg/mL. Mouse and Human antibodies were detected with anti-mouse-HRP and anti-Human-HRP secondary antibodies, respectively, each used at a 1:1000 dilution. Bound goat antibody was detected using anti-goat-HRP at a 1:5000 dilution.

ELISA data for the HEK-293F expression showed a similar pattern to the HEK-293T data. The RH5 pellet produced the highest signal for both AP33 and 1:7 which was significantly higher than the H77-E1E2 background signal ($p<0.0001$) (Figure 4. 9). Interestingly, background signals for HCV-E1E2 and RcapHE1E2 control groups produced higher signals than in HEK-293F than in HEK-293Ts. This increase in background signal was likely due to the increased cell density of HEK-293F cultures which resulted in sedimentation of more cellular debris.

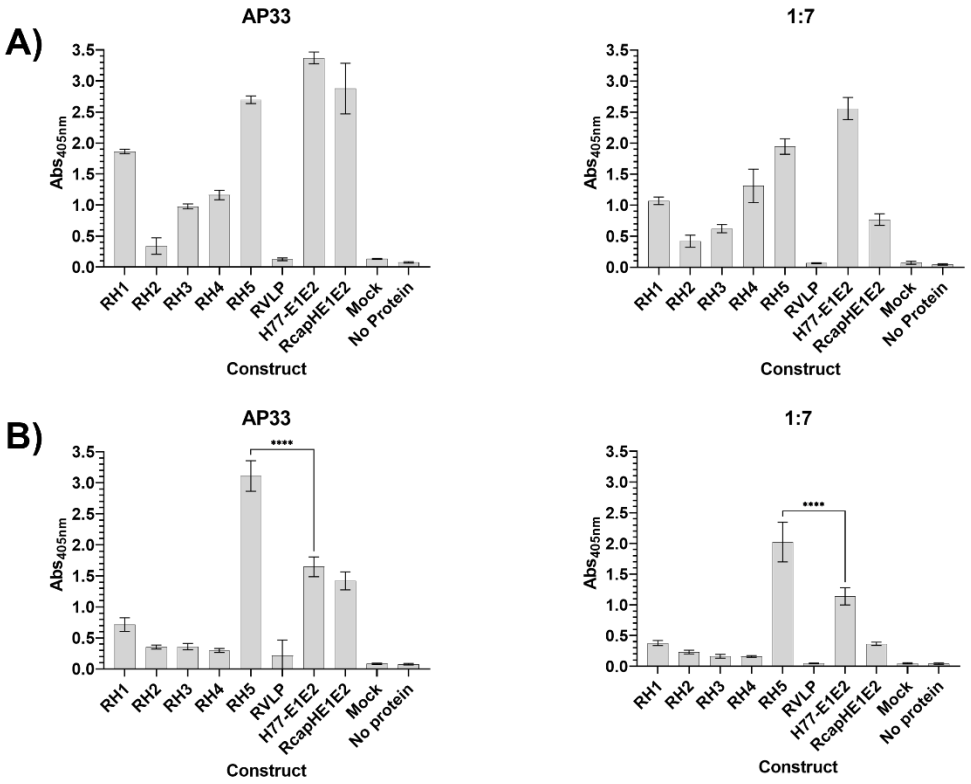

Figure 4. 9 GNA-capture ELISA of RH chimera expressing HEK-293F cell lysates and pellets.

ELISA plates were precoated with GNA lectin at a final concentration of 10 µg/mL in coating buffer. **A**) Lysates of transfected HEK-293F cells were captured on to GNA coated plates. Lysates samples were normalised to a total protein concentration of 1 mg/mL prior to capture. **B**) Pelleted supernatant harvested from transfected HEK-293T cells was loaded onto GNA coated ELISA plates. Samples were normalised to a total protein concentration of 0.5 mg/mL. Detection of bound HCV-E2 was achieved using humanised AP33 and 1:7 each at a final concentration of 10 µg/mL. Bound primary antibodies were detected using an anti-Human-AP conjugated secondary antibody at a 1:2000 dilution. Bound AP activity was measured by addition of a pNPP substrate. Absorbance was measured 30 min after the addition of pNPP.

The ELISA expression data for both HEK-293T and HEK-293F cell lines was analysed statistically. Spearman rank correlation of the two data sets showed that the expression correlates between the two cell lines (Figure 4. 10). When the data sets were split into lysates and pellet samples both cell lines showed a strong correlation ($p<0.0001$). However pelleted samples correlated less well than the lysate samples due to the increase in background signal produced by the HEK-293F cell line. The expression data of both cell lines showed that RH5 was the most promising candidate to further investigate for the formation of RH-VLPs.

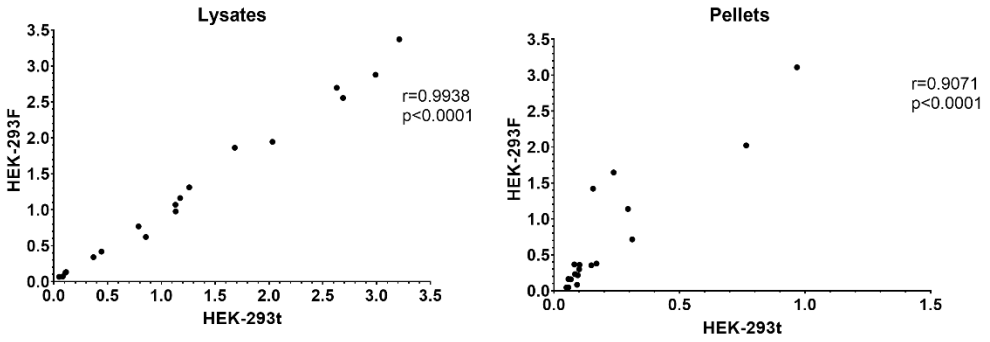

Figure 4. 10 Correlation between ELISA data collect from HEK-293T and HEK-293F cell lines.

The ELISA data collected from intracellular and extracellular HCV-E2 expression between the two cell lines were analysed for correlation. Data point is the mean value (n=3) for each cell line. Correlation was determined using spearman rank method.

4.2.6 Validation of the RH5 chimera

Having shown that the RH5 chimera produced the highest level of extracellular HCV-E2, and that this protein was recognised by a conformation-sensitive anti-HCV-E2 antibody, the next step was to investigate if RH5 produced VLPs. Firstly, to determine if the RH5-E2

secretion was capsid dependent, the RH5 chimeric glycoproteins were amplified from RH5 and subcloned into a pcDNA3.1 plasmid to generate RH5-E1E2. This was then expressed in HEK-293F cells alongside RH5 and RcapHE1E2. Pelleted supernatant samples were used in a GNA-capture ELISA and detected with 1:7 (Figure 4. 11). Extracellular RH5-E2 was significantly higher when expressed in the full RH5 construct compared to the RH5-E1E2 glycoproteins ($p<0.0001$) (Figure 4. 11) and was protein concentration-dependent. Furthermore, as was observed in the chimera panel experiments, RcapHE1E2 produced a detectable HCV-E2 however this was not significant from RH-E1E2 and HCV-E1E2 levels. This showed that capsid-dependency required the RV envelope protein TMD regions that were present in RH5.

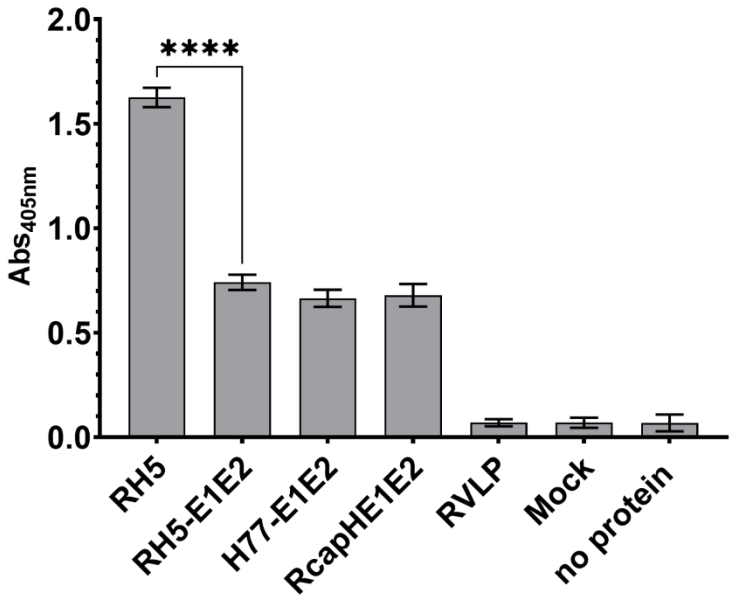

Figure 4. 11 Comparison of HCV-E2 signal between RH5 chimera and glycoproteins expressed in isolation.

GNA-capture ELISA was performed on pelleted supernatant collected from HEK-293F cells transfected with RH5, RH5-E1E2, HCV-E1E2, RcapHE1E2 or RV-24s. Pellets were normalized to a total protein concentration of 0.25 mg/mL. Statistical significance was measured by one-way ANOVA, $p<0.0001$ (****).

The next step was to investigate the release of enveloped RV-C and test for its association with RH5-E2. First a RV-C capture ELISA was performed to detect enveloped RV-C in HEK-293F supernatant. Treatment of the supernatant with Triton for both RVLP and RH5 produced significantly higher amounts of RV-C compared to the untreated control (Figure 4. 12A). The end point dilution for RVLP was 1:16 whilst RH5 was 1:2. Showing that RH5 assembly was less efficient than RVLPs. Finally, association of enveloped RV-C with RH5-E2 was tested using the co-immunoprecipitation approach described for RVLPs in the previous chapter (section 3.2.3). RV-C was eluted from protein G

beads conjugated with AP33, confirming that RH5 supernatant contains RH5-E2-associated enveloped RV-C (Figure 4. 12B). No RV-C was eluted from beads coated with anti-RV-E1 or unconjugated beads incubated with RH5 supernatant, showing that the RV-C was captured in an antibody-dependent manner. The anti-HCV-E2 conformation sensitive antibody, 1:7, did not capture RV-C from any of the samples, including the HCVpp supernatant which was tested for the presence of MLV-p30. To confirm that this antibody was captured, the protein G beads were boiled in Laemmli buffer and reduced protein was separated by SDS-PAGE and detected by silver stain. The eluted protein bands corresponded to the heavy and light chains of antibodies and were present on in all three antibody-containing samples and absent from the beads only group. This confirmed that 1:7 was present on the beads.

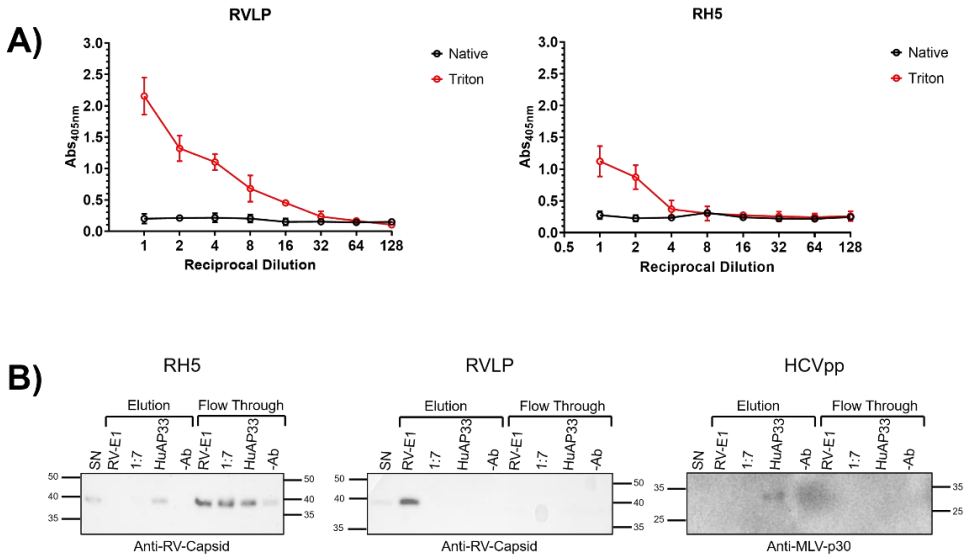

Figure 4. 12 Detection of HCV-E2 associated enveloped RV-C from RH5 expressing HEK-293F cells.

A) RV-C capture ELISA performed on supernatant collected from RVLP and RH5 expressing HEK-293F cells. ELISA plates were precoated with anti-RV-C antibody and incubated with untreated (Native) supernatant or triton lysed supernatant. Captured RV-C was detected using polyclonal rabbit sera, 7w7, at a 1:1000 dilution. Bound rabbit IgG was detected using an anti-rabbit-IgG-AP secondary antibody at a 1:1000 dilution. **B**) co-immunoprecipitation assay was performed on supernatant harvested from HEK-293F cells transfected with RV-24s or RH5, and HEK-293T supernatant from cells expressing HCVpps. Protein G beads were incubated with anti-RV-E1, AP33 or 1:7 monoclonal antibodies. Supernatant collected after incubation with antibody-bound beads was termed flowthrough and elution samples were collected by treatment of beads with 1% triton. Samples were then analysed by western blot for RV-C for RVLP and RH5 samples, and anti-MLV-p30 for HCVpp samples.

To improve the expression of RH5-VLPs, the amount of plasmid transfected into HEK-293F cultures was varied from 1 µg/mL to 8 µg/mL and supernatants were pelleted and VLP production was measured based on E2 signal (Figure 4. 13). Interestingly, there was no significant difference between the HCV-E2 signal between cultures transfected

with 1 µg/mL and 2 µg/mL. Increasing the plasmid concentration above 2 µg/mL led to a reduction in RH5-E2 signal.

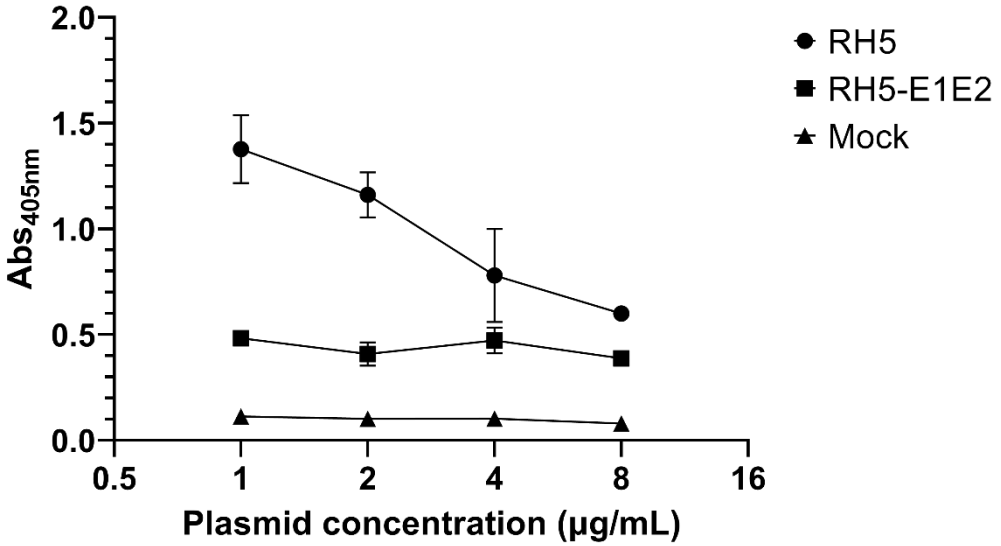

Figure 4. 13 Optimisation of RH5 expression in HEK-293F cells.

The amount of plasmid used to transfect 15 mL HEK-293F suspension cultures was varied. To assess expression, a GNA capture ELISA was performed on pelleted supernatant. A negative control of RH5-E1E2 was also included to measure background signal of glycoprotein in each culture. Pellets from mock cell cultures were also included. Detection of HCV-E2 was achieved using the anti-HCV-E2 antibody, 1:7 at a final concentration of 10 µg/mL.

4.2.7 Characterisation of Chimeric VLPs

The next step was to further characterise the RH5-VLPs. The first step was to investigate the intermolecular covalent interactions of the chimeric glycoproteins. This was done through comparisons between protein migration in the presence and absence of a reducing agent. Under non-reducing conditions, intracellular RH5-E2 showed high molecular weight aggregates that were also observed in HCVpp expressing cell lysates (Figure 4. 14). Monomeric intracellular RH-E2 was also detected which was also seen in the HCVpp cell lysate. When

the same assay was performed on extracellular RH5-E2, all detectable non-reduced RH-E2 displayed a higher molecular weight than the monomer, with the protein migrating as a smear between 100- 140 KDa (Figure 4. 14). This contrasted to the migration pattern of extracellular HCVpp under non-reducing conditions which showed the presence of monomeric HCV-E2, approximately 65 KDa, in addition to aggregates above 140 KDa. Data for HCV-E1 in these experiments was limited since under non-reducing conditions the signal for HCV-E1 was abolished. It was unclear why this occurred since the same samples were used for reducing and non-reducing SDS-PAGE. It was possible that the epitope for the anti-HCV-E1 antibody was occluded under non-reducing conditions. However, given that this antibody successfully detected HCV-E1 and RH5-E1 in a subsequent ELISA assay (Figure 4. 22), in which the protein would be in a native conformation, this explanation is unlikely to be correct. A repeat of this experiment will be needed in which the sample volume is increased.

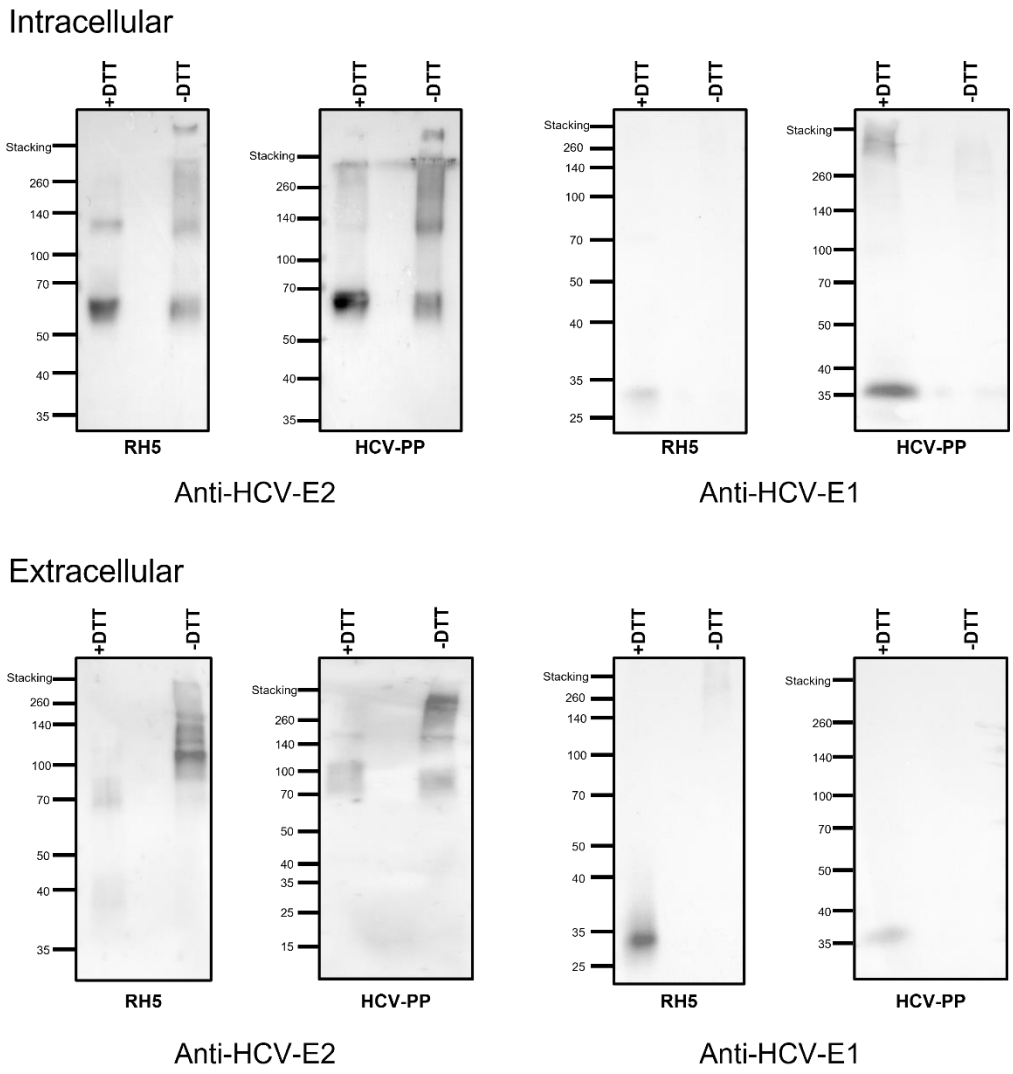

Figure 4. 14 Reducing and non-reducing SDS-PAGE of Intracellular and extracellular RH5 glycoproteins.

For intracellular glycoprotein analysis, transfected cell lysates were used. For extracellular glycoprotein analysis, pelleted supernatant from transfected cells were used. For reducing SDS-PAGE samples were boiled in Laemmli buffer containing 50 mM DTT (+DTT), non-reduced samples were boiled in Laemmli buffer that did not contain DTT (-DTT). Western blotting was performed as previously described.

Another level of characterisation was to investigate the glycosylation of RH5-E2. Glycosylation of proteins can influence the immunogenic properties[382]. Extracellular RH5-E2 was resistant to Endo-H treatment and exhibited a similar migration pattern to the untreated sample (Figure 4. 15). RH5-E2 was sensitive to PNaseF treatment since migration of this protein was faster after treatment with this enzyme and it size corresponded to approximately 40 KDa. This confirmed that RH5-E2 was extensively glycosylated and resistance to Endo-H was suggestive of glycan modification by Golgi associated glycosylase enzymes. Interestingly, following PNGaseF treatment, RH5-E2 produced a double band pattern. This may suggest the presence of glycan groups that were occluded from the PNGaseF enzyme during treatment. RVLPs were tested alongside the RH5 sample and RV-E1 was also shown to be resistant to Endo-H and sensitive to PNGaseF, although this reduction in molecular weight was less than that observed for RH5-E2, suggesting less extensive glycosylation of this protein. Extracellular RV-C was also tested following each treatment to demonstrate that observed changes in molecular weight were due to the activity of the deglycosylase enzymes.

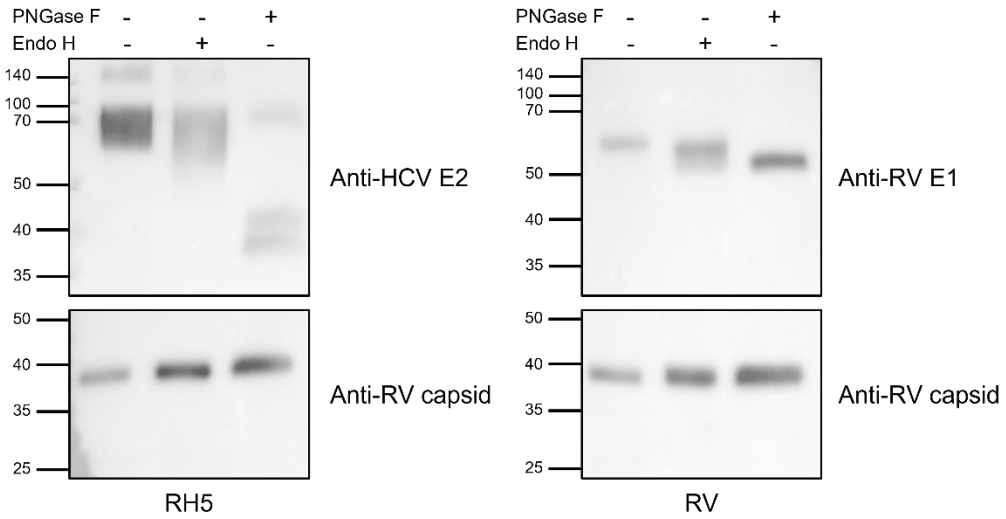

Figure 4. 15 Deglycosylation of RH5-VLPs and RVLPs.

Pelleted supernatant from transfected HEK-293F cells was treated with Endo H or PNGase F deglycosylase enzymes or untreated. Samples were separated by SDS-PAGE and used in western blot analysis. HCV-E2 was detected using the humanised AP33 antibody at a 1.5 µg/mL concentration and RV-E1 was detected using a mouse anti-RV-E1 antibody. A western blot for RV-C was also performed as a negative control as the protein is no glycosylated and thus non-sensitive to Endo H or PNGase F treatment.

4.2.8 Antigenic Characterisation of the RH5 Construct

The antigenicity of RH5 glycoproteins was further tested using a small panel of previously characterised mAbs. These antibodies recognise distinct regions of HCV-E2 (Figure 4. 16) and in the case of AR4A, the HCV-E1E2 heterodimer. Intracellular RH-E1E2 was tested by GNA capture ELISA of transfected cell lysates. Initial experiments were performed at a single point antibody concentration of 10 µg/mL. Mock cell lysates, a lysate from SARS-CoV2 spike protein lysate and an anti-SARS-CoV2 human antibody, AT869, were included as antigen and antibody negative controls (Figure 4. 17A). RH5-E1E2 was recognised by all anti-HCV-E2 antibodies along with HCV-E1E2 lysate. SARS-

CoV2-S lysate was not reactive to anti-HCV-E2 antibodies and was the only lysate to be recognised by AT869 (Figure 4. 17A). These results demonstrated the specificity of the assay and the mAb panel. The reactivity of each anti-HCV antibody was normalized to the HC33.4 value for HCV-E1E2 and RH5-E1E2 lysates (Figure 4. 17B). When normalized, the percentage signal of HC84.26 and AP33 showed no significance between HCV-E1E2 and RH5-E1E2. Significant differences were observed between the binding of 1:7 ($p<0.001$), AR4A ($p<0.0001$) and AR3A ($p<0.0001$). Compared to HC33.4 (100 %), HCV-E1E2 showed mean signal of 84 % for AR3A, 84 % for AR4A and 80 % for 1:7. In contrast, compared to HC33.4 (100 %), RH5-E1E2 showed a mean signal of 56 % for AR3A, 39 % for AR4A and 66 % for 1:7. This showed that whilst RH5-E1E2 was recognised by all the anti-HCV mAbs in the panel however, this sample contained fewer binding sites for AR3A, AR4A and 1:7 compared to HCV-E1E2, highlighting conformational differences.

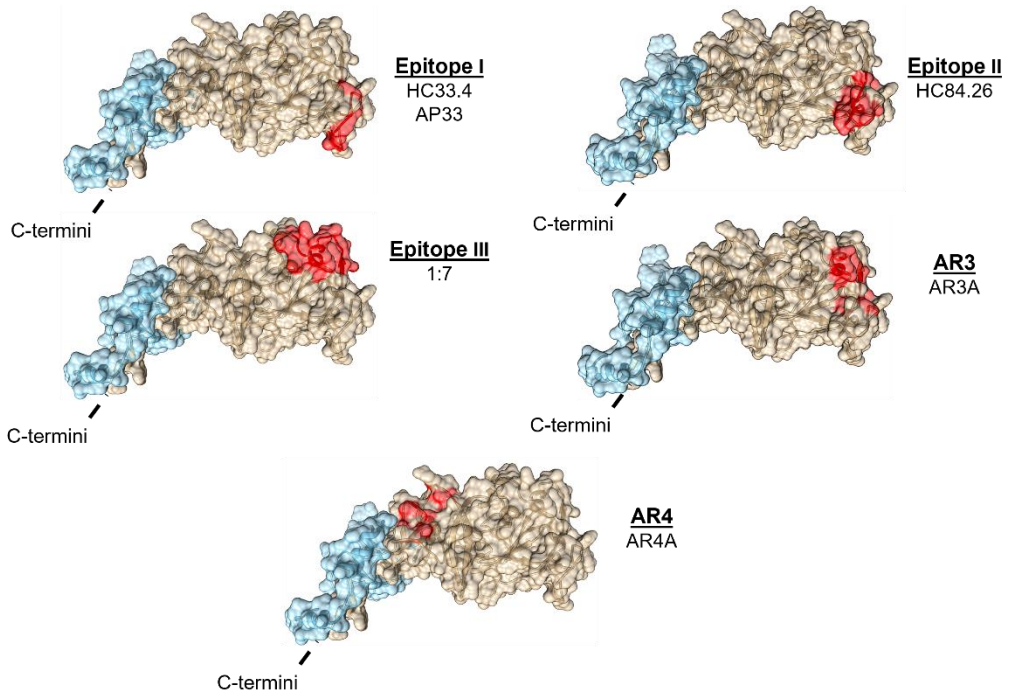

Figure 4. 16 Antigenic regions of HCV-E1E2.

Annotated crystal structure of HCV-E1E2 heterodimer (PDB 7T6X). HCV-E1 is shown in blue and HCV-E2 is shown in tan. Regions highlighted in red depict the position of each antigenic site. Figure was made using chimera[383].

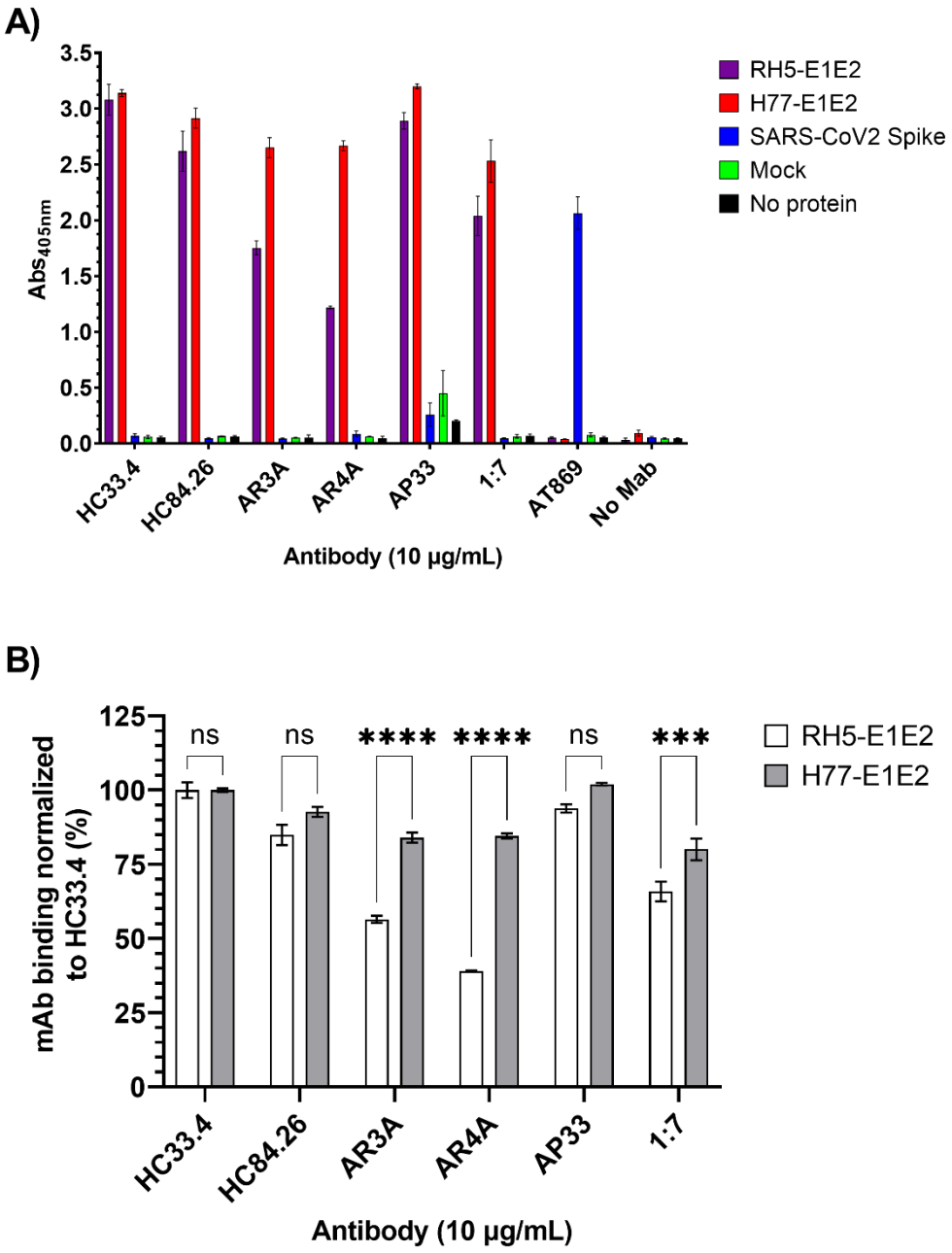

Figure 4. 17 Antigenicity of intracellular RH5 envelope glycoproteins.

A) Lysates of transfected HEK-293F cells were loaded onto GNA-coated ELISA plates at a normalised total protein concentration 1 mg/mL. Primary antibodies were used at a single concentration of 10 µg/mL. The AT869 was an anti-SARS-CoV2-Spike antibody that was used as a negative control. Mock cell lysates and no protein groups were included to demonstrate the specificity of the assay. Absorbance was measured 30 min after the addition of pNPP substrate. **B**) Values obtained from the single point ELISA were normalised to the value of HC33.4.

To further explore the nature of the mAb binding properties to RH-E1E2, binding curves for each antibody were generated (Figure 4. 18). Cell lysates were captured onto GNA coated plates and normalized to a total protein concentration of 1 mg/mL. Each antibody was then diluted in a five-fold series from a starting concentration of 50 µg/mL, and raw absorbance values and normalized values were plotted (Figure 4. 18 and Figure 4. 19, respectively). The raw values of each binding curve showed that a B_{max} was observed for each of the anti-HCV antibodies towards HCV-E1E2 and RH5-E1E2. A plateau in the signal was observed for antibodies HC33.4, AP33, AR3A and AR4A, at the highest concentrations each dilution series. This plateau occurred for both HCV-E1E2 and RH5-E1E2 lysates. The 1:7 antibody did not reach a signal plateau. The EC_{50} values were determined using the data collected in Figure 4. 19(shown in Figure 4. 20). The mAbs; HC33.4, HC84.26, AP33 and AR3A showed comparable affinities for full length H77-E1E2 and RH5-E1E2. The AR4A and 1:7 mAbs displayed a lower affinity for RH5-E1E1 than H77-E1E2 (Figure 4. 20).

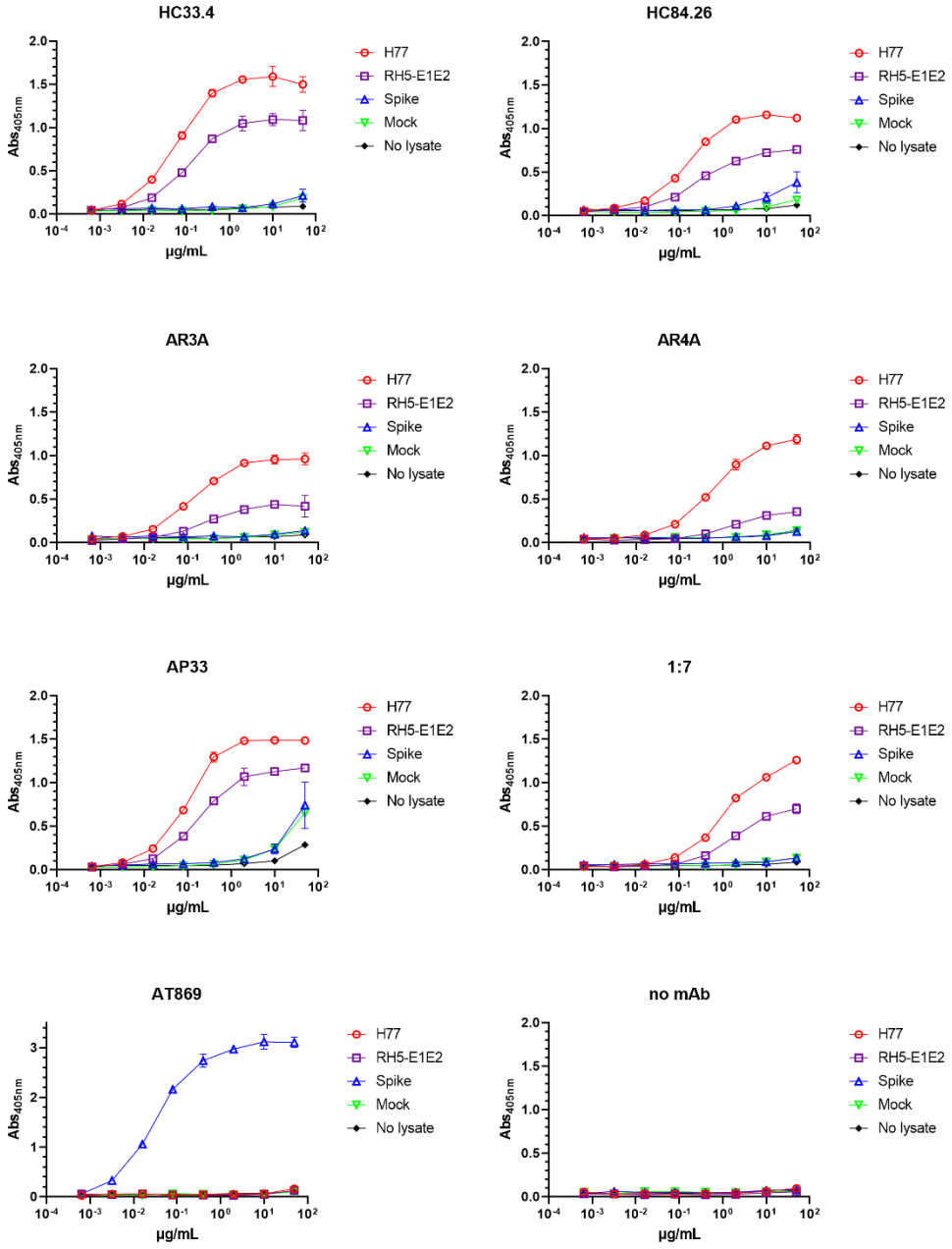

Figure 4. 18 Antigenicity of intracellular RH5 envelope glycoproteins.

GNA capture ELISA was performed on lysates of transfected cells normalised to a total protein concentration of 1 mg/mL. Each antibody was tested in a five-fold serial dilution starting from 50 µg/mL for a total of eight points.

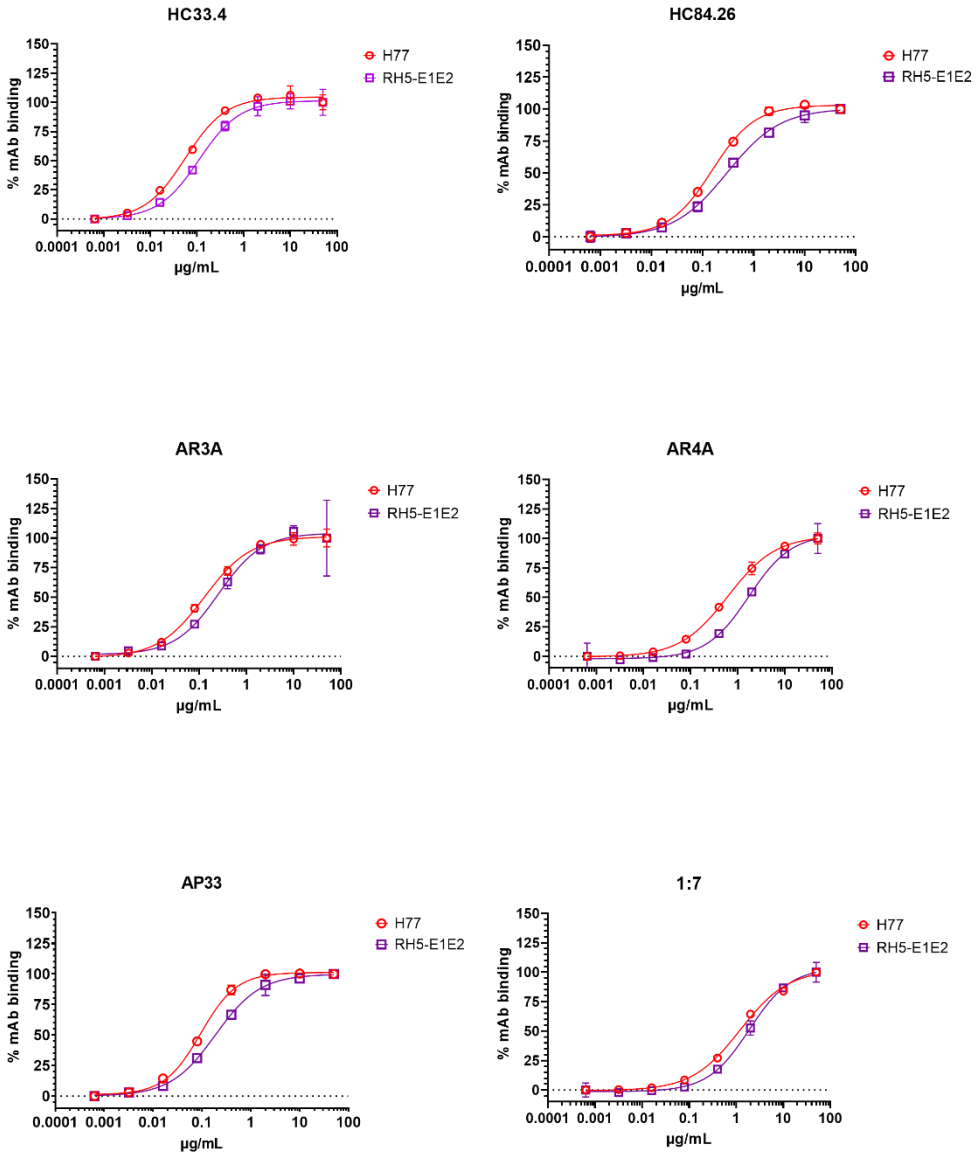

Figure 4. 19 Antigenicity of intracellular RH5 envelope glycoproteins normalised binding curves.

The raw absorbance values for each of the anti-HCV monoclonal antibodies was normalised for HCV-E1E2 and RH5-E1E2 samples. 100 % binding was defined as the absorbance value at 50 µg/mL of antibody. 0% was defined as the absorbance value of the last point in the dilution series. These curves were used to estimate the EC_{50} values for each antibody.

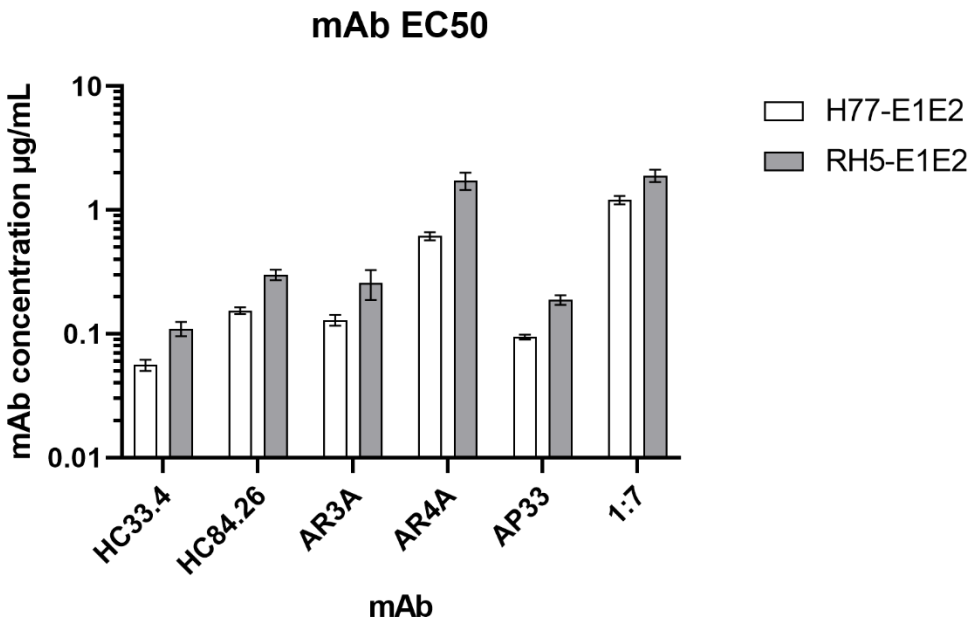

Figure 4. 20 Determined EC50 values for antibody panel against intracellular HCV-E1E2 and RH5-E1E2.

Values were determined from the normalised binding curves in the previous figure 4.19.

The next step was to investigate the antigenicity of extracellular RH5-E1E2. Pelleted HCVpp, RH5, RH5-E1E2, SARS-CoV2pp and mock supernatants were used in a GNA capture ELISA and viral glycoproteins were detected with the mAb panel used at a single point dilution (Figure 4. 21A). All anti-HCV antibodies reacted with HCVpps. HC33.4, HC84.26, AR3A, AP33 and 1:7 reacted to RH5 to a level that was significantly higher to the background signal produce by RH5-E1E2. AR4A did not bind extracellular RH5 or RH5-E1E2. Binding curves for the mAb panel were not performed on extracellular samples due to the requirement for large cultures volumes to generate enough material for this assay. Thus, to gain further insight into the antigenicity

of extracellular RH5, each of the mAbs used in the ELISA experiments in this section were used in a co-IP assay to isolate enveloped RV-C. As previously described, elution was achieved using a Triton X100 lysis method and eluted protein samples were analysed by western blot for RV-C. The results reaffirmed the single point ELISA reactivity data, with all anti-HCV mAbs, with exception to AR4A, isolating RV-C from RH5 supernatant (Figure 4. 21B). Formation of the AR4 region requires the HCV-E1E2 heterodimer, thus a final ELISA assay was performed using the anti-HCV-E1 antibody (Figure 4. 22). Extracellular RH5-E1 was detected and was significantly higher than the RH-E1E2 background level ($p<0.0001$). This showed that both RH5-E1 and RH5-E2 are secreted, however there was no formation of the AR4 region.

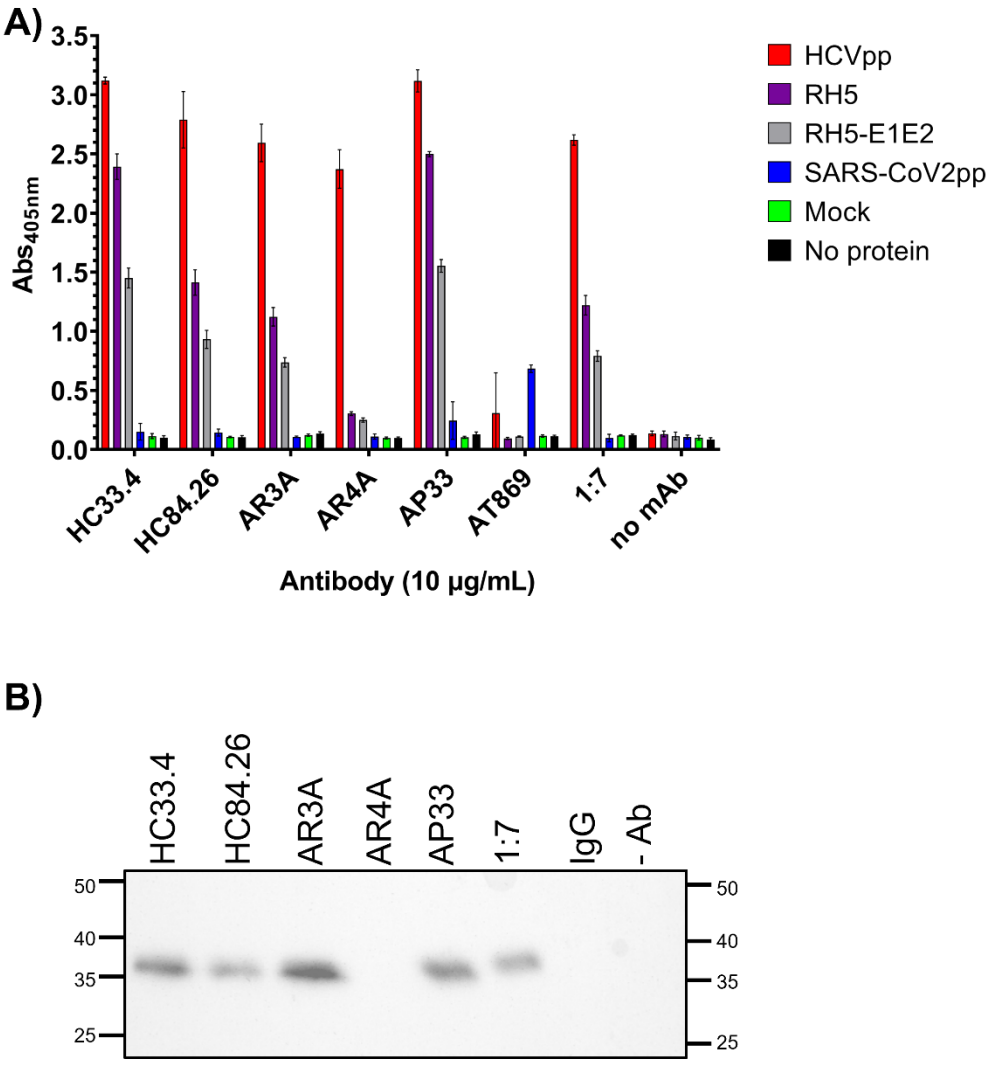

Figure 4. 21 Antigenicity of extracellular RH-5 glycoproteins.

A) Single point GNA-capture ELISA was performed on pelleted supernatant from transfected HEK-293T cells expressing RH5, RH5-E1E2, HCVpps and SARS-CoV2pps. Each antibody was used at a final concentration of 10 µg/mL. Pellet samples were normalised to a total protein concentration of 0.5 mg/mL. **B**) co-immunoprecipitation was performed on RH5 supernatant. Protein G Dynabeads were incubated with each of the monoclonal antibodies. Purified IgG from human sera was used as an irrelevant antibody control alongside a beads only negative control. Following incubation with the RH5 supernatant, bound VLPs were lysed with 1% Triton X100 and eluted protein was analysed by western blot for RV-C as described previously.

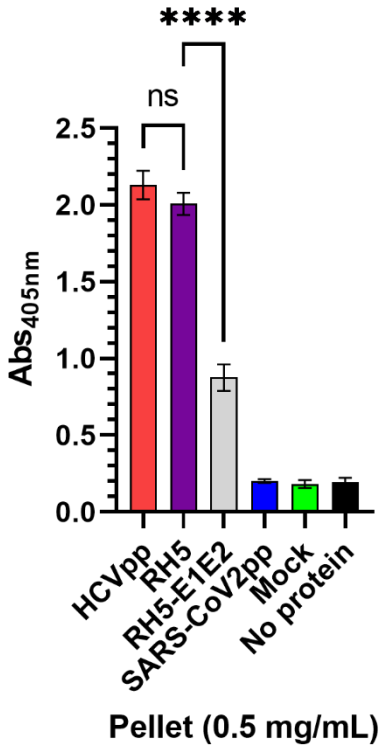

Figure 4. 22 ELISA detection of extracellular RH5-E1.

Single point GNA capture ELISA on pelleted supernatant from HEK-293T cells expressing RH5, HCVpps, RH5-E1E2, SARS-CoV2pps or mock transfected cells. The anti-HCV-E1 antibody was used at a final concentration of 5 µg/mL. Statistical analysis was performed using a one-way ANOVA, $p<0.0001$ (****), $p>0.05$ (ns).

4.3 Discussion

This chapter set out to design and test chimeric RH chimeric constructs to produce VLPs that could have a role as a potential HCV vaccine candidate. Initial design of the chimeras was based on *in silico* prediction of the TMDs and ectodomains of each glycoprotein. Using this information, chimeric glycoproteins were generated using homologous recombination techniques. This approach was initially hampered due to high GC content, however this challenge was overcome with the switch from WT RV-24s to a sequence that was

codon optimised for human cell expression. The small panel of chimeras that were made had varying fusion points for each HCV-E_{ecto} and RV-E_{TMD}. Interestingly the expression of these glycoproteins differed greatly despite some constructs having minor differences in the fusion point position. This suggests limited structural flexibility in the stem regions of these viral glycoproteins. Surprisingly, the RH5 chimera produced promising results during the initial screening of chimeras. This expression was robust and repeatable and showed the secretion of the three viral structural proteins encoded by this construct. Furthermore, it was demonstrated that conformation sensitive anti-HCV-E2 antibodies were capable of isolating detergent sensitive RV-C, providing clear evidence for the generation of chimeric VLPs.

It has previously been shown that the TMD regions of each HCV glycoprotein are critical for the formation of the HCV-E1E2 heterodimer[158]. However, in this work it has been demonstrated that intracellular RH5-E1E2 was present and reactive to the AR4A antibody. At the time of writing this is the first evidence that HCV-E_{ecto} fused to the TMD regions of foreign viral proteins has resulted in the formation of the HCV-E1E2 heterodimer. Perhaps the closest examples of this in the literature are the recent studies describing the formation of soluble HCV-E1E2[270,384]. The discrepancy between intracellular and extracellular AR4A could be explained by two possibilities; firstly, RH5-E1E2 that forms the AR4 epitope does not incorporate into the RH5-VLPs. This may be the result of incorrect trafficking or a steric hinderance caused by this heterodimer at the virus budding site. This

could be investigated by using the mAb panel for immunofluorescence assays on the producer cells to determine the subcellular location of AR4-reactive RH5-E1E2. Secondly, RH5-E1E2 could incorporate into the VLPs which then undergo a conformational change during VLP maturation in Golgi lumen. Testing this theory would be challenging since immature and mature RV particles cannot be distinguished using protein-based methods. This in contrast to other viruses such as Flaviviruses, in which immature and mature virions can be distinguished by western blot detection of prM and M protein[385,386], respectively. To test for AR4A reactivity in immature RH5-VLPs, producer cells would need to be lysed mechanically, in the absence of a detergent followed by purification of immature VLPs using the sucrose cushion method. Further investigation into the loss the AR4 domain in RH5-E1E2 would inform further optimisation of this vaccine candidate.

The absence of AR4 from the RH5-VLPs does not invalidate this construct as a vaccine candidate. There are multiple candidates currently being developed that do not include this region[268,297,387] and there is evidence collected *in vitro*, that the AR3 antibodies alone confer a high barrier to resistance[388]. Additionally, no data was collected in the project on the reactivity of AR5 recognising antibodies, which also requires the HCV-E1E2 heterodimer but does not overlap with AR4[76]. This vaccine candidate may have benefits for its inclusion of HCV-E1 epitopes as has been demonstrated for HBV-chimeric VLPs in which it was found that immunisation of rabbits with a mix of HBV-HCV-E1 and

HBV-HCV-E2 VLPs produced greater nAb titres compared to animals immunized with HBV-HCV-E1E2[294].

A key question that this chapter raises is what is the structure of these chimeric VLPs? For the reasons described in the previous chapter regarding sample purity, no TEM analysis was performed on these VLPs. However, one would expect the structure of these VLPs would be comparable the reported structure of RV. It would be of great interest to observe the spatial arrangement of the chimeric glycoprotein spikes on the surface of the VLP since this would have implications for the immunogenicity of the VLP. Such work would require a highly specialized facility but would be an important step in characterising these VLPs.

Another question raised by this work is are VLPs functional? Testing the VLPs for functionality would give further insight into the structure and presentation of the HCV-E1E2 ectodomains on the surface of the VLP. This question was not answered due to the absence of a RVLP-based reporter system as described in the previous chapter. Additionally, this could not be answered using the commonly used PP systems that are regularly used our laboratory.

This chapter provides a proof of principle for chimeric RH-VLPs and demonstrates a level of structural flexibility not previously described for RV, raising the question of what other foreign viral glycoproteins could be insert into this construct? And does presentation of HCV-E1E2 epitopes in this way elicit an immune response?

Chapter 5 Immunisation of Bovines with Soluble HCV E2 and Chimeric VLPs

5.1 Introduction

Therapeutic mAbs have important roles in combatting viral infections. Recent examples during the COVID-19 pandemic have exemplified the requirement for these treatments to be investigated[389]. Passive immunisation of therapeutic mAbs that block virus entry are of particular interest as possible treatments for HCV[390,391]. Despite the success of DAAs, therapeutic mAbs targeting HCV could offer advantages when used in combination with DAAs or administered following treatment failure. These treatments could also play a protective role following liver transplantation[392]. For example, administration of the antibody, MBL-HCV1 was shown to delay viral rebound following liver transplantation in patients with chronic HCV infection[390] and other mAbs have been shown to prevent HCV infection in transgenic mice[393,394].

The specificity of an Ab is determined by the CDR regions of which there are three located in the variable domain of the heavy and light chains and form a paratope resulting in antigenic specificity. The CDRH3 region has been shown to be a key determinant of antigenic specificity[395]. Regarding antiviral nAbs, the CDRH3 domain has been shown to mediate antigenic interaction for Abs targeting HIV[396], Influenza[397] and HCV[82]. It has been proposed that extended CDRH3s improve nAb potency through subverting the glycan shield of viral glycoproteins. For example, CDRH3 regions of nAbs such as the anti-

HIV envelope mAb, PGT128, has been shown to insert between glycan groups to interact directly with the protein surface[396,398].

In the Human B-cell repertoire, CDRH3s are usually limited to around 26 amino acids long[399,400]. By contrast, the B-cell repertoire of the domestic bovine species, *Bos taurus*, contain a subset of Abs which encode CDRH3s of up to 70 residues long, termed ultra-long[401], which are encoded by the V_{H1-7}, D_{H8-2} and J_{H2-4} genes[401,402]. These UL-CDRH3 regions form a knob and stalk structure projecting form the heavy chain variable region[403] (Figure 5. 1). The knob structure is cysteine-rich with intermolecular disulphide bridges and mediates antigenic interaction[404,405]. As a result of this unique structure, these Abs can access conserved epitopes that are normally occluded from human Abs[405]. It is thought that through targeting these highly conserved regions, mAbs can be generated that exert a high barrier to resistance, thus limiting viral escape.

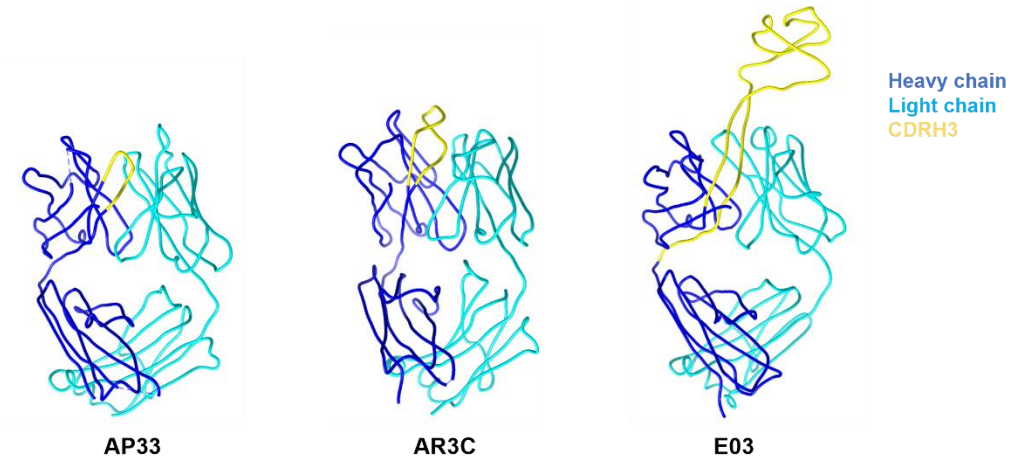

Figure 5. 1 Structures of Mouse, Human and Bovine IgG Fab regions.

Mouse anti-HCV-E2 antibody AP33 (PDB 4GAJ). Human anti-HCV-E2 neutralising antibody AR3C (PDB 6MEF). Bovine E03 fab (PDB 5IJV) isolated from animals immunised with bovine diarrhoea virus although the antigen of this Fab was unknown.

Generation of UL-CDRH3 antibodies can be achieved using both *in vitro* and *in vivo* methods[406,407]. A recent study generated a bovine UL-CDRH3 heavy chain library, expressed as surface scFv, from naive animals that were then screened for neutralizing activity towards SARS-CoV2pps[406]. This approach led to the isolation of a scFv that could target both SARS-CoV2 and SARS-CoV. Since the isolated heavy chain was isolated from a SARS-CoV2 naïve animal, it would be expected that no affinity maturation or somatic hypermutation would have been selected for *in vivo*, thus future work could investigate potential mutations to improve the scFv performance. In contrast, affinity matured antigen specific UL-CDRH3 Abs can be isolated from animals following immunisation[407,408] or infection[409].

Immunisation of bovines with trimeric HIV gp-140 over a course of four years was found to induce high titres of cross-neutralising antibodies in

the colostrum[410]. Interestingly, this study found that repeated homologous boosting did not enhance neutralisation breadth of the sera. In a separate study using a homologous primer/ boost strategy, Sok *et al*.,[407] immunised bovines with the BG505 SOSIP HIV gp-140 trimer[411] for 381 days. In this study cross-neutralising Abs were induced over the course of the experiment, with one animal displaying broad cross neutralising sera after a single boost. In addition to this, anti-HIV UL-CDRH3 nAbs were isolated of which the mAb, NC-Cow1, encoded a CDRH3 region of 60 residues and showed neutralisation activity towards 72 % of a 117 HIVpp panel[407]. This study demonstrated that bovine UL-CDRH3 nAbs can be elicited towards human viruses.

To date there has been no report of the immunogenicity of HCV envelope glycoproteins in bovines. Elicitation of bovine nAbs could lead to the isolation of novel UL-CDRH3 Abs with potent cross reactivity. As such this chapter set out to assess the immunogenicity of HCV glycoproteins in two male *B. taurus*. Firstly, animals were immunised with sE2, based on a previously described construct[82], derived from five HCV isolates. Following six immunisations with sE2, a further three immunisations with the RH5-VLPs described in chapter 4 were administered. Humoral responses were measured over the course of this study by isolating plasma following immunisation and testing for HCV-specific IgG.

5.2 Results

5.2.1 Validation of Immunogens

Soluble HCV-E2 proteins derived from UKNP4.1.1, UKNP3.2.1, 1a80, 1b34 and J6 were validated in house by the groups that produced the protein. For the RH5-VLPs, a single point ELISA was performed for each batch (Figure 5. 2). To show that the single point concentration of pelleted RH5-VLPs was not saturating the ELISA plate, a two-fold dilution series was performed using previously generated RH5 pellets (Figure 5. 2A). This dilution series did not reach a plateau showing that observed similarities between each VLP batch was real and not the result of assay saturation. The three RH5-VLP batches that were generated in house showed no significant difference between the means absorbance values ($p>0.05$) confirming that each immunisation contained similar amounts of VLPs (Figure 5. 2B).

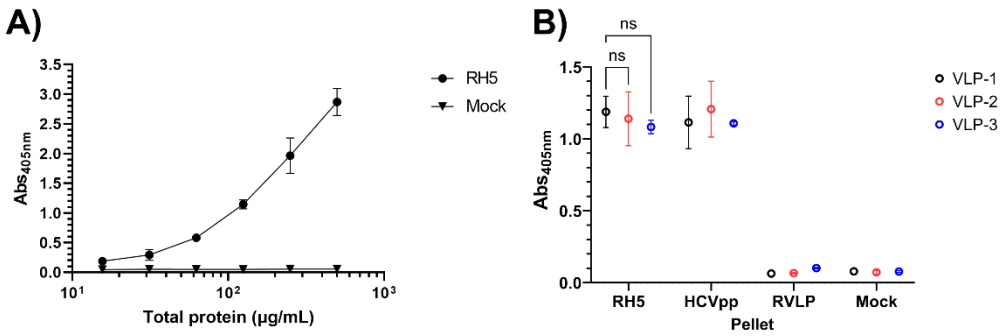

Figure 5. 2 GNA capture ELISA of RH5-VLPs produced for immunisation.

A) A two-fold dilution series was performed using pelleted RH5-VLPs to ensure the ELISA plate to test for saturation. Dilution series started at 500 µg/mL of total protein. **B**) RH5-VLPs were expressed in HEK-293F cells and supernatant was pelleted on a 20 % sucrose cushion. For immunizations VLPs were expressed as 3 independent batches (VLP-1, 2, 3). A GNA ELISA was performed with pellet RH5-VLPs at a normalised total protein concentration of 250 µg/mL. HCVpps expressed in HEK-293t were used as a positive control group. HCV-E2 was detected using the anti-HCV-E2 antibody 1:7 at a concentration of 10 µg/mL. Each data point represents the mean absorbance value with error bars representing the standard deviation. Statistical significance between the means of each RH5-VLP was tested using a one-way ANOVA, ns ($p>0.05$).

The immunisations were performed over a period of 679 days (Figure 5. 3). The first six doses contained a total of 250 µg of sE2 protein and was administered over the first 280 days of the experiment (Figure 5. 3A) Three 250 µg doses of chimeric RH5-VLPs were administered from day 616 to 679. Bovine antibody secreting cells have been shown to peak at four days post boost following immunisation with an inactivated FMDV antigen and remain detectable at least six days afterwards[412]. Based on this observation, blood samples taken within six days of immunisation were harvested for PBMCs. During the course of this experiment the same two animals were immunised with 250 µg S1,

spike and 200 µg trimeric spike antigens derived from SARS-CoV2 (Figure 5. 3B). This provided an oppurtunity to compare the immunogencity of two unrelated viral glycoproteins within the same animals.

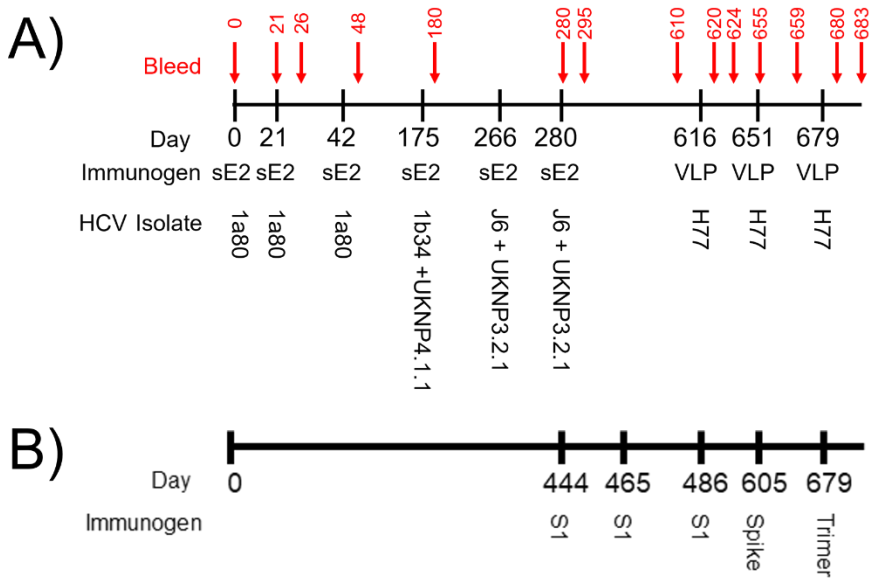

Figure 5. 3 Immunisation schedule.

A) immunisation schedule for HCV immunogens. B) Immunisation schedule for SARS-CoV2 immunogens.

5.2.2 Plasma reactivity following immunisation

The humoral response was assessed by testing the reactivity of isolated plasma with lysates of HCV-E1E2 expressing HEK-293T cells captured on a GNA coated ELISA plate (Figure 5. 4). Immunisation with sE2 elicited limited IgG towards HCV-E2 with days 280 and 295 showing the highest reactivity to H77 and 1a80 for animal 13 (Figure 5. 4A). This reactivity was lost by day 610 and was recovered by day 655 following

immunization with two doses of RH5-VLPs which showed significantly higher reactivity compared to day 0 and was comparable to day 295 in animal 13. A similar pattern was observed for animal 18 although the absorbance values were lower compared to animal 13 and no sE2 immunisations resulted in reactivity above the positive threshold. Interestingly, the peak reactivity towards H77-E1E2 occurred at different time points for each animal. Animal 13 also showed reactivity towards 1b34-E1E2 from day 620 to day 683. This contrasted with animal 18 which showed no reactivity to this isolate. A similar pattern was also observed for the isolate, UKNP4.1.1-E1E2, with animal 18 showing no reactivity towards these glycoproteins and animal 13 showing low level reactivity from day 620 onwards. This level of reactivity did not increase following subsequent RH5-VLP immunisations.

Plasma reactivity was also tested against the chimeric RH5-E1E2 glycoproteins (Figure 5. 4). The reactivity pattern was remarkably like that of the H77-E1E2 glycoproteins. In animal 13, reactivity following RH5-VLP immunisation appeared on day 620 and day 659 for animal 18. Peak reactivity occurred at the same timepoint for each animal as was observed for H77-E1E2 glycoproteins.

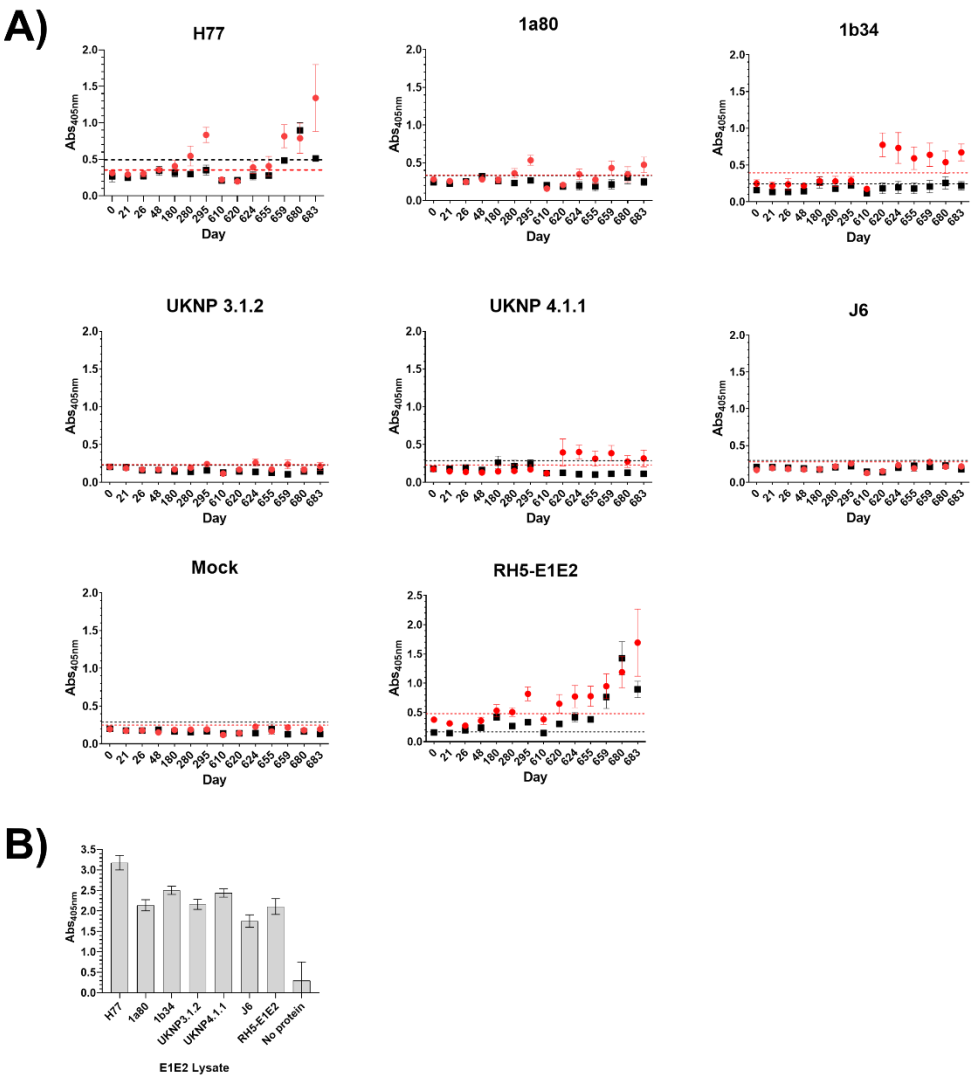

Figure 5. 4 Bovine plasma reactivity towards different HCV isolate glycoproteins.

A) Lysates from HEK-293T cells expressing HCV-E1E2 were captured onto GNA coated ELISA plates. Plasma from each timepoint was used at a 1:100 dilution and bound bovine IgG was detected with a anti-bovine-IgG alkaline phosphatase secondary antibody. Each data point represents the mean absorbance with error bars presenting the standard deviation. Dashed lines represent the positive signal threshold, determined by the mean value of day 0 + 3SD. B) detection of HCV-E2 in all lysates using the 1:7 antibody at a final concentration of 10 µg/mL, performed to confirm the expression of recombinant HCV-E1E2 in lysates used to test plasma reactivity.

To further investigate the magnitude of the humoral response following immunisation, the HCV-specific IgG was titrated for the final two timepoints, day 680 and day 683 (Figure 5. 5). The plasma was diluted in a twofold serial dilution starting at dilution factor of 1:100. For comparison the serially diluted plasma was also tested for SARS-CoV2 spike protein specific IgG. The dilution series demonstrated that the HCV-E1E2 specific IgG was present at a low titre in the plasma. Surprisingly, at a 1:200 dilution the day 683 plasma from animal 13 did not show significantly higher absorbance compared to the day 0 plasma control. In contrast, the same plasma samples contained SARS-CoV2 specific IgG that had an endpoint titration of 1600 and 3200 for animals 13 and 18, respectively (Figure 5. 5).

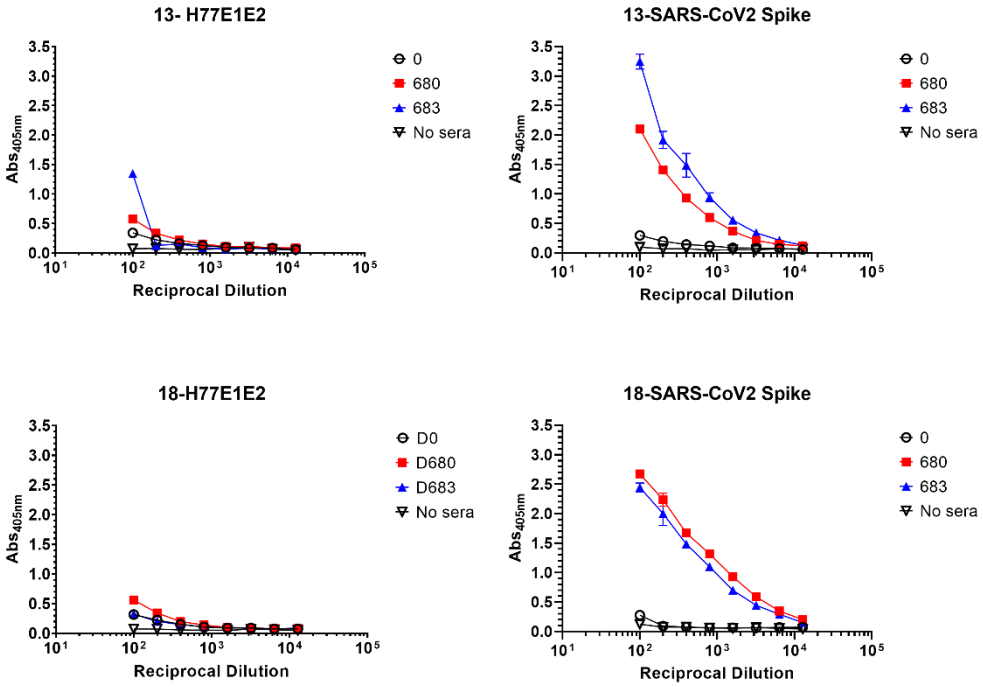

Figure 5. 5 Titration of HCV and SARS-CoV2 specific IgG in bovine plasma.

Bovine plasma was from day 0, 680 and 683 was used in a two-fold serial dilution starting from a 1:100 dilution. Dilutions were added to GNA coated ELISA plates previously incubated with lysates of HCV-E1E2 or SARS-CoV2-Spike expressing HEK-293T cells. Bound IgG was detected with an anti-bovine IgG alkaline phosphatase conjugated secondary antibody.

5.2.3 Generation of neutralising antibodies in plasma

Having shown that the isolated plasma from each animal contained HCV-specific IgG. The next step was to investigate if this humoral response contained nAbs. To test this, HCVpp expressed with the H77 isolate envelope glycoproteins were used in a neutralisation assay (Figure 5. 6A). The plasma from each timepoint was tested at a 1:50 dilution. Timepoints 21-295 showed no significant decrease in HCVpp infectivity compared to the day 0 plasma ($p>0.05$) (Figure 5. 6). At day 610, isolated plasma showed an inhibitory effect on HCVpp entry with animals 13 and 18 showing a 32 % ($p=0.1873$) and 38 % ($p=0.0517$)

decrease in HCVpp infectivity, respectively, compared to day 0. Plasma from animal 13 showed significant decrease in HCVpp infectivity was observed, when compared to day 0, for day 620 ($p<0.01$), day 624, 655, 659, 680 and 683 ($p<0.0001$) (Figure 5. 6A). A similar pattern was observed for animal 18 with all the time points after day 610 showing significant decreases in HCVpp infectivity ($p<0.0001$), compared to day 0 (Figure 5. 6A). The lowest HCVpp infectivity was observed on day 680 and 683 for animal 13 with a mean infectivity of 20 % and 24.5 %, respectively. For animal 18, days 659 and 680 showed the greatest reduction in HCVpp infectivity with a means of 35.6 % and 39.5%, respectively.

To confirm that the neutralising activity exhibited by the bovine plasma was specific HCVpps and not the result of a non-specific interaction in the neutralisation assay. A repeat assay was performed with VSVpps (Figure 5. 6B). These animals had not been immunized with this viral glycoprotein nor had they been immunized with the glycoprotein of a closely related virus, thus it was hypothesized that the plasma would not show any neutralising activity towards this PP. Incubation of plasma from day 0 and day 610-683 showed no neutralising effect upon the VSVpp, confirming that the neutralisation activity observed towards HCVpp was glycoprotein specific. In addition to this, HCVpp inhibition correlated with plasma reactivity towards H77-E1E2 for both animals although this was not significant for animal 18 ($p=0.1$) (Figure 5. 6C). In contrast to HCVpp neutralisation, the plasma from days 610, 680 and 683 showed potent neutralisation of autologous SARS-CoV2pps. With

exception of day 680 for animal 13, all post immunisation plasma led to complete neutralisation of PPs (Figure 5. 7).

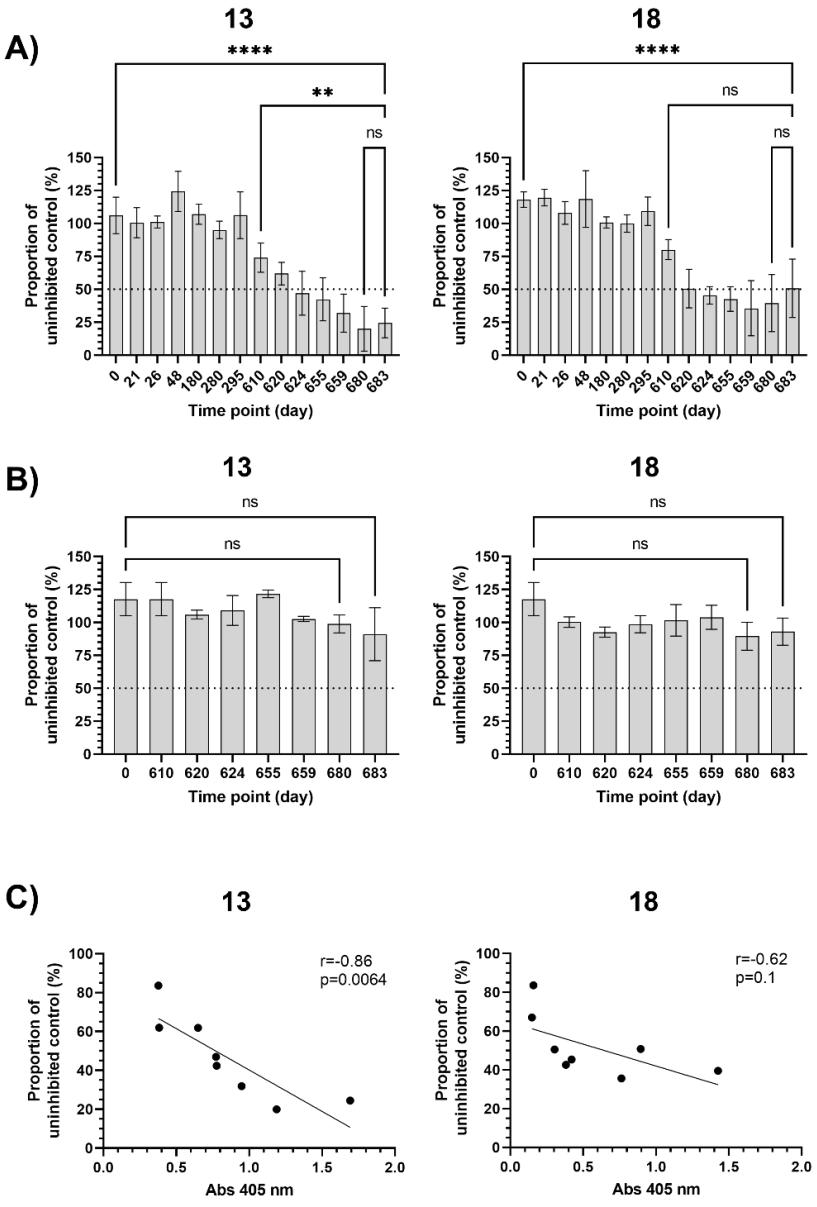

Figure 5. 6 Neutralisation activity towards HCVpps with post-immunisation bovine plasma.

Retroviral HCVpps (H77 isolate) (**A**) and VSVpps (**B**) were incubated with plasma from animal 13 and 18 at a final dilution of 1:100. PPs were then used to infect Huh 7 cells which were the incubated for 72 hrs and measured for luciferase activity. RLU was normalised to a PBS+ HCVpp control (100 % infectivity) and a PBS+ ΔE control (0 % infectivity). Statistical significance was determined using one-way ANOVA. **C**) Spearman correlation was performed to compare autologous plasma reactivity with HCVpp neutralization.

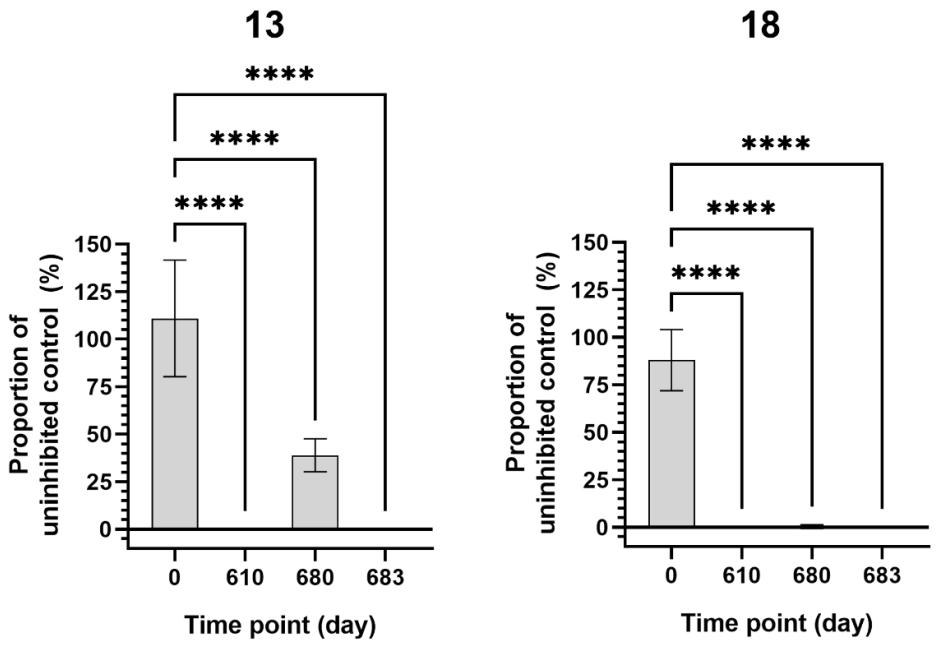

Figure 5. 7 Neutralisation of SARS-CoV2pps using bovine plasma.

Retroviral SARS-COV2pps were incubated with plasma from animal 13 and 18 at a final dilution of 1:100. PPs were then used to infect Huh 7 cells which were the incubated for 72 hrs and measured for luciferase activity. RLU was normalised to a PBS+ HCVpp control (100 % infectivity) and a PBS+ ΔE control (0 % infectivity). This this experiment was performed by Dr Theocharis Tsoleridis (University of Nottingham) and kindly provided for inclusion in this chapter.

5.3 Discussion

This chapter presents the first data on the immunogenicity of HCV glycoproteins in bovines. Immunisation with a previously described sE2 construct elicited limited reactivity in isolated plasma and exhibited no detectable nAbs using an *in vitro* PP neutralisation assay. Immunisation with the chimeric RH5-VLPs induced greater levels of HCV-E1E2 specific IgG that was reactivity to heterologous HCV glycoproteins and correlated with autologous neutralising activity. Titration experiments

demonstrated that HCV-specific IgG was present at low concentrations, even in plasma samples with peak reactivity. In contrast, SARS-CoV2 Spike-specific IgG was shown to be present at significantly higher levels in both animals. This difference between IgG titres suggests that HCV-E1E2 are poorly immunogenic in bovines. This could be the result of poorly ordered glycoprotein as improved immunogenicity has been shown of HIV gp has been shown to elicit bnAbs in shorter time spans compared to more disordered constructs[407]. Soluble HCV-E2 constructs are known to exhibit structural flexibility, making this protein notoriously difficult to crystalise. The sE2 construct used for immunisation in this work was initially developed for structural work and remains the most complete structure of HCV-E2 to date. Whilst this suggests this construct is well ordered it is worth noting that to resolve this structure, the sE2 was co-expressed with the fab fragments of anti-HCV-E2 mAbs to stabilise the structure[82]. As such it is therefore conceivable that the poor immunogenicity of this sE2 was the result of poorly ordered antigen.

Regarding the RH5-VLPs, this immunogen elicited greater humoral responses than the sE2. The structural heterogeny of these VLPs is not known. It can be speculated that the structure would be similar to that of RVLPs which are pleomorphic but share a common feature of anti-parallel arrangements of RV-E2E1 heterodimers[331]. The question of whether a similar pattern of HCV-E1E2 heterodimers is present on the surface of RH5-VLPs remains to be determined. VLPs are regarded as more immunogenic than a subunit vaccine counterpart due to them

containing multiple copies of epitopes[277]. Thus, it is possible that this was one reason for the observed increase in plasma reactivity following immunisation.

This work was not performed to compare sE2 and RH5-VLPs, and such a comparison cannot be made for several reasons. Firstly, immunogens from different isolates were used for sE2 and RH5-VLPs. Thus, it cannot be ruled out that higher plasma reactivity following RH5-VLP immunisation was the result of the H77-E2 being a more potent immunogen than that of the other isolates used for the sE2 construct. Secondly, the dose of each the two immunogens were not normalised. The sE2 dose were based on total protein quantification following purification whilst RH5-VLPs were quantified by total protein of pelleted transfected cell supernatants. The later preparation would contain host cell derived proteins and fewer copies of the HCV-E2 antigen. This issue could be overcome by quantifying the VLPs by the amount of HCV-E2 in the sample. This could be done by performing an ELISA assay that would include a standard curve of purified sE2, derived from the H77 isolate. The dosage of RH5-VLPs could then be defined in terms of HCV-E2 rather than total protein. Finally, the immunisation schedule for these animals was an initial primer/boost with sE2 followed by further booster doses of RH5-VLPs. Therefore, the differences observed in plasma reactivity towards RH5-VLPs could be the result of a B-cell response that was established by the sE2 immunisations. Although plasma from day 610, prior to the first RH5-VLP immunisation, showed no reactivity towards HCV-E1E2 it was likely that an

established pre-existing B-cell response contributed to the observed immunogenicity of RH5-VLPs. This likelihood prevents accurate assessment of the immunogenicity of RH5-VLPs and could be prevented in future experiments by immunising naïve animals with RH5-VLPs and comparing post-immunisation serum reactivity with pre-immunisation serum.

Due to time limitations of this project several experiments were not preformed. One series of experiments was to map the antibody response to HCV-E1E2. This could be done using a competition ELISA assay in which bovine IgG could compete with anti-HCV-E1E2 antibodies with known epitopes such as the panel of mAbs used in the previous chapter. Linear HCV-E2 epitopes could also be used to further characterise the bovine humoral response to HCV-E2 as has been performed for human serum samples[413]. Another approach would be a denaturing ELISA to determine the distinguish between conformational and no-conformation sensitive Abs. One additional area to investigate was the ability of the plasma to neutralise heterologous HCV isolates. Although given the low cross reactivity the plasma exhibited towards the E1E2 proteins of different HCV isolates, cross-neutralisation would likely be limited.

Future work should aim to perform a longer immunisation trial, possibly spanning years, with plasma reactivity monitored throughout this process. A longer immunisation schedule may provide time for immunised animals to generate a high titre cross-neutralising humoral response, which would be essential to proceed to isolating mAbs.

Based on the data in this chapter it can be argued that this immunisation should use RH5-VLPs, since naïve animals immunized with sE2 produced limited response. However, a wider question would be which isolates to immunise with? The isolates selected for the sE2 constructs in this study were identified since they have previously been shown to be resistant to nAbs[209,236,238]. However, in a recent study characterising Ab responses following reinfection following SVC, Frumento *et al*.,[414] demonstrated that greater neutralising breadth was observed in the sera of individuals that were infected with nAb sensitive isolates compared to those that were reinfected with more nAb resistant strains. This has clear implications for vaccine design, such as which isolates to base immunogens on, but also on how a vaccine might be administered such as a heterologous primer/ boost strategy with nAb sensitive isolates. Although this study was regarding natural infection and clearance in humans, it would be of interest and relevance to this work, to test immunisation with nAb-sensitive isolates to elicit potent cross reactivity UL-CDRH3 bovine mAbs.

Chapter 6 Discussion and Future Work

This project set out to design a chimeric RH VLP vaccine platform. To that end, the work detailed in this thesis described the successful production of such chimeric VLPs that have been validated with western blot, co-IP and ELISA based techniques. The successful assembly of RH5-VLPs demonstrated a level of structural flexibility not previously described for RV. The recognition of RH5-VLPs by a panel of anti-HCV has shown that that these VLPs present important HCV-E antigenic regions, such as AR3, which will be vital for B cell targeting vaccines against HCV.

One aspect to consider when designing chimeric vaccines is the impact of pre-existing immunity towards the vector virus. This is of particular concern if neutralising epitopes of the vector virus are included in the vaccine. For example, the previously described RV vaccine vector system includes the full ectodomain of the RV-E1, the main target of RV-specific nAbs[341]. Therefore, the ability of this vaccine to induce responses the foreign viral epitope target, could be hinder especially if the individual has previously been vaccinated against RV. This problem could be circumvented or minimised if it was administered as childhood vaccine. Regarding the RH5 vaccine platform, pre-existing RV nAbs are expected to be non-reactive to these VLPs since the ectodomains of the RV envelope glycoproteins are not present. It would be expected that immunisation with these VLPs would stimulate pre-existing cellular immunity, however the impact of this upon the establishment of new B cell responses to HCV-E1E2 may not impact vaccine efficacy.

The most immediate experiments required to further progress this project would be a small animal immunisation study. This is a common requirement for early preclinical vaccine candidates. For this study four groups should be included which would be immunised with either: Rh5-VLPs, HCV-sE2, RVLPs and PBS only control group. In order to normalise the dose of antigen, animals should be immunised with a dose of RH5-VLP, equivalent to HCV-sE2 to allow for accurate comparison of the two immunogens. The Dosage of RVLPs should be determined based on the amount of enveloped RV-C in a dose of the normalised RH5-VLPs to ensure a similar amount of RVLPs are used in the immunisation. Sera from the animals should be screened initially for homologous reactivity and *in vitro* neutralising activity followed by extensive characterisation against a panel of HCV isolates with varying neutralisation sensitivities[287].

This work focused on chimeras that incorporated HCV-E1E2 from the reference isolate strain H77, an isolate that originates from HCV passaged in Chimpanzees[352]. This isolate has been commonly used in early testing of HCV vaccine candidates. However, it could be argued that proteins derived from patient isolates may be better suited, particularly those derived from patients that went on to achieve SVC. Furthermore, it is possible that a vaccine that induces pan-neutralising immune responses will be needed to be multivalent, requiring antigens derived from multiple HCV isolates to enhance targeting breadth. Thus, one avenue for future work on this vaccine candidate should involve testing the production of RH5-VLPs using a variety of genetically

diverse HCV isolates. Selection of these isolates could be based on the neutralisation profile of each isolate. Characterisation of neutralisation sensitivities for different HCV isolates has demonstrated that isolates form clusters that are do not correlate with genetic distance[415]. Thus, it may be advantageous to selected HCV-E1E2 sequences from distinct neutralisation clusters to be included in a multivalent vaccine. An alternative approach could be to use isolates that engage unmutated ancestors of nAbs. For example, the HCV-E2 protein of isolate 1b57 can be recognised by predicted unmutated ancestors of nAbs suggesting a potential role for this antigen in B cell priming. Importantly for this work, the expansion of the RH5 construct to include a panel of HCV isolates would be relatively simple to establish since the stem regions of HCV-E1 and HCV-E2 are relatively conserved making it clear which residues are analogous to the H77 isolate included in RH5. Indeed, the challenge of generating a panel of vaccine constructs lies in what immunisation schedule induces the best immune response. This work would require considerable resources since a multivalent vaccine could be administered as a homologous or heterologous prime/ boost strategy.

The use of RH5-VLPs could also extend to the presentation of modified HCV-E antigens. Immunisation with rationally designed HCV-E glycoproteins has become increasingly common[18]. For example, a recent study showed that immunogenicity of a mutated HCV-sE2, harbouring a F442NYT mutation that introduced a glycosylation site to reduce CD81 binding, was enhanced in mice[416]. It would be of interest

to test these immunogens in the context of RH5-VLPs to assess immunogenicity.

It would also be insightful to explore the performance of RH5 with envelope glycoproteins derived from different *Hepacivirus* species, particularly EqHV. This could be done for two reasons. Firstly, there is currently no EqHV vaccine, thus the Rubella-EqHV chimera VLP could be considered a vaccine candidate towards this virus. Secondly, EqHV is the closest relative of HCV, and it could be argued that successful generation of chimeric VLPs using this virus would infer that other HCV isolates could be successfully incorporated into this system. Thirdly, as already discussed in the introduction chapter of this thesis, EqHV provides an analogous model for HCV infection and so characterisation the Rubella-EqHV candidate in this model would of interest. This piece of work was initially started during this project, with two chimeric constructs based on EqHV-E1E2 sequences isolated in our laboratory. However due to time limitations, the plasmids for these constructs were made but not tested.

Another aspect of future work would be to investigate the use of the RH5 chimera in the context of a full-length RV-genome with the 24s ORF replaced with RH5 construct. This could produce a replication-competent, attenuated chimeric virus. A similar approach has been used successfully in the rVSV-ΔG-EBOV vaccine[417]. The next step towards developing this system would be to generate a RV-based reporter system that can then be used to assess the functionality of the RH5 envelope glycoproteins.

This project has proposed a novel HCV vaccine candidate. As a result of this, several questions have arisen from this work that were unable to be answered in this thesis. There are a wealth of experiments required to fully explore the potential of this candidate.

Despite the advances in the treatment of HCV using DAAs, pressure for an effective vaccine remains. The ability to provide long lasting, protective immunity towards infection will be essential for meeting current elimination targets. Current understanding of immune responses in individuals who achieved SVC have highlighted the importance of both humoral and cellular immune responses. VLP based vaccines are highly immunogenic, stimulating both cellular and humoral arms of the adaptive immune system. VLPs therefore provide a valid line of research into the development of novel HCV vaccines.

Chapter 7 References

1. Blach S, Zeuzem S, Manns M, et al. Global prevalence and genotype distribution of hepatitis C virus infection in 2015: a modelling study. *lancet Gastroenterol Hepatol*. 2017;2(3):161-176. doi:10.1016/S2468-1253(16)30181-9

2. Calvaruso V, Petta S, Craxì A. Is global elimination of HCV realistic? *Liver Int*. 2018;38 Suppl 1:40-46. doi:10.1111/LIV.13668

3. Dultz G, Graubard BI, Martin P, et al. Liver transplantation for chronic hepatitis C virus infection in the United States 2002–2014: An analysis of the UNOS/OPTN registry. *PLoS One*. 2017;12(10):e0186898. doi:10.1371/JOURNAL.PONE.0186898

4. Ly KN, Xing J, Klevens RM, Jiles RB, Holmberg SD. Causes of death and characteristics of decedents with viral hepatitis, United States, 2010. *Clin Infect Dis*. 2014;58(1):40-49. doi:10.1093/CID/CIT642

5. Dore GJ, Bajis S. Hepatitis C virus elimination: laying the foundation for achieving 2030 targets. *Nat Rev Gastroenterol Hepatol 2020 182*. 2020;18(2):91-92. doi:10.1038/s41575-020-00392-3

6. Williams IT, Bell BP, Kuhnert W, Alter MJ. Incidence and Transmission Patterns of Acute Hepatitis C in the United States, 1982-2006. *Arch Intern Med*. 2011;171(3):242-248. doi:10.1001/ARCHINTERNMED.2010.511

7. Lanphear BP, Linnemann CC, Cannon CG, DeRonde MM, Pendy L, Kerley LM. Hepatitis C virus infection in healthcare workers: risk of exposure and infection. *Infect Control Hosp Epidemiol*. 1994;15(12):745-750. doi:10.1086/646851

8. Alter HJ, Harvey GK. The hazards of blood transfusion in historical perspective. *Blood*. 2008;112(7):2617-2626. doi:10.1182/BLOOD-2008-07-077370

9. Prati D. Transmission of hepatitis C virus by blood transfusions and other medical procedures: A global review. *J Hepatol*. 2006;45(4):607-616. doi:10.1016/J.JHEP.2006.07.003

10. Novati R, Thiers V, D'ArminioMonforte A, et al. Mother-to-child transmission of hepatitis C virus detected by nested polymerase chain reaction. *J Infect Dis*. 1992;165(4):720-723. doi:10.1093/INFDIS/165.4.720

11. Armstrong GL, Wasley A, Simard EP, McQuillan GM, Kuhnert WL, Alter MJ. The prevalence of hepatitis C virus infection in the United States, 1999 through 2002. *Ann Intern Med*. 2006;144(10):705-714. doi:10.7326/0003-4819-144-10-200605160-00004

12. Hagan H, Jordan AE, Neurer J, Cleland CM. Incidence of sexually

transmitted hepatitis C virus infection in HIV-positive men who have sex with men. *AIDS*. 2015;29(17):2335-2345. doi:10.1097/QAD.0000000000000834

13. Ghany MG, Strader DB, Thomas DL, Seeff LB. Diagnosis, management, and treatment of hepatitis C: an update. *Hepatology*. 2009;49(4):1335-1374. doi:10.1002/HEP.22759

14. Osburn WO, Fisher BE, Dowd KA, et al. Spontaneous control of primary hepatitis C virus infection and immunity against persistent reinfection. *Gastroenterology*. 2010;138(1):315-324. doi:10.1053/J.GASTRO.2009.09.017

15. Jacobson IM, Cacoub P, Dal Maso L, Harrison SA, Younossi ZM. Manifestations of Chronic Hepatitis C Virus Infection Beyond the Liver. *Clin Gastroenterol Hepatol*. 2010;8(12):1017-1029. doi:10.1016/J.CGH.2010.08.026

16. Thein HH, Yi Q, Dore GJ, Krahn MD. Estimation of stage-specific fibrosis progression rates in chronic hepatitis C virus infection: a meta-analysis and meta-regression. *Hepatology*. 2008;48(2):418-431. doi:10.1002/HEP.22375

17. El-Serag HB. Epidemiology of viral hepatitis and hepatocellular carcinoma. *Gastroenterology*. 2012;142(6). doi:10.1053/J.GASTRO.2011.12.061

18. Duncan JD, Urbanowicz RA, Tarr AW, Ball JK. Hepatitis C Virus Vaccine: Challenges and Prospects. *Vaccines 2020, Vol 8, Page 90*. 2020;8(1):90. doi:10.3390/VACCINES8010090

19. Palumbo E. Pegylated interferon and ribavirin treatment for hepatitis C virus infection. *Ther Adv Chronic Dis*. 2011;2(1):39-45. doi:10.1177/2040622310384308

20. Liang TJ, Ghany MG. Current and future therapies for hepatitis C virus infection. *N Engl J Med*. 2013;368(20):1907-1917. doi:10.1056/NEJMRA1213651

21. Falade-Nwulia O, Suarez-Cuervo C, Nelson DR, Fried MW, Segal JB, Sulkowski MS. Oral Direct-Acting Agent Therapy for Hepatitis C Virus Infection: A Systematic Review. *Ann Intern Med*. 2017;166(9):637-648. doi:10.7326/M16-2575

22. Marquez LK, Chaillon A, Soe KP, et al. Cost and cost-effectiveness of a real-world HCV treatment program among HIV-infected individuals in Myanmar. *BMJ Glob Heal*. 2021;6(2):e004181. doi:10.1136/BMJGH-2020-004181

23. Foster GR, Hézode C, Bronowicki J, et al. Telaprevir alone or with peginterferon and ribavirin reduces HCV RNA in patients with chronic genotype 2 but not genotype 3 infections. *Gastroenterology*. 2011;141(3). doi:10.1053/J.GASTRO.2011.05.046

24. Newman RM, Kuntzen T, Weiner B, et al. Whole genome pyrosequencing of rare hepatitis C virus genotypes enhances subtype classification and identification of naturally occurring drug resistance variants. *J Infect Dis*. 2013;208(1):17-31. doi:10.1093/INFDIS/JIS679

25. Sonderup MW, Afihene M, Ally R, et al. Hepatitis C in sub-Saharan Africa: the current status and recommendations for achieving elimination by 2030. *Lancet Gastroenterol Hepatol*. 2017;2(12):910-919. doi:10.1016/S2468-1253(17)30249-2

26. Njouom R, Frost E, Deslandes S, et al. Predominance of hepatitis C virus genotype 4 infection and rapid transmission between 1935 and 1965 in the Central African Republic. *J Gen Virol*. 2009;90(Pt 10):2452-2456. doi:10.1099/VIR.0.011981-0

27. Shah R, Ahovegbe L, Niebel M, Shepherd J, Thomson EC. Non-epidemic HCV genotypes in low- and middle-income countries and the risk of resistance to current direct-acting antiviral regimens. *J Hepatol*. 2021;75(2):462-473. doi:10.1016/J.JHEP.2021.04.045

28. da Silva Filipe A, Sreenu V, Hughes J, et al. Response to DAA therapy in the NHS England Early Access Programme for rare HCV subtypes from low and middle income countries. *J Hepatol*. 2017;67(6):1348-1350. doi:10.1016/J.JHEP.2017.06.035

29. Rossi C, Butt ZA, Wong S, et al. Hepatitis C virus reinfection after successful treatment with direct-acting antiviral therapy in a large population-based cohort. *J Hepatol*. 2018;69(5):1007-1014. doi:10.1016/J.JHEP.2018.07.025

30. Moureau G, Cook S, Lemey P, et al. New insights into flavivirus evolution, taxonomy and biogeographic history, extended by analysis of canonical and alternative coding sequences. *PLoS One*. 2015;10(2). doi:10.1371/JOURNAL.PONE.0117849

31. Smith DB, Becher P, Bukh J, et al. Proposed update to the taxonomy of the genera Hepacivirus and Pegivirus within the Flaviviridae family. *J Gen Virol*. 2016;97(11):2894-2907. doi:10.1099/jgv.0.000612

32. Tegtmeyer B, Echelmeyer J, Pfankuche VM, et al. Chronic equine hepacivirus infection in an adult gelding with severe hepatopathy. *Vet Med Sci*. 2019;5(3):372. doi:10.1002/VMS3.181

33. Pfaender S, Brown RJP, Pietschmann T, Steinmann E. Natural reservoirs for homologs of hepatitis C virus. *Emerg Microbes Infect*. 2014;3(3). doi:10.1038/EMI.2014.19

34. Echeverría N, Moratorio G, Cristina J, Moreno P. Hepatitis C virus genetic variability and evolution. *World J Hepatol*. 2015;7(6):831-845. doi:10.4254/WJH.V7.I6.831

35. Smith DB, Bukh J, Kuiken C, et al. Expanded classification of

hepatitis C virus into 7 genotypes and 67 subtypes: updated criteria and genotype assignment web resource. *Hepatology*. 2014;59(1):318-327. doi:10.1002/HEP.26744

36. Borgia SM, Hedskog C, Parhy B, et al. Identification of a Novel Hepatitis C Virus Genotype From Punjab, India: Expanding Classification of Hepatitis C Virus Into 8 Genotypes. *J Infect Dis*. 2018;218(11):1722-1729. doi:10.1093/INFDIS/JIY401

37. Bukh J, Miller RH, Purcell RH. Genetic heterogeneity of hepatitis C virus: quasispecies and genotypes. *Semin Liver Dis*. 1995;15(1):41-63. doi:10.1055/S-2007-1007262

38. Forns X, Purcell RH, Bukh J. Quasispecies in viral persistence and pathogenesis of hepatitis C virus. *Trends Microbiol*. 1999;7(10):402-410. doi:10.1016/S0966-842X(99)01590-5

39. Liu L, Fisher BE, Dowd KA, Astemborski J, Cox AL, Ray SC. Acceleration of Hepatitis C Virus Envelope Evolution in Humans Is Consistent with Progressive Humoral Immune Selection during the Transition from Acute to Chronic Infection. *J Virol*. 2010;84(10):5067-5077. doi:10.1128/JVI.02265-09/ASSET/FD129016-2CE0-4754-8873-C7D3D7337028/ASSETS/GRAPHIC/ZJV9990931990006.JPEG

40. Farci P, Shimoda A, Coiana A, et al. The outcome of acute hepatitis C predicted by the evolution of the viral quasispecies. *Science*. 2000;288(5464):339-344. doi:10.1126/SCIENCE.288.5464.339

41. Petruzziello A, Marigliano S, Loquercio G, Cozzolino A, Cacciapuoti C. Global epidemiology of hepatitis C virus infection: An up-date of the distribution and circulation of hepatitis C virus genotypes. *World J Gastroenterol*. 2016;22(34):7824. doi:10.3748/WJG.V22.I34.7824

42. Choo QL, Richman KH, Han JH, et al. Genetic organization and diversity of the hepatitis C virus. *Proc Natl Acad Sci*. 1991;88(6):2451-2455. doi:10.1073/PNAS.88.6.2451

43. Tsukiyama-Kohara K, Iizuka N, Kohara M, Nomoto A. Internal ribosome entry site within hepatitis C virus RNA. *J Virol*. 1992;66(3):1476-1483. doi:10.1128/JVI.66.3.1476-1483.1992

44. Ashfaq UA, Javed T, Rehman S, Nawaz Z, Riazuddin S. An overview of HCV molecular biology, replication and immune responses. *Virol J*. 2011;8(Figure 1):1-10. doi:10.1186/1743-422X-8-161

45. Ito T, Tahara SM, Lai MMC. The 3′-Untranslated Region of Hepatitis C Virus RNA Enhances Translation from an Internal Ribosomal Entry Site. *J Virol*. 1998;72(11):8789. Accessed September 18, 2021. /pmc/articles/PMC110295/

46. T T, N K, MJ C, K S, K S. Structure of the 3' terminus of the

hepatitis C virus genome. *J Virol*. 1996;70(5):3307-3312. doi:10.1128/JVI.70.5.3307-3312.1996

47. Shi G, Ando T, Suzuki R, et al. Involvement of the 3' Untranslated Region in Encapsidation of the Hepatitis C Virus. *PLOS Pathog*. 2016;12(2):e1005441. doi:10.1371/JOURNAL.PPAT.1005441

48. Kopp M, Murray CL, Jones CT, Rice CM. Genetic Analysis of the Carboxy-Terminal Region of the Hepatitis C Virus Core Protein. *J Virol*. 2010;84(4):1666. doi:10.1128/JVI.02043-09

49. Gawlik K, Gallay PA. HCV core protein and virus assembly: what we know without structures. *Immunol Res*. 2014;60(1):1-10. doi:10.1007/s12026-014-8494-3

50. Ivanyi-Nagy R, Kanevsky I, Gabus C, et al. Analysis of hepatitis C virus RNA dimerization and core-RNA interactions. *Nucleic Acids Res*. 2006;34(9):2618-2633. doi:10.1093/NAR/GKL240

51. Klein KC, Dellos SR, Lingappa JR. Identification of residues in the hepatitis C virus core protein that are critical for capsid assembly in a cell-free system. *J Virol*. 2005;79(11):6814-6826. doi:10.1128/JVI.79.11.6814-6826.2005

52. Boulant S, Montserret R, Hope RG, et al. Structural determinants that target the hepatitis C virus core protein to lipid droplets. *J Biol Chem*. 2006;281(31):22236-22247. doi:10.1074/JBC.M601031200

53. Vieyres G, Thomas X, Descamps V, Duverlie G, Patel AH, Dubuisson J. Characterization of the Envelope Glycoproteins Associated with Infectious Hepatitis C Virus. *J Virol*. 2010;84(19):10159-10168. doi:10.1128/jvi.01180-10

54. Vieyres G, Dubuisson J, Pietschmann T. Incorporation of hepatitis C virus E1 and E2 glycoproteins: the keystones on a peculiar virion. *Viruses*. 2014;6(3):1149-1187. doi:10.3390/V6031149

55. Ball JK, Tarr AW, McKeating JA. The past, present and future of neutralizing antibodies for hepatitis C virus. *Antiviral Res*. 2014;105(100):100-111. doi:10.1016/J.ANTIVIRAL.2014.02.013

56. Helle F, Vieyres G, Elkrief L, et al. Role of N-Linked Glycans in the Functions of Hepatitis C Virus Envelope Proteins Incorporated into Infectious Virions. *J Virol*. 2010;84(22):11905-11915. doi:10.1128/jvi.01548-10

57. Meunier JC, Fournillier A, Choukhi A, et al. Analysis of the glycosylation sites of hepatitis C virus (HCV) glycoprotein E1 and the influence of E1 glycans on the formation of the HCV glycoprotein complex. *J Gen Virol*. 1999;80 (Pt 4)(4):887-896. doi:10.1099/0022-1317-80-4-887

58. Wahid A, Helle F, Descamps V, Duverlie G, Penin F, Dubuisson J. Disulfide bonds in hepatitis C virus glycoprotein E1 control the

assembly and entry functions of E2 glycoprotein. *J Virol*. 2013;87(3):1605-1617. doi:10.1128/JVI.02659-12

59. Cocquerel L, Duvet S, Meunier J-C, et al. The transmembrane domain of hepatitis C virus glycoprotein E1 is a signal for static retention in the endoplasmic reticulum. *J Virol*. 1999;73(4):2641-2649. doi:10.1128/JVI.73.4.2641-2649.1999

60. Ciczora Y, Callens N, Penin F, Pécheur E-I, Dubuisson J. Transmembrane Domains of Hepatitis C Virus Envelope Glycoproteins: Residues Involved in E1E2 Heterodimerization and Involvement of These Domains in Virus Entry. *J Virol*. 2007;81(5):2372-2381. doi:10.1128/jvi.02198-06

61. JP M, C W, A C, et al. Characterization of truncated forms of hepatitis C virus glycoproteins. *J Gen Virol*. 1997;78 (Pt 9)(9):2299-2306. doi:10.1099/0022-1317-78-9-2299

62. Botti V, Bianchi A, Foung SKH, Merola M. The Hepatitis C Virus E1 Glycoprotein Undergoes Productive Folding but Accelerated Degradation When Expressed as an Individual Subunit in CHO Cells. *PLoS One*. 2011;6(8). doi:10.1371/JOURNAL.PONE.0023838

63. Pfaff-Kilgore JM, Davidson E, Kadash-Edmondson K, et al. Sites of vulnerability in HCV E1E2 identified by comprehensive functional screening. *Cell Rep*. 2022;39(8):110859. doi:10.1016/J.CELREP.2022.110859

64. Garry RF, Dash S. Proteomics computational analyses suggest that hepatitis C virus E1 and pestivirus E2 envelope glycoproteins are truncated class II fusion proteins. *Virology*. 2003;307(2):255-265. doi:10.1016/S0042-6822(02)00065-X

65. El Omari K, Iourin O, Kadlec J, et al. Unexpected structure for the N-terminal domain of hepatitis C virus envelope glycoprotein E1. *Nat Commun 2014 51*. 2014;5(1):1-5. doi:10.1038/ncomms5874

66. Drummer HE, Boo I, Poumbourios P. Mutagenesis of a conserved fusion peptide-like motif and membrane-proximal heptad-repeat region of hepatitis C virus glycoprotein E1. *J Gen Virol*. 2007;88(Pt 4):1144-1148. doi:10.1099/VIR.0.82567-0

67. Tong Y, Lavillette D, Li Q, Zhong J. Role of Hepatitis C Virus Envelope Glycoprotein E1 in Virus Entry and Assembly. *Front Immunol*. 2018;9(JUN). doi:10.3389/FIMMU.2018.01411

68. El Omari K, Iourin O, Harlos K, Grimes JM, Stuart DI. Structure of a Pestivirus Envelope Glycoprotein E2 Clarifies Its Role in Cell Entry. *Cell Rep*. 2013;3(1):30-35. doi:10.1016/J.CELREP.2012.12.001

69. Falson P, Bartosch B, Alsaleh K, et al. Hepatitis C Virus Envelope Glycoprotein E1 Forms Trimers at the Surface of the Virion. *J Virol*. 2015;89(20):10333-10346. doi:10.1128/jvi.00991-15

70. Kima IS, Jenni S, Stanifer ML, et al. Mechanism of membrane fusion induced by vesicular stomatitis virus G protein. *Proc Natl Acad Sci U S A*. 2017;114(1):E28-E36. doi:10.1073/PNAS.1618883114/-/DCSUPPLEMENTAL

71. Dubois RM, Vaney MC, Tortorici MA, et al. Functional and evolutionary insight from the crystal structure of rubella virus protein E1. *Nat 2012 4937433*. 2013;493(7433):552-556. doi:10.1038/nature11741

72. Kato N, Ootsuyama Y, Ohkoshi S, et al. Characterization of hypervariable regions in the putative envelope protein of hepatitis C virus. *Biochem Biophys Res Commun*. 1992;189(1):119-127. doi:10.1016/0006-291X(92)91533-V

73. McCaffrey K, Boo I, Poumbourios P, Drummer HE. Expression and characterization of a minimal hepatitis C virus glycoprotein E2 core domain that retains CD81 binding. *J Virol*. 2007;81(17):9584-9590. doi:10.1128/JVI.02782-06

74. Keck Z, Wang W, Wang Y, et al. Cooperativity in virus neutralization by human monoclonal antibodies to two adjacent regions located at the amino terminus of hepatitis C virus E2 glycoprotein. *J Virol*. 2013;87(1):37-51. doi:10.1128/JVI.01941-12

75. Keck Z-Y, Op De Beeck A, Hadlock KG, et al. Hepatitis C Virus E2 Has Three Immunogenic Domains Containing Conformational Epitopes with Distinct Properties and Biological Functions. *J Virol*. 2004;78(17):9224-9232. doi:10.1128/jvi.78.17.9224-9232.2004

76. Giang E, Dorner M, Prentoe JC, et al. Human broadly neutralizing antibodies to the envelope glycoprotein complex of hepatitis C virus. *Proc Natl Acad Sci U S A*. 2012;109(16):6205-6210. doi:10.1073/PNAS.1114927109/-/DCSUPPLEMENTAL

77. Drummer HE. Challenges to the development of vaccines to hepatitis C virus that elicit neutralizing antibodies. *Front Microbiol*. 2014;5(JULY):329. doi:10.3389/FMICB.2014.00329/BIBTEX

78. Yagnik AT, Lahm A, Meola A, et al. A model for the hepatitis C virus envelope glycoprotein E2. *Proteins*. 2000;40(3):355-366. doi:10.1002/1097-0134(20000815)40:3<355::aid-prot20>3.0.co;2-k

79. Krey T, D'Alayer J, Kikuti CM, et al. The disulfide bonds in glycoprotein E2 of hepatitis C virus reveal the tertiary organization of the molecule. *PLoS Pathog*. 2010;6(2). doi:10.1371/JOURNAL.PPAT.1000762

80. Kong L, Giang E, Nieusma T, et al. Hepatitis C virus E2 envelope glycoprotein core structure. *Science (80-)*. 2013;342(6162):1090-1094. doi:10.1126/science.1243876

81. Khan AG, Whidby J, Miller MT, et al. Structure of the core ectodomain of the hepatitis C virus envelope glycoprotein 2.

Nature. 2014;509(7500):381-384. doi:10.1038/nature13117

82. Flyak AI, Ruiz S, Colbert MD, et al. HCV Broadly Neutralizing Antibodies Use a CDRH3 Disulfide Motif to Recognize an E2 Glycoprotein Site that Can Be Targeted for Vaccine Design. *Cell Host Microbe*. 2018;24(5):703-716.e3. doi:10.1016/j.chom.2018.10.009

83. Torrents De La Peña A, Sliepen K, Eshun-Wilson L, et al. Structure of the hepatitis C virus E1E2 glycoprotein complex. doi:10.1101/2021.12.16.472992

84. Schnell JR, Chou JJ. Structure and mechanism of the M2 proton channel of influenza A virus. *Nat 2008 4517178*. 2008;451(7178):591-595. doi:10.1038/nature06531

85. González ME. Vpu Protein: The Viroporin Encoded by HIV-1. *Viruses*. 2015;7(8):4352. doi:10.3390/V7082824

86. Lin C, Lindenbach BD, Prágai BM, McCourt DW, Rice CM. Processing in the hepatitis C virus E2-NS2 region: identification of p7 and two distinct E2-specific products with different C termini. *J Virol*. 1994;68(8):5063-5073. doi:10.1128/JVI.68.8.5063-5073.1994

87. Carrère-Kremer S, Montpellier-Pala C, Cocquerel L, Wychowski C, Penin F, Dubuisson J. Subcellular Localization and Topology of the p7 Polypeptide of Hepatitis C Virus. *J Virol*. 2002;76(8):3720. doi:10.1128/JVI.76.8.3720-3730.2002

88. Montserret R, Saint N, Vanbelle C, et al. NMR structure and ion channel activity of the p7 protein from hepatitis C virus. *J Biol Chem*. 2010;285(41):31446-31461. doi:10.1074/JBC.M110.122895/ATTACHMENT/38FF4B99-0563-4349-A744-62B60270F5EA/MMC1.PDF

89. Griffin SDC, Harvey R, Clarke DS, Barclay WS, Harris M, Rowlands DJ. A conserved basic loop in hepatitis C virus p7 protein is required for amantadine-sensitive ion channel activity in mammalian cells but is dispensable for localization to mitochondria. *J Gen Virol*. 2004;85(2):451-461. doi:10.1099/VIR.0.19634-0/CITE/REFWORKS

90. Chandler DE, Penin F, Schulten K, Chipot C. The p7 Protein of Hepatitis C Virus Forms Structurally Plastic, Minimalist Ion Channels. *PLOS Comput Biol*. 2012;8(9):e1002702. doi:10.1371/JOURNAL.PCBI.1002702

91. Pavlovic D, Neville DCA, Argaud O, et al. The hepatitis C virus p7 protein forms an ion channel that is inhibited by long-alkyl-chain iminosugar derivatives. *Proc Natl Acad Sci U S A*. 2003;100(10):6104-6108. doi:10.1073/PNAS.1031527100

92. Griffin SDC, Beales LP, Clarke DS, et al. The p7 protein of hepatitis C virus forms an ion channel that is blocked by the

antiviral drug, Amantadine. *FEBS Lett*. 2003;535(1-3):34-38. doi:10.1016/S0014-5793(02)03851-6

93. Steinmann E, Penin F, Kallis S, Patel AH, Bartenschlager R, Pietschmann T. Hepatitis C Virus p7 Protein Is Crucial for Assembly and Release of Infectious Virions. *PLOS Pathog*. 2007;3(7):e103. doi:10.1371/JOURNAL.PPAT.0030103

94. Wozniak AL, Griffin S, Rowlands D, et al. Intracellular Proton Conductance of the Hepatitis C Virus p7 Protein and Its Contribution to Infectious Virus Production. *PLOS Pathog*. 2010;6(9):e1001087. doi:10.1371/JOURNAL.PPAT.1001087

95. Jones CT, Murray CL, Eastman DK, Tassello J, Rice CM. Hepatitis C Virus p7 and NS2 Proteins Are Essential for Production of Infectious Virus. *J Virol*. 2007;81(16):8374. doi:10.1128/JVI.00690-07

96. Sakai A, St. Claire M, Faulk K, et al. The p7 polypeptide of hepatitis C virus is critical for infectivity and contains functionally important genotype-specific sequences. *Proc Natl Acad Sci U S A*. 2003;100(20):11646-11651. doi:10.1073/PNAS.1834545100

97. E S, L P, C F, G M, N M. The NS2 protein of hepatitis C virus is a transmembrane polypeptide. *J Virol*. 1995;69(12):7461-7471. doi:10.1128/JVI.69.12.7461-7471.1995

98. Grakoui A, McCourt DW, Wychowski C, Feinstone SM, Rice CM. A second hepatitis C virus-encoded proteinase. *Proc Natl Acad Sci U S A*. 1993;90(22):10583-10587. doi:10.1073/PNAS.90.22.10583

99. Lorenz IC, Marcotrigiano J, Dentzer TG, Rice CM. Structure of the catalytic domain of the hepatitis C virus NS2-3 protease. *Nature*. 2006;442(7104):831-835. doi:10.1038/NATURE04975

100. Lohmann V, Körner F, Koch JO, Herian U, Theilmann L, Bartenschlager R. Replication of subgenomic hepatitis C virus RNAs in a hepatoma cell line. *Science*. 1999;285(5424):110-113. doi:10.1126/SCIENCE.285.5424.110

101. Pietschmann T, Kaul A, Koutsoudakis G, et al. Construction and characterization of infectious intragenotypic and intergenotypic hepatitis C virus chimeras. *Proc Natl Acad Sci U S A*. 2006;103(19):7408. doi:10.1073/PNAS.0504877103

102. Hijikata M, Mizushima H, Akagi T, et al. Two distinct proteinase activities required for the processing of a putative nonstructural precursor protein of hepatitis C virus. *J Virol*. 1993;67(8):4665. doi:10.1128/JVI.67.8.4665-4675.1993

103. Love RA, Parge HE, Wickersham JA, et al. The Crystal Structure of Hepatitis C Virus NS3 Proteinase Reveals a Trypsin-like Fold and a Structural Zinc Binding Site. *Cell*. 1996;87(2):331-342. doi:10.1016/S0092-8674(00)81350-1

104. Bartenschlager R, Ahlborn-Laake L, Mous J, Jacobsen H. Kinetic and structural analyses of hepatitis C virus polyprotein processing. *J Virol*. 1994;68(8):5045. doi:10.1128/JVI.68.8.5045-5055.1994

105. Tomei L, Failla C, Vitale RL, Bianchi E, De Francesco R. A central hydrophobic domain of the hepatitis C virus NS4A protein is necessary and sufficient for the activation of the NS3 protease. *J Gen Virol*. 1996;77 (Pt 5)(5):1065-1070. doi:10.1099/0022-1317-77-5-1065

106. Frick DN. The Hepatitis C Virus NS3 Protein: A Model RNA Helicase and Potential Drug Target. *Curr Issues Mol Biol 2007, Vol 9, Pages 1-20*. 2007;9(1):1-20. doi:10.21775/CIMB.009.001

107. Koch JO, Lohmann V, Herian U, Bartenschlager R. In VitroStudies on the Activation of the Hepatitis C Virus NS3 Proteinase by the NS4A Cofactor. *Virology*. 1996;221(1):54-66. doi:10.1006/VIRO.1996.0352

108. Kim JL, Morgenstern KA, Lin C, et al. Crystal Structure of the Hepatitis C Virus NS3 Protease Domain Complexed with a Synthetic NS4A Cofactor Peptide. *Cell*. 1996;87(2):343-355. doi:10.1016/S0092-8674(00)81351-3

109. Roder AE, Vazquez C, Horner SM. The acidic domain of the hepatitis C virus NS4A protein is required for viral assembly and envelopment through interactions with the viral E1 glycoprotein. *PLOS Pathog*. 2019;15(2):e1007163. doi:10.1371/JOURNAL.PPAT.1007163

110. Aligo J, Jia S, Manna D, Konan K V. Formation and function of hepatitis C virus replication complexes require residues in the carboxy-terminal domain of NS4B protein. *Virology*. 2009;393(1):68-83. doi:10.1016/J.VIROL.2009.07.033

111. Gouttenoire J, Penin F, Moradpour D. Hepatitis C virus nonstructural protein 4B: a journey into unexplored territory. *Rev Med Virol*. 2010;20(2):117-129. doi:10.1002/RMV.640

112. Gouttenoire J, Castet V, Montserret R, et al. Identification of a novel determinant for membrane association in hepatitis C virus nonstructural protein 4B. *J Virol*. 2009;83(12):6257-6268. doi:10.1128/JVI.02663-08

113. Gouttenoire J, Roingeard P, Penin F, Moradpour D. Amphipathic alpha-helix AH2 is a major determinant for the oligomerization of hepatitis C virus nonstructural protein 4B. *J Virol*. 2010;84(24):12529-12537. doi:10.1128/JVI.01798-10

114. Egger D, Wölk B, Gosert R, et al. Expression of Hepatitis C Virus Proteins Induces Distinct Membrane Alterations Including a Candidate Viral Replication Complex. *J Virol*. 2002;76(12):5974. doi:10.1128/JVI.76.12.5974-5984.2002

115. Thompson AA, Zou A, Yan J, et al. Biochemical characterization of recombinant hepatitis C virus nonstructural protein 4B: evidence for ATP/GTP hydrolysis and adenylate kinase activity. *Biochemistry*. 2009;48(5):906-916. doi:10.1021/BI801747P

116. Blight KJ. Charged Residues in Hepatitis C Virus NS4B Are Critical for Multiple NS4B Functions in RNA Replication. *J Virol*. 2011;85(16):8158. doi:10.1128/JVI.00858-11

117. Kaneko T, Tanji Y, Satoh S, et al. Production of two phosphoproteins from the NS5A region of the hepatitis C viral genome. *Biochem Biophys Res Commun*. 1994;205(1):320-326. doi:10.1006/BBRC.1994.2667

118. Bartenschlager R, Lohmann V, Penin F. The molecular and structural basis of advanced antiviral therapy for hepatitis C virus infection. *Nat Rev Microbiol 2013 117*. 2013;11(7):482-496. doi:10.1038/nrmicro3046

119. Lee KJ, Choi J, Ou J, Lai MMC. The C-Terminal Transmembrane Domain of Hepatitis C Virus (HCV) RNA Polymerase Is Essential for HCV Replication In Vivo. *J Virol*. 2004;78(7):3797-3802. doi:10.1128/JVI.78.7.3797-3802.2004/ASSET/CA8A44DE-F087-495B-8AE7-D9E16DD04DA3/ASSETS/GRAPHIC/ZJV0070414670006.JPEG

120. Lesburg CA, Cable MB, Ferrari E, Hong Z, Mannarino AF, Weber PC. Crystal structure of the RNA-dependent RNA polymerase from hepatitis C virus reveals a fully encircled active site. *Nat Struct Biol*. 1999;6(10):937-943. doi:10.1038/13305

121. Luo G, Hamatake RK, Mathis DM, et al. De novo initiation of RNA synthesis by the RNA-dependent RNA polymerase (NS5B) of hepatitis C virus. *J Virol*. 2000;74(2):851-863. doi:10.1128/JVI.74.2.851-863.2000

122. Gao L, Aizaki H, He J-W, Lai MMC. Interactions between Viral Nonstructural Proteins and Host Protein hVAP-33 Mediate the Formation of Hepatitis C Virus RNA Replication Complex on Lipid Raft. *J Virol*. 2004;78(7):3480-3488. doi:10.1128/JVI.78.7.3480-3488.2004/ASSET/476804F5-6B2C-4053-B24D-EDC1673DF9F9/ASSETS/GRAPHIC/ZJV0070411870006.JPEG

123. Catanese MT, Uryu K, Kopp M, et al. Ultrastructural analysis of hepatitis C virus particles. *Proc Natl Acad Sci U S A*. 2013;110(23):9505-9510. doi:10.1073/PNAS.1307527110/-/DCSUPPLEMENTAL

124. Piver E, Boyer A, Gaillard J, et al. Ultrastructural organisation of HCV from the bloodstream of infected patients revealed by electron microscopy after specific immunocapture. *Gut*. 2017;66(8):1487-1495. doi:10.1136/GUTJNL-2016-311726

125. Zhang Y, Corver J, Chipman PR, et al. Structures of immature

flavivirus particles. *EMBO J*. 2003;22(11):2604-2613. doi:10.1093/EMBOJ/CDG270

126. Collett S, Torresi J, Earnest-Silveira L, Christiansen D, Elbourne A, Ramsland PA. Probing and pressing surfaces of hepatitis C virus-like particles. *J Colloid Interface Sci*. 2019;545:259-268. doi:10.1016/j.jcis.2019.03.022

127. Bankwitz D, Doepke M, Hueging K, et al. Maturation of secreted HCV particles by incorporation of secreted ApoE protects from antibodies by enhancing infectivity. *J Hepatol*. 2017;67(3):480-489. doi:10.1016/j.jhep.2017.04.010

128. Nielsen SU, Bassendine MF, Burt AD, Martin C, Pumeechockchai W, Toms GL. Association between Hepatitis C Virus and Very-Low-Density Lipoprotein (VLDL)/LDL Analyzed in Iodixanol Density Gradients. *J Virol*. 2006;80(5):2418-2428. doi:10.1128/JVI.80.5.2418-2428.2006/FORMAT/EPUB

129. Nielsen SU, Bassendine MF, Martin C, et al. Characterization of hepatitis C RNA-containing particles from human liver by density and size. *J Gen Virol*. 2008;89(Pt 10):2507-2617. doi:10.1099/VIR.0.2008/000083-0

130. André P, Komurian-Pradel F, Deforges S, et al. Characterization of low- and very-low-density hepatitis C virus RNA-containing particles. *J Virol*. 2002;76(14):6919-6928. doi:10.1128/JVI.76.14.6919-6928.2002

131. Lindenbach BD, Rice CM. The ins and outs of hepatitis C virus entry and assembly. *Nat Rev Microbiol*. 2013;11(10):688-700. doi:10.1038/nrmicro3098

132. Shi Q, Jiang J, Luo G. Syndecan-1 serves as the major receptor for attachment of hepatitis C virus to the surfaces of hepatocytes. *J Virol*. 2013;87(12):6866-6875. doi:10.1128/JVI.03475-12

133. Lefèvre M, Felmlee DJ, Parnot M, Baumert TF, Schuster C. Syndecan 4 Is Involved in Mediating HCV Entry through Interaction with Lipoviral Particle-Associated Apolipoprotein E. *PLoS One*. 2014;9(4):e95550. doi:10.1371/JOURNAL.PONE.0095550

134. Jiang J, Cun W, Wu X, Shi Q, Tang H, Luo G. Hepatitis C Virus Attachment Mediated by Apolipoprotein E Binding to Cell Surface Heparan Sulfate. *J Virol*. 2012;86(13):7256-7267. doi:10.1128/jvi.07222-11

135. Barth H, Schafer C, Adah MI, et al. Cellular binding of hepatitis C virus envelope glycoprotein E2 requires cell surface heparan sulfate. *J Biol Chem*. 2003;278(42):41003-41012. doi:10.1074/jbc.M302267200

136. Wang J, Qiao L, Hou Z, Luo G. TIM-1 Promotes Hepatitis C Virus Cell Attachment and Infection. *J Virol*. 2017;91(2).

doi:10.1128/JVI.01583-16

137. Bartosch B, Vitelli A, Granier C, et al. Cell entry of hepatitis C virus requires a set of co-receptors that include the CD81 tetraspanin and the SR-B1 scavenger receptor. *J Biol Chem*. 2003;278(43):41624-41630. doi:10.1074/JBC.M305289200

138. Pileri P, Uematsu Y, Campagnoli S, et al. Binding of hepatitis C virus to CD81. *Science*. 1998;282(5390):938-941. doi:10.1126/SCIENCE.282.5390.938

139. Scarselli E, Ansuini H, Cerino R, et al. The human scavenger receptor class B type I is a novel candidate receptor for the hepatitis C virus. *EMBO J*. 2002;21(19):5017-5025. doi:10.1093/EMBOJ/CDF529

140. Ploss A, Evans MJ, Gaysinskaya VA, et al. Human occludin is a hepatitis C virus entry factor required for infection of mouse cells. *Nature*. 2009;457(7231):882-886. doi:10.1038/NATURE07684

141. Liu S, Yang W, Shen L, Turner JR, Coyne CB, Wang T. Tight junction proteins claudin-1 and occludin control hepatitis C virus entry and are downregulated during infection to prevent superinfection. *J Virol*. 2009;83(4):2011-2014. doi:10.1128/JVI.01888-08

142. Evans MJ, Von Hahn T, Tscherne DM, et al. Claudin-1 is a hepatitis C virus co-receptor required for a late step in entry. *Nature*. 2007;446(7137):801-805. doi:10.1038/NATURE05654

143. Augestad EH, Bukh J, Prentoe J. Hepatitis C virus envelope protein dynamics and the link to hypervariable region 1. *Curr Opin Virol*. 2021;50:69-75. doi:10.1016/J.COVIRO.2021.07.006

144. Roccasecca R, Ansuini H, Vitelli A, et al. Binding of the hepatitis C virus E2 glycoprotein to CD81 is strain specific and is modulated by a complex interplay between hypervariable regions 1 and 2. *J Virol*. 2003;77(3):1856-1867. doi:10.1128/JVI.77.3.1856-1867.2003

145. Penin F, Combet C, Germanidis G, Frainais P-O, Deléage G, Pawlotsky J-M. Conservation of the conformation and positive charges of hepatitis C virus E2 envelope glycoprotein hypervariable region 1 points to a role in cell attachment. *J Virol*. 2001;75(12):5703-5710. doi:10.1128/JVI.75.12.5703-5710.2001

146. Bonander N, Jamshad M, Hu K, et al. Structural characterization of CD81-Claudin-1 hepatitis C virus receptor complexes. *Biochem Soc Trans*. 2011;39(2):537-540. doi:10.1042/BST0390537

147. Tscherne DM, Jones CT, Evans MJ, Lindenbach BD, McKeating JA, Rice CM. Time- and temperature-dependent activation of hepatitis C virus for low-pH-triggered entry. *J Virol*. 2006;80(4):1734-1741. doi:10.1128/JVI.80.4.1734-1741.2006

148. Colpitts CC, Tsai PL, Zeisel MB. Hepatitis C Virus Entry: An Intriguingly Complex and Highly Regulated Process. *Int J Mol Sci*. 2020;21(6). doi:10.3390/IJMS21062091

149. Pestova T V., Shatsky IN, Fletcher SP, Jackson RJ, Hellen CUT. A prokaryotic-like mode of cytoplasmic eukaryotic ribosome binding to the initiation codon during internal translation initiation of hepatitis C and classical swine fever virus RNAs. *Genes Dev*. 1998;12(1):67-83. doi:10.1101/GAD.12.1.67

150. Hashem Y, Des Georges A, Dhote V, et al. Hepatitis-C-virus-like internal ribosome entry sites displace eIF3 to gain access to the 40S subunit. *Nature*. 2013;503(7477):539-543. doi:10.1038/NATURE12658

151. Lukavsky PJ. Structure and function of HCV IRES domains. *Virus Res*. 2009;139(2):166-171. doi:10.1016/J.VIRUSRES.2008.06.004

152. Jopling CL. Liver-specific microRNA-122: Biogenesis and function. *RNA Biol*. 2012;9(2):137-142. doi:10.4161/RNA.18827

153. Schult P, Roth H, Adams RL, et al. microRNA-122 amplifies hepatitis C virus translation by shaping the structure of the internal ribosomal entry site. *Nat Commun 2018 91*. 2018;9(1):1-14. doi:10.1038/s41467-018-05053-3

154. Masaki T, Arend KC, Li Y, et al. miR-122 stimulates hepatitis C virus RNA synthesis by altering the balance of viral RNAs engaged in replication versus translation. *Cell Host Microbe*. 2015;17(2):217-228. doi:10.1016/J.CHOM.2014.12.014

155. Romero-Brey I, Merz A, Chiramel A, et al. Three-Dimensional Architecture and Biogenesis of Membrane Structures Associated with Hepatitis C Virus Replication. *PLoS Pathog*. 2012;8(12). doi:10.1371/JOURNAL.PPAT.1003056

156. Paul D, Hoppe S, Saher G, Krijnse-Locker J, Bartenschlager R. Morphological and Biochemical Characterization of the Membranous Hepatitis C Virus Replication Compartment. *J Virol*. 2013;87(19):10612. doi:10.1128/JVI.01370-13

157. Dubuisson J, Rice CM. Hepatitis C virus glycoprotein folding: disulfide bond formation and association with calnexin. *J Virol*. 1996;70(2):778-786. doi:10.1128/JVI.70.2.778-786.1996

158. De Beeck AO, Montserret R, Duvet S, et al. The transmembrane domains of hepatitis C virus envelope glycoproteins E1 and E2 play a major role in heterodimerization. *J Biol Chem*. 2000;275(40):31428-31437. doi:10.1074/JBC.M003003200

159. Coller KE, Heaton NS, Berger KL, Cooper JD, Saunders JL, Randall G. Molecular Determinants and Dynamics of Hepatitis C Virus Secretion. *PLoS Pathog*. 2012;8(1):1002466. doi:10.1371/JOURNAL.PPAT.1002466

160. Vieyres G, Pietschmann T. HCV Pit Stop at the Lipid Droplet: Refuel Lipids and Put on a Lipoprotein Coat before Exit. *Cells*. 2019;8(3):233. doi:10.3390/cells8030233

161. Syed GH, Khan M, Yang S, Siddiqui A. Hepatitis C Virus Lipoviroparticles Assemble in the Endoplasmic Reticulum (ER) and Bud off from the ER to the Golgi Compartment in COPII Vesicles. Ou J-HJ, ed. *J Virol*. 2017;91(15). doi:10.1128/JVI.00499-17

162. Mina MM, Luciani F, Cameron B, et al. Resistance to hepatitis C virus: potential genetic and immunological determinants. *Lancet Infect Dis*. 2015;15(4):451-460. doi:10.1016/S1473-3099(14)70965-X

163. Gao B, Jeong W Il, Tian Z. Liver: An organ with predominant innate immunity. *Hepatology*. 2008;47(2):729-736. doi:10.1002/HEP.22034

164. Brown KS, Keogh MJ, Owsianka AM, et al. Specific interaction of hepatitis C virus glycoproteins with mannan binding lectin inhibits virus entry. *Protein Cell*. 2010;1(7):664-674. doi:10.1007/S13238-010-0088-9

165. Hamed MR, Brown RJP, Zothner C, et al. Recombinant human L-ficolin directly neutralizes hepatitis C virus entry. *J Innate Immun*. 2014;6(5):676-684. doi:10.1159/000362209

166. Lozach PY, Lortat-Jacob H, De Lacroix de Lavalette A, et al. DC-SIGN and L-SIGN are high affinity binding receptors for hepatitis C virus glycoprotein E2. *J Biol Chem*. 2003;278(22):20358-20366. doi:10.1074/JBC.M301284200

167. Xu Y, Zhong J. Innate immunity against hepatitis C virus. *Curr Opin Immunol*. 2016;42:98-104. doi:10.1016/J.COI.2016.06.009

168. Chigbu DI, Loonawat R, Sehgal M, Patel D, Jain P. Hepatitis C Virus Infection: Host–Virus Interaction and Mechanisms of Viral Persistence. *Cells 2019, Vol 8, Page 376*. 2019;8(4):376. doi:10.3390/CELLS8040376

169. Li D, Wu M. Pattern recognition receptors in health and diseases. *Signal Transduct Target Ther 2021 61*. 2021;6(1):1-24. doi:10.1038/s41392-021-00687-0

170. Fensterl V, Chattopadhyay S, Sen GC. No Love Lost Between Viruses and Interferons. *Annu Rev Virol*. 2015;2(1):549-572. doi:10.1146/ANNUREV-VIROLOGY-100114-055249

171. Patra T, Ray R, Ray R. Strategies to Circumvent Host Innate Immune Response by Hepatitis C Virus. *Cells*. 2019;8(3):274. doi:10.3390/cells8030274

172. Heim MH. Innate immunity and HCV. *J Hepatol*. 2013;58(3):564-574. doi:10.1016/J.JHEP.2012.10.005

173. Li XD, Sun L, Seth RB, Pineda G, Chen ZJ. Hepatitis C virus protease NS3/4A cleaves mitochondrial antiviral signaling protein off the mitochondria to evade innate immunity. *Proc Natl Acad Sci U S A*. 2005;102(49):17717-17722. doi:10.1073/PNAS.0508531102/SUPPL_FILE/08531FIG6.JPG

174. Abe T, Minami N, Bawono RG, et al. ISGylation of Hepatitis C Virus NS5A Protein Promotes Viral RNA Replication via Recruitment of Cyclophilin A. *J Virol*. 2020;94(20):532-552. doi:10.1128/JVI.00532-20

175. Thomas DL, Thio CL, Martin MP, et al. Genetic variation in IL28B and spontaneous clearance of hepatitis C virus. *Nature*. 2009;461(7265):798-801. doi:10.1038/NATURE08463

176. Ge D, Fellay J, Thompson AJ, et al. Genetic variation in IL28B predicts hepatitis C treatment-induced viral clearance. *Nature*. 2009;461(7262):399-401. doi:10.1038/NATURE08309

177. Khakoo SI, Thio CL, Martin MP, et al. HLA and NK cell inhibitory receptor genes in resolving hepatitis C virus infection. *Science*. 2004;305(5685):872-874. doi:10.1126/SCIENCE.1097670

178. Romero V, Azocar J, Zúñiga J, et al. Interaction of NK inhibitory receptor genes with HLA-C and MHC class II alleles in Hepatitis C virus infection outcome. *Mol Immunol*. 2008;45(9):2429-2436. doi:10.1016/J.MOLIMM.2008.01.002

179. Yoon JC, Yang CM, Song Y, Lee JM. Natural killer cells in hepatitis C: Current progress. *World J Gastroenterol*. 2016;22(4):1449-1460. doi:10.3748/WJG.V22.I4.1449

180. Mittrücker HW, Visekruna A, Huber M. Heterogeneity in the differentiation and function of $CD8^+$ T cells. *Arch Immunol Ther Exp (Warsz)*. 2014;62(6):449-458. doi:10.1007/S00005-014-0293-Y

181. Laidlaw BJ, Craft JE, Kaech SM. The multifaceted role of CD4(+) T cells in CD8(+) T cell memory. *Nat Rev Immunol*. 2016;16(2):102-111. doi:10.1038/NRI.2015.10

182. Swain SL, McKinstry KK, Strutt TM. Expanding roles for CD4+ T cells in immunity to viruses. *Nat Rev Immunol*. 2012;12(2):136. doi:10.1038/NRI3152

183. Luckheeram RV, Zhou R, Verma AD, Xia B. $CD4^+$T cells: differentiation and functions. *Clin Dev Immunol*. 2012;2012. doi:10.1155/2012/925135

184. Missale G, Bertoni R, Lamonaca V, et al. Different clinical behaviors of acute hepatitis C virus infection are associated with different vigor of the anti-viral cell-mediated immune response. *J Clin Invest*. 1996;98(3):706-714. doi:10.1172/JCI118842

185. Semmo N, Klenerman P. CD4+ T cell reponses in hepatitis C

virus infection. *World J Gastroenterol*. 2007;13(36):4831-4838. doi:10.3748/wjg.v13.i36.4831

186. Schulze zur Wiesch J, Ciuffreda D, Lewis-Ximenez L, et al. Broadly directed virus-specific CD4+ T cell responses are primed during acute hepatitis C infection, but rapidly disappear from human blood with viral persistence. *J Exp Med*. 2012;209(1):61. doi:10.1084/JEM.20100388

187. Holz L, Rehermann B. T Cell Responses in Hepatitis C Virus Infection: Historical Overview and Goals for Future Research. *Antiviral Res*. 2015;114:96. doi:10.1016/J.ANTIVIRAL.2014.11.009

188. Vranjkovic A, Deonarine F, Kaka S, Angel JB, Cooper CL, Crawley AM. Direct-acting antiviral treatment of hcv infection does not resolve the dysfunction of circulating CD8+ T-cells in advanced liver disease. *Front Immunol*. 2019;10(AUG):1926. doi:10.3389/FIMMU.2019.01926/BIBTEX

189. Cox AL, Mosbruger T, Mao Q, et al. Cellular immune selection with hepatitis C virus persistence in humans. *J Exp Med*. 2005;201(11):1741-1752. doi:10.1084/JEM.20050121

190. Smits M, Zoldan K, Ishaque N, et al. Follicular T helper cells shape the HCV-specific CD4+ T cell repertoire after virus elimination. *J Clin Invest*. 2020;130(2):998. doi:10.1172/JCI129642

191. Salinas E, Boisvert M, Upadhyay AA, et al. Early T follicular helper cell activity accelerates hepatitis C virus-specific B cell expansion. *J Clin Invest*. 2021;131(2). doi:10.1172/JCI140590

192. Khanam A, Kottilil S, Wilson E. Reconstitution of T follicular helper-humoral immune axis with elimination of hepatitis C virus. *Sci Rep*. 2020;10(1). doi:10.1038/S41598-020-77020-2

193. Grakoui A, Shoukry NH, Woollard DJ, et al. HCV Persistence and Immune Evasion in the Absence of Memory T Cell Help. *Science (80-)*. 2003;302(5645):659-662. doi:10.1126/SCIENCE.1088774/SUPPL_FILE/GRAKOUI.SOM.REV1.PDF

194. Shoukry NH, Grakoui A, Houghton M, et al. Memory CD8+ T Cells Are Required for Protection from Persistent Hepatitis C Virus Infection. *J Exp Med*. 2003;197(12):1645-1655. doi:10.1084/JEM.20030239

195. Diepolder HM, Zachoval R, Hoffmann RM, et al. Possible mechanism involving T-lymphocyte response to non-structural protein 3 in viral clearance in acute hepatitis C virus infection. *Lancet (London, England)*. 1995;346(8981):1006-1007. doi:10.1016/S0140-6736(95)91691-1

196. Chang KM, Thimme R, Melpolder JJ, et al. Differential CD4(+)

and CD8(+) T-cell responsiveness in hepatitis C virus infection. *Hepatology*. 2001;33(1):267-276. doi:10.1053/JHEP.2001.21162

197. McHeyzer-Williams M, Okitsu S, Wang N, McHeyzer-Williams L. Molecular programming of B cell memory. *Nat Rev Immunol 2011 121*. 2011;12(1):24-34. doi:10.1038/nri3128

198. Ellebedy AH, Jackson KJL, Kissick HT, et al. Defining antigen-specific plasmablast and memory B cell subsets in human blood after viral infection or vaccination. *Nat Immunol 2016 1710*. 2016;17(10):1226-1234. doi:10.1038/ni.3533

199. Vidarsson G, Dekkers G, Rispens T. IgG subclasses and allotypes: from structure to effector functions. *Front Immunol*. 2014;5(OCT). doi:10.3389/FIMMU.2014.00520

200. Schroeder HW, Cavacini L. Structure and Function of Immunoglobulins. *J Allergy Clin Immunol*. 2010;125(2 0 2):S41. doi:10.1016/J.JACI.2009.09.046

201. Klasse PJ, Sattentau QJ. Occupancy and mechanism in antibody-mediated neutralization of animal viruses. *J Gen Virol*. 2002;83(Pt 9):2091-2108. doi:10.1099/0022-1317-83-9-2091

202. Reading SA, Dimmock NJ. Neutralization of animal virus infectivity by antibody. *Arch Virol*. 2007;152(6):1047-1059. doi:10.1007/S00705-006-0923-8

203. Chen M, Sallaberg M, Sonneborg A, et al. Limited humoral immunity in hepatitis C virus infection. *Gastroenterology*. 1999;116(1):135-143. doi:10.1016/S0016-5085(99)70237-4

204. Netski DM, Mosbruger T, Depla E, et al. Humoral immune response in acute hepatitis C virus infection. *Clin Infect Dis*. 2005;41(5):667-675. doi:10.1086/432478

205. Walker MR, Eltahla AA, Mina MM, Li H, Lloyd AR, Bull RA. Envelope-Specific IgG3 and IgG1 Responses Are Associated with Clearance of Acute Hepatitis C Virus Infection. *Viruses*. 2020;12(1). doi:10.3390/V12010075

206. Sagnelli E, Coppola N, Marrocco C, et al. Diagnosis of HCV related acute hepatitis by serial determination of IgM to HCV: a preliminary observation. *J Biol Regul Homeost Agents*. 2003;17(2):207-210.

207. Sato S, Fujiyama S, Tanaka M, et al. IgM and IgA antibodies generated against hepatitis C virus core antigen in patients with acute and chronic HCV infection. *Dig Dis Sci*. 1994;39(9):2022-2031. doi:10.1007/BF02088141

208. P F, HJ A, DC W, et al. Prevention of hepatitis C virus infection in chimpanzees after antibody-mediated in vitro neutralization. *Proc Natl Acad Sci U S A*. 1994;91(16):7792-7796. doi:10.1073/PNAS.91.16.7792

209. Osburn WO, Snider AE, Wells BL, et al. Clearance of hepatitis C infection is associated with the early appearance of broad neutralizing antibody responses. *Hepatology*. 2014;59(6):2140-2151. doi:10.1002/hep.27013

210. Dowd KA, Netski DM, Wang XH, Cox AL, Ray SC. Selection Pressure From Neutralizing Antibodies Drives Sequence Evolution During Acute Infection With Hepatitis C Virus. *Gastroenterology*. 2009;136(7):2377-2386. doi:10.1053/J.GASTRO.2009.02.080/ATTACHMENT/69DEAE75-8920-4A98-B7D2-CA12CC1E83D9/MMC2.JPG

211. Allander T, Drakenberg K, Beyene A, et al. Recombinant human monoclonal antibodies against different conformational epitopes of the E2 envelope glycoprotein of hepatitis C virus that inhibit its interaction with CD81. *J Gen Virol*. 2000;81(10):2451-2459. doi:10.1099/0022-1317-81-10-2451

212. Johansson DX, Voisset C, Tarr AW, et al. Human combinatorial libraries yield rare antibodies that broadly neutralize hepatitis C virus. *Proc Natl Acad Sci U S A*. 2007;104(41):16269-16274. doi:10.1073/pnas.0705522104

213. Post JJ, Pan Y, Freeman AJ, et al. Clearance of hepatitis C viremia associated with cellular immunity in the absence of seroconversion in the hepatitis C incidence and transmission in prisons study cohort. *J Infect Dis*. 2004;189(10):1846-1855. doi:10.1086/383279

214. Zeremski M, Shu MA, Brown Q, et al. Hepatitis C virus-specific T-cell immune responses in seronegative injection drug users. *J Viral Hepat*. 2009;16(1):10-20. doi:10.1111/J.1365-2893.2008.01016.X

215. Mina M, Underwood A, Eltahla A, et al. Anti-envelope antibody responses in highly exposed seronegative individuals may be associated with protection from HCV infection. *J Viral Hepat*. 2020;27(10):1012-1021. doi:10.1111/jvh.13339

216. Pestka JM, Zeisel MB, Bläser E, et al. Rapid induction of virus-neutralizing antibodies and viral clearance in a single-source outbreak of hepatitis C. *Proc Natl Acad Sci*. 2007;104(14):6025-6030. doi:10.1073/PNAS.0607026104

217. Walker MR, Leung P, Eltahla AA, et al. Clearance of hepatitis C virus is associated with early and potent but narrowly-directed, Envelope-specific antibodies. *Sci Rep*. 2019;9(1):1-14. doi:10.1038/s41598-019-49454-w

218. Kinchen VJ, Massaccesi G, Flyak AI, et al. Plasma deconvolution identifies broadly neutralizing antibodies associated with hepatitis C virus clearance. *J Clin Invest*. 2019;129(11):4786-4796. doi:10.1172/JCI130720

219. Merat SJ, Bru C, van de Berg D, et al. Cross-genotype AR3-specific neutralizing antibodies confer long-term protection in injecting drug users after HCV clearance. *J Hepatol*. 2019;71(1):14-24. doi:10.1016/j.jhep.2019.02.013

220. Bailey JR, Flyak AI, Cohen VJ, et al. Broadly neutralizing antibodies with few somatic mutations and hepatitis C virus clearance. *JCI insight*. 2017;2(9):1-17. doi:10.1172/jci.insight.92872

221. Colbert MD, Flyak AI, Ogega CO, et al. Broadly Neutralizing Antibodies Targeting New Sites of Vulnerability in Hepatitis C Virus E1E2. *J Virol*. 2019;93(14):1-19. doi:10.1128/jvi.02070-18

222. Chan CH, Hadlock KG, Foung SKH, Levy S. VH1-69 gene is preferentially used by hepatitis C virus–associated B cell lymphomas and by normal B cells responding to the E2 viral antigen. *Blood*. 2001;97(4):1023-1026. doi:10.1182/BLOOD.V97.4.1023

223. Merat SJ, Molenkamp R, Wagner K, et al. Hepatitis C virus Broadly Neutralizing Monoclonal Antibodies Isolated 25 Years after Spontaneous Clearance. *PLoS One*. 2016;11(10). doi:10.1371/JOURNAL.PONE.0165047

224. Chen F, Tzarum N, Wilson IA, Law M. VH1-69 antiviral broadly neutralizing antibodies: genetics, structures, and relevance to rational vaccine design. *Curr Opin Virol*. 2019;34:149-159. doi:10.1016/J.COVIRO.2019.02.004

225. Lohmann V, Bartenschlager R. On the history of hepatitis C virus cell culture systems. *J Med Chem*. 2014;57(5):1627-1642. doi:10.1021/JM401401N/ASSET/IMAGES/JM401401N.SOCIAL.JPEG_V03

226. McClure CP, Urbanowicz RA, King BJ, Cano-Crespo S, Tarr AW, Ball JK. Flexible and rapid construction of viral chimeras applied to hepatitis c virus. *J Gen Virol*. 2016;97(9):2187-2193. doi:10.1099/jgv.0.000530

227. Wakita T, Pietschmann T, Kato T, et al. Production of infectious hepatitis C virus in tissue culture from a cloned viral genome. *Nat Med*. 2005;11(7):791-796. doi:10.1038/NM1268

228. Aubry F, Nougairède A, Gould EA, Lamballerie X de. Flavivirus reverse genetic systems, construction techniques and applications: A historical perspective. *Antiviral Res*. 2015;114:67. doi:10.1016/J.ANTIVIRAL.2014.12.007

229. Zhong J, Gastaminza P, Cheng G, et al. Robust hepatitis C virus infection in vitro. *Proc Natl Acad Sci U S A*. 2005;102(26):9294-9299. doi:10.1073/PNAS.0503596102

230. Blight KJ, McKeating JA, Rice CM. Highly permissive cell lines for subgenomic and genomic hepatitis C virus RNA replication. *J*

Virol. 2002;76(24):13001-13014. doi:10.1128/JVI.76.24.13001-13014.2002

231. Sumpter R, Loo Y-M, Foy E, et al. Regulating intracellular antiviral defense and permissiveness to hepatitis C virus RNA replication through a cellular RNA helicase, RIG-I. *J Virol*. 2005;79(5):2689-2699. doi:10.1128/JVI.79.5.2689-2699.2005

232. King B, Temperton NJ, Grehan K, et al. Technical considerations for the generation of novel pseudotyped viruses. *Future Virol*. 2016;11(1):47-59. doi:10.2217/fvl.15.106

233. Bartosch B, Dubuisson J, Cosset FL. Infectious hepatitis C virus pseudo-particles containing functional E1-E2 envelope protein complexes. *J Exp Med*. 2003;197(5):633-642. doi:10.1084/jem.20021756

234. Flint M, Logvinoff C, Rice CM, McKeating JA. Characterization of Infectious Retroviral Pseudotype Particles Bearing Hepatitis C Virus Glycoproteins. *J Virol*. 2004;78(13):6875-6882. doi:10.1128/jvi.78.13.6875-6882.2004

235. Wasilewski LN, Ray SC, Bailey JR. Hepatitis C virus resistance to broadly neutralizing antibodies measured using replication-competent virus and pseudoparticles. *J Gen Virol*. 2016;97(11):2883-2893. doi:10.1099/jgv.0.000608

236. Salas JH, Urbanowicz RA, Guest JD, et al. An antigenically diverse, representative panel of envelope glycoproteins for HCV vaccine development. *Gastroenterology*. Published online October 13, 2021. doi:10.1053/J.GASTRO.2021.10.005

237. Tarr AW, Urbanowicz RA, Hamed MR, et al. Hepatitis C Patient-Derived Glycoproteins Exhibit Marked Differences in Susceptibility to Serum Neutralizing Antibodies: Genetic Subtype Defines Antigenic but Not Neutralization Serotype. *J Virol*. 2011;85(9):4246-4257. doi:10.1128/jvi.01332-10

238. Urbanowicz RA, McClure CP, Brown RJP, et al. A Diverse Panel of Hepatitis C Virus Glycoproteins for Use in Vaccine Research Reveals Extremes of Monoclonal Antibody Neutralization Resistance. *J Virol*. 2016;90(7):3288-3301. doi:10.1128/jvi.02700-15

239. Seaman MS, Janes H, Hawkins N, et al. Tiered categorization of a diverse panel of HIV-1 Env pseudoviruses for assessment of neutralizing antibodies. *J Virol*. 2010;84(3):1439-1452. doi:10.1128/JVI.02108-09

240. Lanford RE, Bigger C, Bassett S, Klimpel G. The chimpanzee model of hepatitis C virus infections. *ILAR J*. 2001;42(2):117-126. doi:10.1093/ILAR.42.2.117

241. Mercer DF, Schiller DE, Elliott JF, et al. Hepatitis C virus replication in mice with chimeric human livers. *Nat Med*.

2001;7(8):927-933. doi:10.1038/90968

242. Meuleman P, Libbrecht L, De Vos R, et al. Morphological and biochemical characterization of a human liver in a uPA-SCID mouse chimera. *Hepatology*. 2005;41(4):847-856. doi:10.1002/HEP.20657

243. Chen J, Zhao Y, Zhang C, et al. Persistent hepatitis C virus infections and hepatopathological manifestations in immune-competent humanized mice. *Cell Res 2014 249*. 2014;24(9):1050-1066. doi:10.1038/cr.2014.116

244. Ding Q, von Schaewen M, Hrebikova G, et al. Mice Expressing Minimally Humanized CD81 and Occludin Genes Support Hepatitis C Virus Uptake In Vivo. *J Virol*. 2017;91(4). doi:10.1128/JVI.01799-16

245. Yong KSM, Her Z, Chen Q. Humanized Mouse Models for the Study of Hepatitis C and Host Interactions. *Cells*. 2019;8(6):604. doi:10.3390/CELLS8060604

246. Chen F, Nagy K, Chavez D, et al. Antibody Responses to Immunization With HCV Envelope Glycoproteins as a Baseline for B-Cell-Based Vaccine Development. *Gastroenterology*. 2020;158(4):1058-1071.e6. doi:10.1053/J.GASTRO.2019.11.282

247. Ramsay JD, Evanoff R, Wilkinson TE, Divers TJ, Knowles DP, Mealey RH. Experimental transmission of equine hepacivirus in horses as a model for hepatitis C virus. *Hepatology*. 2015;61(5):1533-1546. doi:10.1002/HEP.27689

248. Trivedi S, Murthy S, Sharma H, et al. Viral persistence, liver disease, and host response in a hepatitis C-like virus rat model. *Hepatology*. 2018;68(2):435-448. doi:10.1002/HEP.29494

249. Atcheson E, Li W, Bliss CM, et al. Use of an Outbred Rat Hepacivirus Challenge Model for Design and Evaluation of Efficacy of Different Immunization Strategies for Hepatitis C Virus. *Hepatology*. 2020;71(3):794-807. doi:10.1002/HEP.30894

250. Pfaender S, Cavalleri JMV, Walter S, et al. Clinical course of infection and viral tissue tropism of hepatitis C virus-like nonprimate hepaciviruses in horses. *Hepatology*. 2015;61(2):447-459. doi:10.1002/HEP.27440

251. Plotkin SA, Plotkin SL. The development of vaccines: how the past led to the future. *Nat Rev Microbiol 2011 912*. 2011;9(12):889-893. doi:10.1038/nrmicro2668

252. Kubinski M, Beicht J, Gerlach T, Volz A, Sutter G, Rimmelzwaan GF. Tick-Borne Encephalitis Virus: A Quest for Better Vaccines against a Virus on the Rise. *Vaccines*. 2020;8(3):1-45. doi:10.3390/VACCINES8030451

253. Koch C, Jensen SS, Øster A, Houen G. A comparison of the

immunogenicity of the native and denatured forms of a protein. *APMIS*. 1996;104(2):115-125. doi:10.1111/J.1699-0463.1996.TB00696.X

254. Warfield KL, Swenson DL, Olinger GG, et al. Ebola Virus Inactivation with Preservation of Antigenic and Structural Integrity by a Photoinducible Alkylating Agent. *J Infect Dis*. 2007;196(Supplement_2):S276-S283. doi:10.1086/520605

255. Akazawa D, Moriyama M, Yokokawa H, et al. Neutralizing antibodies induced by cell culture-derived hepatitis C virus protect against infection in mice. *Gastroenterology*. 2013;145(2):447-455.e4. doi:10.1053/j.gastro.2013.05.007

256. Yokokawa H, Higashino A, Suzuki S, et al. Induction of humoural and cellular immunity by immunisation with HCV particle vaccine in a non-human primate model. *Gut*. 2018;67(2):372-379. doi:10.1136/gutjnl-2016-312208

257. Pihl AF, Feng S, Offersgaard A, et al. Inactivated whole hepatitis C virus vaccine employing a licensed adjuvant elicits cross-genotype neutralizing antibodies in mice. *J Hepatol*. 2022;76(5):1051-1061. doi:10.1016/J.JHEP.2021.12.026/ATTACHMENT/3C1E986F-380C-412E-8FA3-0457F274F47D/MMC3.PDF

258. Offersgaard A, Duarte Hernandez CR, Finne Pihl A, et al. High-Titer Hepatitis C Virus Production in a Scalable Single-Use High Cell Density Bioreactor. *Vaccines 2022, Vol 10, Page 249*. 2022;10(2):249. doi:10.3390/VACCINES10020249

259. Lothert K, Offersgaard AF, Pihl AF, et al. Development of a downstream process for the production of an inactivated whole hepatitis C virus vaccine. *Sci Rep*. 2020;10(1):1-13. doi:10.1038/s41598-020-72328-5

260. Plotkin SA. Vaccines: past, present and future. *Nat Med 2005 114*. 2005;11(4):S5-S11. doi:10.1038/nm1209

261. Frey SE, Houghton M, Coates S, et al. Safety and immunogenicity of HCV E1E2 vaccine adjuvanted with MF59 administered to healthy adults. *Vaccine*. 2010;28(38):6367-6373. doi:10.1016/J.VACCINE.2010.06.084

262. Choo QL, Kuo G, Ralston R, et al. Vaccination of chimpanzees against infection by the hepatitis C virus. *Proc Natl Acad Sci*. 1994;91(4):1294-1298. doi:10.1073/PNAS.91.4.1294

263. Ray R, Meyer K, Banerjee A, et al. Characterization of antibodies induced by vaccination with hepatitis C virus envelope glycoproteins. *J Infect Dis*. 2010;202(6):862-866. doi:10.1086/655902

264. Wong JAJ-X, Bhat R, Hockman D, et al. Recombinant Hepatitis C Virus Envelope Glycoprotein Vaccine Elicits Antibodies Targeting

Multiple Epitopes on the Envelope Glycoproteins Associated with Broad Cross-Neutralization. *J Virol*. 2014;88(24):14278-14288. doi:10.1128/jvi.01911-14

265. Law JLM, Chen C, Wong J, et al. A hepatitis C virus (HCV) vaccine comprising envelope glycoproteins gpE1/gpE2 derived from a single isolate elicits broad cross-genotype neutralizing antibodies in humans. *PLoS One*. 2013;8(3). doi:10.1371/JOURNAL.PONE.0059776

266. Logan M, Law J, Wong JAJ-X, et al. Native Folding of a Recombinant gpE1/gpE2 Heterodimer Vaccine Antigen from a Precursor Protein Fused with Fc IgG. *J Virol*. 2017;91(1):1552-1568. doi:10.1128/JVI.01552-16

267. Li D, von Schaewen M, Wang X, et al. Altered Glycosylation Patterns Increase Immunogenicity of a Subunit Hepatitis C Virus Vaccine, Inducing Neutralizing Antibodies Which Confer Protection in Mice. *J Virol*. 2016;90(23):10486-10498. doi:10.1128/JVI.01462-16

268. Vietheer PT, Boo I, Gu J, et al. The core domain of hepatitis C virus glycoprotein E2 generates potent cross-neutralizing antibodies in guinea pigs. *Hepatology*. 2017;65(4):1117-1131. doi:10.1002/HEP.28989/SUPPINFO

269. Prentoe J, Janitzek CM, Velázquez-Moctezuma R, et al. Antigenic and immunogenic evaluation of permutations of soluble hepatitis C virus envelope protein E2 and E1 antigens. Ho PL, ed. *PLoS One*. 2021;16(7):e0255336. doi:10.1371/JOURNAL.PONE.0255336

270. Guest JD, Wang R, Elkholy KH, et al. Design of a native-like secreted form of the hepatitis C virus E1E2 heterodimer. *Proc Natl Acad Sci U S A*. 2021;118(3). doi:10.1073/pnas.2015149118

271. Ura T, Okuda K, Shimada M. Developments in Viral Vector-Based Vaccines. *Vaccines*. 2014;2(3):624. doi:10.3390/VACCINES2030624

272. Barnes E, Folgori A, Capone S, et al. Novel adenovirus-based vaccines induce broad and sustained T cell responses to HCV in man. *Sci Transl Med*. 2012;4(115). doi:10.1126/SCITRANSLMED.3003155

273. Swadling L, Capone S, Antrobus RD, et al. A human vaccine strategy based on chimpanzee adenoviral and MVA vectors that primes, boosts, and sustains functional HCV-specific T cell memory. *Sci Transl Med*. 2014;6(261). doi:10.1126/SCITRANSLMED.3009185

274. Capone S, Zampaglione I, Vitelli A, et al. Modulation of the Immune Response Induced by Gene Electrotransfer of a Hepatitis C Virus DNA Vaccine in Nonhuman Primates. *J Immunol*.

2006;177(10):7462-7471. doi:10.4049/JIMMUNOL.177.10.7462

275. Swadling L, Halliday J, Kelly C, et al. Highly-immunogenic virally-vectored T-cell vaccines cannot overcome subversion of the T-cell response by HCV during chronic infection. *Vaccines*. 2016;4(3). doi:10.3390/vaccines4030027

276. Page K, Melia MT, Veenhuis RT, et al. Randomized Trial of a Vaccine Regimen to Prevent Chronic HCV Infection. *N Engl J Med*. 2021;384(6):541. doi:10.1056/NEJMOA2023345

277. Bachmann MF, Jennings GT. Vaccine delivery: a matter of size, geometry, kinetics and molecular patterns. *Nat Rev Immunol*. 2010;10(11):787-796. doi:10.1038/NRI2868

278. Sun C, Yuan R-Y, Xie C, et al. Induction of Broadly Cross-Reactive Antibody Responses to SARS-CoV-2 Variants by S1 Nanoparticle Vaccines. Heise MT, ed. *J Virol*. Published online June 14, 2022. doi:10.1128/JVI.00383-22

279. Baumert TF, Ito S, Wong DT, Liang ATJ. Hepatitis C Virus Structural Proteins Assemble into Viruslike Particles in Insect Cells. *J Virol*. 1998;72(5):3827. doi:10.1128/jvi.72.5.3827-3836.1998

280. Lechmann M, Murata K, Satoi J, Vergalla J, Baumert TF, Liang TJ. Hepatitis C virus-like particles induce virus-specific humoral and cellular immune responses in mice. *Hepatology*. 2001;34(2):417-423. doi:10.1053/jhep.2001.26523

281. Jeong S-H, Qiao M, Nascimbeni M, et al. Immunization with hepatitis C virus-like particles induces humoral and cellular immune responses in nonhuman primates. *J Virol*. 2004;78(13):6995-7003. doi:10.1128/JVI.78.13.6995-7003.2004

282. Chua BY, Johnson D, Tan A, et al. Hepatitis C VLPs Delivered to Dendritic Cells by a TLR2 Targeting Lipopeptide Results in Enhanced Antibody and Cell-Mediated Responses. *PLoS One*. 2012;7(10):1-10. doi:10.1371/journal.pone.0047492

283. Earnest-Silveira L, Christiansen D, Herrmann S, et al. Large scale production of a mammalian cell derived quadrivalent hepatitis C virus like particle vaccine. *J Virol Methods*. 2016;236:87-92. doi:10.1016/j.jviromet.2016.06.012

284. Earnest-Silveira L, Chua B, Chin R, et al. Characterization of a hepatitis C virus-like particle vaccine produced in a human hepatocyte-derived cell line. *J Gen Virol*. 2016;97(8):1865-1876. doi:10.1099/JGV.0.000493/CITE/REFWORKS

285. Christiansen D, Earnest-Silveira L, Chua B, et al. Immunological responses following administration of a genotype 1a/1b/2/3a quadrivalent HCV VLP vaccine. *Sci Rep*. 2018;8(1):1-13. doi:10.1038/s41598-018-24762-9

286. Christiansen D, Earnest-Silveira L, Grubor-Bauk B, et al. Pre-clinical evaluation of a quadrivalent HCV VLP vaccine in pigs following microneedle delivery. *Sci Rep*. 2019;9(1):1-13. doi:10.1038/s41598-019-45461-z

287. Salas JH, Urbanowicz RA, Guest JD, et al. An antigenically diverse, representative panel of envelope glycoproteins for HCV vaccine development. *Gastroenterology*. Published online October 13, 2021. doi:10.1053/J.GASTRO.2021.10.005

288. Nakabayashi H, Taketa K, Miyano K, Yamane T, Sato J. Growth of human hepatoma cells lines with differentiated functions in chemically defined medium. *Cancer Res*. 1982;42(9):3858-3863.

289. Kruger DH, Ulrich R, Gerlich WH. Chimeric virus-like particles as vaccines. *Biol Chem*. 1999;380(3):275-276. doi:10.1515/BC.1999.037

290. Wampler DE, Lehman ED, Boger J, McAleer WJ, Scolnick EM. Multiple chemical forms of hepatitis B surface antigen produced in yeast. *Proc Natl Acad Sci U S A*. 1985;82(20):6830-6834. doi:10.1073/PNAS.82.20.6830

291. Valenzuela P, Medina A, Rutter WJ, Ammerer G, Hall BD. Synthesis and assembly of hepatitis B virus surface antigen particles in yeast. *Nature*. 1982;298(5872):347-350. doi:10.1038/298347A0

292. Czarnota A, Offersgaard A, Pihl AF, et al. Specific antibodies induced by immunization with hepatitis B virus-like particles carrying hepatitis C virus envelope glycoprotein 2 epitopes show differential neutralization efficiency. *Vaccines*. 2020;8(2):1-19. doi:10.3390/vaccines8020294

293. Wei S, Lei Y, Yang J, et al. Neutralization effects of antibody elicited by chimeric HBV S antigen viral-like particles presenting HCV neutralization epitopes. *Vaccine*. 2018;36(17):2273-2281. doi:10.1016/J.VACCINE.2018.03.036

294. Beaumont E, Roch E, Chopin L, Roingeard P. Hepatitis C virus E1 and E2 proteins used as separate immunogens induce neutralizing antibodies with additive properties. *PLoS One*. 2016;11(3). doi:10.1371/journal.pone.0151626

295. Beaumont E, Joël Clément B, Guérin V, et al. Mixing particles from various HCV genotypes increases the HBV-HCV vaccine ability to elicit broadly cross-neutralizing antibodies. *Liver Int*. 2020;40(8):1865-1871. doi:10.1111/liv.14541

296. Beaumont E, Patient R, Hourioux C, Dimier-Poisson I, Roingeard P. Chimeric hepatitis B virus/hepatitis C virus envelope proteins elicit broadly neutralizing antibodies and constitute a potential bivalent prophylactic vaccine. *Hepatology*. 2013;57(4):1303-1313. doi:10.1002/HEP.26132

297. McGregor J, Hardy JM, Lay C-S, et al. Virus-Like Particles Containing the E2 Core Domain of Hepatitis C Virus Generate Broadly Neutralizing Antibodies in Guinea Pigs. *J Virol*. Published online January 5, 2022. doi:10.1128/JVI.01675-21

298. PARKMAN PD, BUESCHER EL, ARTENSTEIN MS. Recovery of rubella virus from army recruits. *Proc Soc Exp Biol Med Soc Exp Biol Med (New York, NY)*. 1962;111:225-230. doi:10.3181/00379727-111-27750

299. Lee J-Y, Bowden DS. Rubella Virus Replication and Links to Teratogenicity. *Clin Microbiol Rev*. 2000;13(4):571-587. doi:10.1128/CMR.13.4.571

300. Chess S, Fernandez P. Impulsivity in rubella deaf children: a longitudinal study. *Am Ann Deaf*. 1980;125(4):505-509. doi:10.1353/aad.2012.1329

301. Mekonnen D. Clinically Confirmed Congenital Rubella Syndrome: The Role of Echocardiography. *Ethiop J Health Sci*. 2017;27(2):197-202. doi:10.4314/EJHS.V27I2.13

302. Fenner F, Pereira HG, Porterfield JS, Joklik WK, Downie AW. Family and generic names for viruses approved by the International Committee on Taxonomy of Viruses, June 1974. *Intervirology*. 1974;3(3):193-198. doi:10.1159/000149755

303. Dominguez G, Wang CY, Frey TK. Sequence of the genome RNA of rubella virus: evidence for genetic rearrangement during togavirus evolution. *Virology*. 1990;177(1):225-238. doi:10.1016/0042-6822(90)90476-8

304. Shi M, Lin XD, Chen X, et al. The evolutionary history of vertebrate RNA viruses. *Nat 2018 5567700*. 2018;556(7700):197-202. doi:10.1038/s41586-018-0012-7

305. M S, XD L, X C, et al. The evolutionary history of vertebrate RNA viruses. *Nature*. 2018;556(7700):197-202. doi:10.1038/S41586-018-0012-7

306. Bennett AJ, Paskey AC, Ebinger A, et al. Relatives of rubella virus in diverse mammals. *Nature*. 2020;586(7829):424-428. doi:10.1038/s41586-020-2812-9

307. JL G, F DG, M W, et al. Virome composition in marine fish revealed by meta-transcriptomics. *Virus Evol*. 2021;7(1). doi:10.1093/VE/VEAB005

308. Grimwood RM, Holmes EC, Geoghegan JL. A Novel Rubi-Like Virus in the Pacific Electric Ray (Tetronarce californica) Reveals the Complex Evolutionary History of the Matonaviridae. *Viruses*. 2021;13(4). doi:10.3390/V13040585

309. Pfaff F, Breithaupt A, Rubbenstroth D, et al. Revisiting Rustrela Virus: New Cases of Encephalitis and a Solution to the Capsid

Enigma. *Microbiol Spectr*. 2022;10(2). doi:10.1128/SPECTRUM.00103-22

310. World Health Organization. Standardization of the nomenclature for genetic characteristics of wild-type rubella viruses. *Wkly Epidemiol Rec*. 2005;80(14):126-132. Accessed October 24, 2021. https://pubmed.ncbi.nlm.nih.gov/15850226/

311. ES A, JM H, CP M, et al. Status of global virologic surveillance for rubella viruses. *J Infect Dis*. 2011;204 Suppl 1(SUPPL. 1). doi:10.1093/INFDIS/JIR099

312. E P, D W-K, E A, et al. Genotypes of rubella virus and the epidemiology of rubella infections in the Democratic Republic of the Congo, 2004-2013. *J Med Virol*. 2016;88(10):1677-1684. doi:10.1002/JMV.24517

313. Frey TK, Marr LD. Sequence of the region coding for virion proteins C and E2 and the carboxy terminus of the nonstructural proteins of rubella virus: comparison with alphaviruses. *Gene*. 1988;62(1):85-99. doi:10.1016/0378-1119(88)90582-3

314. Oker-Blom C, Ulmanen I, Kääriäinen L, Pettersson RF. Rubella virus 40S genome RNA specifies a 24S subgenomic mRNA that codes for a precursor to structural proteins. *J Virol*. 1984;49(2):403. Accessed August 18, 2021. /pmc/articles/PMC255479/?report=abstract

315. Tzeng W-P, Frey TK. Mapping the Rubella Virus Subgenomic Promoter. *J Virol*. 2002;76(7):3189-3201. doi:10.1128/jvi.76.7.3189-3201.2002

316. Claus C, Tzeng WP, Liebert UG, Frey TK. Rubella virus-like replicon particles: Analysis of encapsidation determinants and non-structural roles of capsid protein in early post-entry replication. *J Gen Virol*. 2012;93(3):516-525. doi:10.1099/vir.0.038984-0

317. Frey TK. Molecular Biology of Rubella Virus. *Adv Virus Res*. 1994;44(C):69-160. doi:10.1016/S0065-3527(08)60328-0

318. Baron MD, Forsell K. Oligomerisation of the structural proteins of Rubella virus. *Virology*. 1991;185(2):811-819. doi:10.1016/0042-6822(91)90552-M

319. Prasad VM, Willows SD, Fokine A, et al. Rubella virus capsid protein structure and its role in virus assembly and infection. *Proc Natl Acad Sci U S A*. 2013;110(50):20105-20110. doi:10.1073/pnas.1316681110

320. Garbutt M, Law LMJ, Chan H, Hobman TC. Role of Rubella Virus Glycoprotein Domains in Assembly of Virus-Like Particles. *J Virol*. 1999;73(5):3524-3533. doi:10.1128/jvi.73.5.3524-3533.1999

321. Dubé M, Etienne L, Fels M, Kielian M. Calcium-Dependent

Rubella Virus Fusion Occurs in Early Endosomes. *J Virol*. 2016;90(14):6303-6313. doi:10.1128/jvi.00634-16

322. Qiu Z, Ou D, Hobman TC, Gillam S. Expression and characterization of virus-like particles containing rubella virus structural proteins. *J Virol*. 1994;68(6):4086-4091. doi:10.1128/jvi.68.6.4086-4091.1994

323. Brown RS, Wan JJ, Kielian M. The Alphavirus Exit Pathway: What We Know and What We Wish We Knew. *Viruses*. 2018;10(2). doi:10.3390/V10020089

324. Hobman TC, Woodward L, Farquhar MG. The Rubella Virus E2 and E1 spike glycoproteins are targeted to the Golgi complex. *J Cell Biol*. 1993;121(2):269-281. doi:10.1083/jcb.121.2.269

325. Hobman TC, Woodward L, Farquhar MG. The rubella virus E1 glycoprotein is arrested in a novel post-ER, pre-Golgi compartment. *J Cell Biol*. 1992;118(4):795-811. doi:10.1083/jcb.118.4.795

326. Hobman TC, Woodward L, Farquhar MG. Targeting of a heterodimeric membrane protein complex to the Golgi: Rubella virus E2 glycoprotein contains a transmembrane Golgi retention signal. *Mol Biol Cell*. 1995;6(1):7-20. doi:10.1091/mbc.6.1.7

327. Hobman TC, Lundstrom ML, Mauracher CA, Woodward L, Gillam S, Farquhar MG. Assembly of Rubella Virus Structural Proteins into Virus-like Particles in Transfected Cells. *Virology*. 1994;202(2):574-585. doi:10.1006/viro.1994.1379

328. Accola MA, Strack B, Göttlinger HG. Efficient particle production by minimal Gag constructs which retain the carboxy-terminal domain of human immunodeficiency virus type 1 capsid-p2 and a late assembly domain. *J Virol*. 2000;74(12):5395-5402. doi:10.1128/JVI.74.12.5395-5402.2000

329. Risco C, Carrascosa JL, Frey TK. Structural maturation of rubella virus in the Golgi complex. *Virology*. 2003;312(2):261-269. doi:10.1016/S0042-6822(03)00384-2

330. Mangala Prasad V, Klose T, Rossmann MG. Assembly, maturation and three-dimensional helical structure of the teratogenic rubella virus. *PLOS Pathog*. 2017;13(6):e1006377. doi:10.1371/JOURNAL.PPAT.1006377

331. Battisti AJ, Yoder JD, Plevka P, et al. Cryo-Electron Tomography of Rubella Virus. *J Virol*. 2012;86(20):11078-11085. doi:10.1128/jvi.01390-12

332. Honeyman MC, Forrest JM, Dorman DC. Cell-mediated immune response following natural rubella and rubella vaccination. *Clin Exp Immunol*. 1974;17(4):665-671.

333. Dhiman N, Ovsyannikova IG, Jacobson RM, et al. Correlates of

lymphoproliferative responses to measles, mumps, and rubella (MMR) virus vaccines following MMR-II vaccination in healthy children. *Clin Immunol*. 2005;115(2):154-161. doi:10.1016/J.CLIM.2004.12.010

334. Ou D, Chong P, Tingle AJ, Gillam S. Mapping T-cell epitopes of rubella virus structural proteins E1, E2, and C recognized by T-cell lines and clones derived from infected and immunized populations. *J Med Virol*. 1993;40(3):175-183. doi:10.1002/JMV.1890400302

335. McCarthy M, Lovett A, Kerman RH, Overstreet A, Wolinsky JS. Immunodominant T-cell epitopes of rubella virus structural proteins defined by synthetic peptides. *J Virol*. 1993;67(2):673-681. doi:10.1128/JVI.67.2.673-681.1993

336. Chaye HH, Mauracher CA, Tingle AJ, Gillam S. Cellular and humoral immune responses to rubella virus structural proteins E1, E2, and C. *J Clin Microbiol*. 1992;30(9):2323-2329. doi:10.1128/JCM.30.9.2323-2329.1992

337. Lovett AE, Hahn CS, Rice CM, Frey TK, Wolinsky JS. Rubella virus-specific cytotoxic T-lymphocyte responses: identification of the capsid as a target of major histocompatibility complex class I-restricted lysis and definition of two epitopes. *J Virol*. 1993;67(10):5849-5858. doi:10.1128/JVI.67.10.5849-5858.1993

338. Lovett AE, McCarthy M, Wolinsky JS. Mapping cell-mediated immunodominant domains of the rubella virus structural proteins using recombinant proteins and synthetic peptides. *J Gen Virol*. 1993;74 (Pt 3)(3):445-452. doi:10.1099/0022-1317-74-3-445

339. Vauloup-Fellous C, Grangeot-Keros L. Humoral Immune Response after Primary Rubella Virus Infection and after Vaccination. *Clin Vaccine Immunol*. 2007;14(5):644. doi:10.1128/CVI.00032-07

340. Cradock-Watson JE, Bourne MS, Vandervelde EM. IgG, IgA and IgM responses in acute rubella determined by the immunofluorescent technique. *J Hyg (Lond)*. 1972;70(3):473. doi:10.1017/S0022172400063063

341. Petrova EK, Dmitrieva AA, Trifonova EA, Nikitin NA, Karpova O V. The key role of rubella virus glycoproteins in the formation of immune response, and perspectives on their use in the development of new recombinant vaccines. *Vaccine*. 2016;34(8):1006-1011. doi:10.1016/j.vaccine.2016.01.010

342. SA P, D C, TH I. Studies of immunization with living rubella virus. Trials in children with a strain cultured from an aborted fetus. *Am J Dis Child*. 1965;110(4):381-389. doi:10.1001/ARCHPEDI.1965.02090030401007

343. Weibel RE, Benor DE. Chronic arthropathy and musculoskeletal

symptoms associated with rubella vaccines. A review of 124 claims submitted to the national vaccine injury compensation program. *Arthritis Rheum*. 1996;39(9):1529-1534. doi:10.1002/ART.1780390913

344. Atkins MC, Esmonde TFG. Guillain-Barré syndrome associated with rubella. *Postgrad Med J*. 1991;67(786):375-376. doi:10.1136/PGMJ.67.786.375

345. Plotkin SA. The History of Rubella and Rubella Vaccination Leading to Elimination. Accessed October 22, 2021. https://academic.oup.com/cid/article/43/Supplement_3/S164/288915

346. O'Shea S, Woodward S, Best JM, Banatvala JE, Holzel H, Dudgeon JA. RUBELLA VACCINATION: PERSISTENCE OF ANTIBODIES FOR 10-21 YEARS. *Lancet*. 1988;332(8616):909. doi:10.1016/S0140-6736(88)92512-3

347. Virnik K, Ni Y, Berkower I. Live attenuated rubella viral vectors stably express HIV and SIV vaccine antigens while reaching high titers. *Vaccine*. 2012;30(37):5453-5458. doi:10.1016/J.VACCINE.2012.06.074

348. Virnik K, Ni Y, Berkower I. Enhanced expression of HIV and SIV vaccine antigens in the structural gene region of live attenuated rubella viral vectors and their incorporation into virions. *Vaccine*. 2013;31(17):2119-2125. doi:10.1016/J.VACCINE.2013.02.055

349. Virnik K, Hockenbury M, Ni Y, et al. Live attenuated rubella vectors expressing SIV and HIV vaccine antigens replicate and elicit durable immune responses in rhesus macaques. *Retrovirology 2013 101*. 2013;10(1):1-15. doi:10.1186/1742-4690-10-99

350. Spadaccini A, Virnik K, Ni Y, Prutzman K, Berkower I. Stable expression of a foreign protein by a replication-competent rubella viral vector. *Vaccine*. 2010;28(5):1181-1187. doi:10.1016/J.VACCINE.2009.11.037

351. Pugachev K V., Galinski MS, Frey TK. Infectious cDNA clone of the RA27/3 vaccine strain of Rubella Virus. *Virology*. 2000;273(1):189-197. doi:10.1006/viro.2000.0408

352. Yanagi M, Purcell RH, Emerson SU, Bukh J. Transcripts from a single full-length cDNA clone of hepatitis C virus are infectious when directly transfected into the liver of a chimpanzee. *Proc Natl Acad Sci U S A*. 1997;94(16):8738-8743. doi:10.1073/pnas.94.16.8738

353. Pugachev K V., Abernathy ES, Frey TK. Genomic sequence of the RA27/3 vaccine strain of rubella virus. *Arch Virol*. 1997;142(6):1165-1180. doi:10.1007/s007050050150

354. Beatch MD, Hobman TC. Rubella Virus Capsid Associates with

Host Cell Protein p32 and Localizes to Mitochondria. *J Virol*. 2000;74(12):5569. doi:10.1128/JVI.74.12.5569-5576.2000

355. Cserzo M, Eisenhaber F, Eisenhaber B, Simon I. TM or not TM: transmembrane protein prediction with low false positive rate using DAS-TMfilter. *Bioinformatics*. 2004;20(1):136-137. doi:10.1093/BIOINFORMATICS/BTG394

356. Urbanowicz RA, McClure CP, King B, Mason CP, Ball JK, Tarr AW. Novel functional hepatitis C virus glycoprotein isolates identified using an optimized viral pseudotype entry assay. *J Gen Virol*. 2016;97(9):2265-2279. doi:10.1099/jgv.0.000537

357. Laemmli UK. Cleavage of structural proteins during the assembly of the head of bacteriophage T4. *Nature*. 1970;227(5259):680-685. doi:10.1038/227680A0

358. Owsianka A, Clayton RF, Loomis-Price LD, McKeating JA, Patel AH. Functional analysis of hepatitis C virus E2 glycoproteins and virus-like particles reveals structural dissimilarities between different forms of E2. *J Gen Virol*. 2001;82(8):1877-1883. doi:10.1099/0022-1317-82-8-1877

359. Hobman TC, Gillam S. In vitro and in vivo expression of rubella virus glycoprotein E2: The signal peptide is contained in the c-terminal region of capsid protein. *Virology*. 1989;173(1):241-250. doi:10.1016/0042-6822(89)90240-7

360. Garg H, Sedano M, Plata G, Punke EB, Joshi A. Development of Virus-Like-Particle Vaccine and Reporter Assay for Zika Virus. *J Virol*. 2017;91(20). doi:10.1128/JVI.00834-17

361. Walpita P, Barr J, Sherman M, Basler CF, Wang L. Vaccine potential of Nipah virus-like particles. *PLoS One*. 2011;6(4). doi:10.1371/JOURNAL.PONE.0018437

362. Warfield KL, Bosio CM, Welcher BC, et al. Ebola virus-like particles protect from lethal Ebola virus infection. *Proc Natl Acad Sci U S A*. 2003;100(26):15889-15894. doi:10.1073/PNAS.2237038100

363. Akahata W, Yang ZY, Andersen H, et al. A virus-like particle vaccine for epidemic Chikungunya virus protects nonhuman primates against infection. *Nat Med*. 2010;16(3):334-338. doi:10.1038/NM.2105

364. Syed AM, Taha TY, Tabata T, et al. Rapid assessment of SARS-CoV-2-evolved variants using virus-like particles. *Science*. 2021;374(6575):1626-1632. doi:10.1126/SCIENCE.ABL6184

365. DuBridge RB, Tang P, Hsia HC, Leong PM, Miller JH, Calos MP. Analysis of mutation in human cells by using an Epstein-Barr virus shuttle system. *Mol Cell Biol*. 1987;7(1):379-387. doi:10.1128/MCB.7.1.379-387.1987

366. Lin YC, Boone M, Meuris L, et al. Genome dynamics of the human embryonic kidney 293 lineage in response to cell biology manipulations. *Nat Commun*. 2014;5. doi:10.1038/NCOMMS5767

367. Rio DC, Clark SG, Tjian R. A mammalian host-vector system that regulates expression and amplification of transfected genes by temperature induction. *Science*. 1985;227(4682):23-28. doi:10.1126/SCIENCE.2981116

368. Lee JY, Hwang D, Gillam S. Dimerization of Rubella Virus Capsid Protein Is Not Required for Virus Particle Formation. *Virology*. 1996;216(1):223-227. doi:10.1006/VIRO.1996.0051

369. Goldsmith CS, Miller SE. Modern uses of electron microscopy for detection of viruses. *Clin Microbiol Rev*. 2009;22(4):552-563. doi:10.1128/CMR.00027-09

370. Vaheri A, von Bonsdorff CH, Vesikari T, Hovi T, Väänänen P. Purification of rubella virus particles. *J Gen Virol*. 1969;5(1):39-46. doi:10.1099/0022-1317-5-1-39/CITE/REFWORKS

371. Zahn T, Mhedhbi I, Hein S, et al. Persistence of infectious SARS-CoV-2 particles for up to 37 days in patients with mild COVID-19. *Allergy*. 2021;00:1-14. doi:10.1111/ALL.15138

372. Clayton RF, Owsianka A, Aitken J, Graham S, Bhella D, Patel AH. Analysis of antigenicity and topology of E2 glycoprotein present on recombinant hepatitis C virus-like particles. *J Virol*. 2002;76(15):7672-7682. doi:10.1128/JVI.76.15.7672-7682.2002

373. Tzeng WP, Chen MH, Derdeyn CA, Frey TK. Rubella Virus DI RNAs and Replicons: Requirement for Nonstructural Proteins Acting in Cis for Amplification by Helper Virus. *Virology*. 2001;289(1):63-73. doi:10.1006/VIRO.2001.1088

374. Engelman DM, Steitz TA, Goldman A. Identifying nonpolar transbilayer helices in amino acid sequences of membrane proteins. *Annu Rev Biophys Biophys Chem*. 1986;15:321-353. doi:10.1146/annurev.bb.15.060186.001541

375. Hobman TC, Lemon HF, Jewell K. Characterization of an endoplasmic reticulum retention signal in the rubella virus E1 glycoprotein. *J Virol*. 1997;71(10):7670-7680. doi:10.1128/jvi.71.10.7670-7680.1997

376. Cocquerel L, De Beeck AO, Lambot M, et al. Topological changes in the transmembrane domains of hepatitis C virus envelope glycoproteins. *EMBO J*. 2002;21(12):2893-2902. doi:10.1093/emboj/cdf295

377. Law LMJ, Duncan R, Esmaili A, Nakhasi HL, Hobman TC. Rubella Virus E2 Signal Peptide Is Required for Perinuclear Localization of Capsid Protein and Virus Assembly. *J Virol*. 2001;75(4):1978. doi:10.1128/JVI.75.4.1978-1983.2001

378. Suomalainen M, Garoff H, Baron MD. The E2 signal sequence of rubella virus remains part of the capsid protein and confers membrane association in vitro. *J Virol*. 1990;64(11):5500-5509. doi:10.1128/JVI.64.11.5500-5509.1990

379. Gibson DG, Young L, Chuang RY, Venter JC, Hutchison CA, Smith HO. Enzymatic assembly of DNA molecules up to several hundred kilobases. *Nat Methods*. 2009;6(5):343-345. doi:10.1038/NMETH.1318

380. Op De Beeck A, Voisset C, Bartosch B, et al. Characterization of Functional Hepatitis C Virus Envelope Glycoproteins. *J Virol*. 2004;78(6):2994-3002. doi:10.1128/JVI.78.6.2994-3002.2004/ASSET/2B5ED75B-8A55-4584-95EE-DD7BEF1D0871/ASSETS/GRAPHIC/ZJV0060418160008.JPEG

381. Tarr AW, Owsianka AM, Timms JM, et al. Characterization of the hepatitis C virus E2 epitope defined by the broadly neutralizing monoclonal antibody AP33. *Hepatology*. 2006;43(3):592-601. doi:10.1002/hep.21088

382. Urbanowicz RA, Wang R, Schiel JE, et al. Antigenicity and Immunogenicity of Differentially Glycosylated Hepatitis C Virus E2 Envelope Proteins Expressed in Mammalian and Insect Cells. *J Virol*. 2019;93(7):1-19. doi:10.1128/jvi.01403-18

383. Pettersen EF, Goddard TD, Huang CC, et al. UCSF Chimera--a visualization system for exploratory research and analysis. *J Comput Chem*. 2004;25(13):1605-1612. doi:10.1002/jcc.20084

384. Ruwona TB, Giang E, Nieusma T, Law M. Fine Mapping of Murine Antibody Responses to Immunization with a Novel Soluble Form of Hepatitis C Virus Envelope Glycoprotein Complex. *J Virol*. 2014;88(18):10459. doi:10.1128/JVI.01584-14

385. Elshuber S, Allison SL, Heinz FX, Mandl CW. Cleavage of protein prM is necessary for infection of BHK-21 cells by tick-borne encephalitis virus. *J Gen Virol*. 2003;84(1):183-191. doi:10.1099/VIR.0.18723-0/CITE/REFWORKS

386. Newton ND, Hardy JM, Modhiran N, et al. The structure of an infectious immature flavivirus redefines viral architecture and maturation. *Sci Adv*. 2021;7(20):4507-4521. doi:10.1126/SCIADV.ABE4507/SUPPL_FILE/ABE4507_SM.PDF

387. Mosa AI, Urbanowicz RA, AbouHaidar MG, Tavis JE, Ball JK, Feld JJ. A bivalent HCV peptide vaccine elicits pan-genotypic neutralizing antibodies in mice. *Vaccine*. 2020;38(44):6864-6867. doi:10.1016/j.vaccine.2020.08.066

388. Velázquez-Moctezuma R, Galli A, Law M, Bukh J, Prentoe J. Hepatitis C Virus Escape Studies of Human Antibody AR3A Reveal a High Barrier to Resistance and Novel Insights on Viral Antibody Evasion Mechanisms. *J Virol*. 2019;93(4).

doi:10.1128/JVI.01909-18

389. Taylor PC, Adams AC, Hufford MM, de la Torre I, Winthrop K, Gottlieb RL. Neutralizing monoclonal antibodies for treatment of COVID-19. *Nat Rev Immunol*. 2021;21(6):382-393. doi:10.1038/S41577-021-00542-X

390. Chung RT, Gordon FD, Curry MP, et al. Human monoclonal antibody MBL-HCV1 delays HCV viral rebound following liver transplantation: a randomized controlled study. *Am J Transplant*. 2013;13(4):1047-1054. doi:10.1111/AJT.12083

391. Colpitts CC, Tawar RG, Mailly L, et al. Humanisation of a claudin-1-specific monoclonal antibody for clinical prevention and cure of HCV infection without escape. *Gut*. 2018;67(4):736-745. doi:10.1136/GUTJNL-2016-312577

392. Felmlee DJ, Coilly A, Chung RT, Samuel D, Baumert TF. New perspectives for preventing hepatitis C virus liver graft infection. *Lancet Infect Dis*. 2016;16(6):735-745. doi:10.1016/S1473-3099(16)00120-1

393. O'Shea D, Law J, Egli A, et al. Prevention of hepatitis C virus infection using a broad cross-neutralizing monoclonal antibody (AR4A) and epigallocatechin gallate. *Liver Transpl*. 2016;22(3):324-332. doi:10.1002/LT.24344

394. Desombere I, Mesalam AA, Urbanowicz RA, et al. A novel neutralizing human monoclonal antibody broadly abrogates hepatitis C virus infection in vitro and in vivo. *Antiviral Res*. 2017;148:53-64. doi:10.1016/J.ANTIVIRAL.2017.10.015

395. Xu JL, Davis MM. Diversity in the CDR3 region of V(H) is sufficient for most antibody specificities. *Immunity*. 2000;13(1):37-45. doi:10.1016/S1074-7613(00)00006-6

396. Julien JP, Cupo A, Sok D, et al. Crystal structure of a soluble cleaved HIV-1 envelope trimer. *Science*. 2013;342(6165):1477-1483. doi:10.1126/SCIENCE.1245625

397. Fu Y, Zhang Z, Sheehan J, et al. A broadly neutralizing anti-influenza antibody reveals ongoing capacity of haemagglutinin-specific memory B cells to evolve. *Nat Commun*. 2016;7. doi:10.1038/NCOMMS12780

398. Crispin M, Ward AB, Wilson IA. Structure and Immune Recognition of the HIV Glycan Shield. *Annu Rev Biophys*. 2018;47:499-523. doi:10.1146/ANNUREV-BIOPHYS-060414-034156

399. Wu T Te, Johnson G, Kabat EA. Length distribution of CDRH3 in antibodies. *Proteins*. 1993;16(1):1-7. doi:10.1002/PROT.340160102

400. DeWitt WS, Lindau P, Snyder TM, et al. A Public Database of

Memory and Naive B-Cell Receptor Sequences. *PLoS One*. 2016;11(8). doi:10.1371/JOURNAL.PONE.0160853

401. JK H, R H, VV S. Diversity in the Cow Ultralong CDR H3 Antibody Repertoire. *Front Immunol*. 2018;9(JUN). doi:10.3389/FIMMU.2018.01262

402. Wang F, Ekiert DC, Ahmad I, et al. Reshaping antibody diversity. *Cell*. 2013;153(6). doi:10.1016/J.CELL.2013.04.049

403. Stanfield RL, Wilson IA, Smider V V. Conservation and diversity in the ultralong third heavy-chain complementarity-determining region of bovine antibodies. *Sci Immunol*. 2016;1(1). doi:10.1126/SCIIMMUNOL.AAF7962

404. Svilenov HL, Sacherl J, Protzer U, Zacharias M, Buchner J. Mechanistic principles of an ultra-long bovine CDR reveal strategies for antibody design. *Nat Commun 2021 121*. 2021;12(1):1-13. doi:10.1038/s41467-021-27103-z

405. Stanfield RL, Berndsen ZT, Huang R, et al. Structural basis of broad HIV neutralization by a vaccine-induced cow antibody. *Sci Adv*. 2020;6(22). doi:10.1126/SCIADV.ABA0468/SUPPL_FILE/ABA0468_SM.PDF

406. Burke MJ, Scott JNF, Minshull T, Stockley PG, Calabrese AN, Boyes J. An Ultralong Bovine CDRH3 that Targets a Conserved, Cryptic Epitope on SARS-CoV and SARS-CoV-2. *bioRxiv*. Published online April 6, 2022:2022.04.06.487306. doi:10.1101/2022.04.06.487306

407. Sok D, Le KM, Vadnais M, et al. Rapid elicitation of broadly neutralizing antibodies to HIV by immunization in cows. *Nature*. 2017;548(7665):108-111. doi:10.1038/NATURE23301

408. Macpherson A, Scott-Tucker A, Spiliotopoulos A, et al. Isolation of antigen-specific, disulphide-rich knob domain peptides from bovine antibodies. *PLoS Biol*. 2020;18(9). doi:10.1371/JOURNAL.PBIO.3000821

409. Li K, Wang S, Cao Y, et al. Development of Foot-and-Mouth Disease Virus-Neutralizing Monoclonal Antibodies Derived From Plasmablasts of Infected Cattle and Their Germline Gene Usage. *Front Immunol*. 2019;10. doi:10.3389/FIMMU.2019.02870

410. Heydarchi B, Center RJ, Gonelli C, et al. Repeated Vaccination of Cows with HIV Env gp140 during Subsequent Pregnancies Elicits and Sustains an Enduring Strong Env-Binding and Neutralising Antibody Response. *PLoS One*. 2016;11(6). doi:10.1371/JOURNAL.PONE.0157353

411. Sanders RW, Derking R, Cupo A, et al. A next-generation cleaved, soluble HIV-1 Env trimer, BG505 SOSIP.664 gp140, expresses multiple epitopes for broadly neutralizing but not non-neutralizing antibodies. *PLoS Pathog*. 2013;9(9).

doi:10.1371/JOURNAL.PPAT.1003618

412. Grant CFJ, Carr BV, Kotecha A, et al. The B Cell Response to Foot-and-Mouth Disease Virus in Cattle following Sequential Vaccination with Multiple Serotypes. *J Virol*. 2017;91(9). doi:10.1128/JVI.02157-16/FORMAT/EPUB

413. Ahsan A, Dar S, Hassan F, Ghafoor F, Yousuf MH, Shahzad-Ul-Hussan S. Characterization of linear epitope specificity of antibodies potentially contributing to spontaneous clearance of hepatitis C virus. *PLoS One*. 2021;16(8):e0256816. doi:10.1371/JOURNAL.PONE.0256816

414. Frumento N, Figueroa A, Wang T, et al. Repeated exposure to heterologous hepatitis C viruses associates with enhanced neutralizing antibody breadth and potency. *J Clin Invest*. Published online May 19, 2022. doi:10.1172/JCI160058

415. Bankwitz D, Bahai A, Labuhn M, et al. Hepatitis C reference viruses highlight potent antibody responses and diverse viral functional interactions with neutralising antibodies. *Gut*. 2021;70(9):1734-1745. doi:10.1136/GUTJNL-2020-321190

416. Vijayamahantesh V, Patra T, Meyer K, et al. Modified E2 Glycoprotein of Hepatitis C Virus Enhances Proinflammatory Cytokines and Protective Immune Response. James Ou J-H, ed. *J Virol*. Published online May 25, 2022. doi:10.1128/JVI.00523-22

417. Fathi A, Dahlke C, Addo MM. Recombinant vesicular stomatitis virus vector vaccines for WHO blueprint priority pathogens. *Hum Vaccin Immunother*. 2019;15(10):2269-2285. doi:10.1080/21645515.2019.1649532

Appendix 1- Chimera cloning primers

Cloning approach 1 primers.

RV and HCV regions are coloured blue and red, respectively. Orange bases were introduced to form a BsiWI restriction site following recombination. Sites involved in homologous recombination are in bold underlined font.

Name	Nucleotide Sequence (5'-3')
RubcasR	ACGGCGCGCGCGGTGCCAAC
Rubcas2F	ACGCTCACTCTGGGCGCCATTTGCG
Rubcas3F	ACGCCAAATGCTTGTACTACTTGCGCGGC
RH-E1F	**TGGCACCGCGCGCGCC**TACCAAGTGCGCAATTCCT
RH2-E1R	**GCGGCGACAGGCGCGGCG**GCACACCATAAATATCAGGACCCAC GGGACCAACAGGACAAAGGCCGCGAACGCGTGGTCAAGAGACA GCGCCCAGTGAGCACCAGCGAT
RH2-E2F	**CGCCGCGCCTGTCGCCGC**CGCGGCGCCGCCGCCGCCCTCACC GCAGTCGTCCTGCAGGGGTACAACCCCCCCGCCTATGGCGAAA CCCACGTCACCG
RH2-E2R	**CAAATGGCGCCC**AGAGTGAGCTTAATGGCCCAGGACG
RH3-E1R	**CCCCTGCAGGACGACTGCGG**TGAGGGCGGCGGCGGCGCCGC GGCGGCGACAGGCGCGGCGCGCGTCGACGCC
RH3-E2F	**CCGCAGTCGTCCTGCAGGGG**TACAACCCCCCCGCCTATGGCGA AACCCACGTCACCG
RH3-E2R	**GTACAAGCATTTGGC**CGCCTCCGCTTGG

Cloning approach 2 primers. RV and HCV regions are coloured blue and red, respectively.

Name	Nucleotide Sequence (5'-3')
RH-VecR	AGCTCTGGCTGTTCCAAC
RH-E1F	CCGTTGGAACAGCCAGAGCTTACCAAGTGCGCAATTCCTC
RH1-VecF	CTGAATGGGCCGCTGCTCACTGGTGGCAACTGACACTGGGAGCTATC
RH1-E1R	GCCAGCCACAGAGCAGAGGCTGGGGACCAGTTCATCATCATA
RH1-E2F	GCCTCTGCTCTGTGGCTGGCCACAGCCAATGCTCTGTCTCTGGATCAT
RH1-E2R	GTGAGCAGCGGCCCATTCAGCCCATGTCTGTCTGGTTTCGGACACGGCGCTTGACCCTACCC
RH2-E1R	TTCTGCAGACCATGAAGATCAGCACCCAAGGAACCAGCAGCACAAAGGCGGCCAGGGCATGATCCAGAGACAGAGCCCAGTGAGCACCAGCGAT
RH2-E2F	GATCTTCATGGTCTGCAGAAGGGCCTGCAGAAGAAGAGGCGCTGCTGCTGCTCTGACAGCCGTGGTTCTGCAGGGCTATAACCCTCCTGCCTATGGCGAAACCCACGTCACC
RH2-E2R	CAGATAGCTCCCAGTGTCAGCTTAATGGCCCAGGACG
RH2-VecF	CTGACACTGGGAGCTATCTG
RH3-E1R	CCCTGCAGAACCACGGCTGTCAGAGCAGCAGCAGCGCCTCTTCTTCTGCAGGCCCTTCTGCAGGCAAATAGCAGCAGCACTA
RH3-E2F	ACAGCCGTGGTTCTGCAGGGCTATAACCCTCCTGCCTATGGCGAAACCCACGTCACCG
RH3-E2R	CGCAGGTAGTACAGGCACTTGGCCTCAGCCTGGGATAT
RH3-VecF	AAGTGCCTGTACTACCTGCG
RH4-E2R	CGCAGGTAGTACAGGCACTTCCACAAGCAGGAGCAGA
RH5-E1R	TTCTGCAGACCATGAAGATCAGCACCCAAGGAACCAGCAGCACAAAGGCGGCCAGGGCATGATCCAGAGACAGAGCATTGGCTGTGGCCAGCCACAGCCAGTGAGCACCAGCGAT